Regulation of centromeric histone localization in budding yeast

Erica Hildebrand

A dissertation

submitted in partial fulfillment of the

requirements for the degree of

Doctor of Philosophy

University of Washington

2016

Reading Committee:

Susan Biggins, Chair

Toshio Tsukiyama

Steven Henikoff

Program Authorized to Offer Degree:

Molecular and Cellular Biology

University of Washington

Abstract

Regulation of centromeric histone localization in budding yeast

Erica Hildebrand

Chair of the Supervisory Committee:
Dr. Susan Biggins
Howard Hughes Medical Institute,
Division of Basic Sciences, Fred Hutchinson Cancer Research Center

The exclusive localization of the histone H3 variant CENP-A to centromeres is essential for accurate chromosome segregation. Ubiquitin-mediated proteolysis helps to ensure that CENP-A does not mislocalize to euchromatin, which can lead to genomic instability. Consistent with this, overexpression of budding yeast CENP-A^{Cse4} is lethal in cells lacking Psh1, the E3 ubiquitin ligase that targets CENP-A^{Cse4} for degradation. To identify additional mechanisms that prevent CENP-A^{Cse4} misincorporation and lethality, I analyzed the genome-wide mislocalization pattern of overexpressed CENP-A^{Cse4} in the presence and absence of Psh1 by chromatin immunoprecipitation followed by high throughput sequencing. I found that ectopic CENP-A^{Cse4} is enriched at promoters that contain histone H2A.Z^{Htz1} nucleosomes, but that H2A.Z^{Htz1} is not required for CENP-A^{Cse4} mislocalization. Instead, INO80-C, which removes H2A.Z^{Htz1} from

nucleosomes, promotes the ectopic deposition of CENP-A^{Cse4}. Transcriptional profiling revealed gene expression changes in the *psh1*Δ cells overexpressing CENP-A^{Cse4}. The down-regulated genes are enriched for CENP-A^{Cse4} mislocalization to promoters, while the up-regulated genes correlate with those that are also transcriptionally upregulated in an *htz1*Δ strain. Together, these data show that regulating centromeric nucleosome localization is not only critical for maintaining centromere function, but also for ensuring accurate promoter function and transcriptional regulation. To determine whether there are features of the CENP-A^{Cse4} nucleosome that facilitate Psh1-mediated proteolysis, a genetic screen was performed to identify histone H4 residues that regulate CENP-A^{Cse4} degradation. H4-R36 is a key residue identified from this screen that promotes the interaction between CENP-A^{Cse4} and Psh1. Consistent with this, CENP-A^{Cse4} protein levels are stabilized in H4-R36A mutant cells and CENP-A^{Cse4} is enriched in the euchromatin. The defects in CENP-A^{Cse4} proteolysis may be related to changes in Psh1 localization, as Psh1 becomes enriched at 3' intergenic regions in H4-R36A mutant cells. These data reveal a key residue in histone H4 that is important for efficient CENP-A^{Cse4} degradation, likely by facilitating the interaction between Psh1 and CENP-A^{Cse4}. My work reveals details of the Psh1 regulated mislocalization pathway for CENP-A^{Cse4} in budding yeast. As CENP-A is mislocalized in some cancer cells, it is important to understand the regulatory mechanisms involved with controlling centromeric histone mislocalization. Future work will determine if any of the mechanisms identified here are conserved in other organisms, or if they are perturbed during oncogenesis.

TABLE OF CONTENTS

LIST OF FIGURES

LIST OF TABLES

LIST OF SUPPLEMENTAL FIGURES

LIST OF SUPPLEMENTAL TABLES

LIST OF SUPPLEMENTAL FILES

ACKNOWLEDGEMENTS

I am so grateful to the many people who have supported me through my education, and who have made finishing this thesis possible. First, I would like to thank two people who started me on this path: my high school AP biology teacher, Karen Smereka, who is an amazing teacher, and mentored me through my first independent biology research project, and my first PI, Deborah Eastman, who I worked with for two years at Connecticut College as an undergraduate. Dr. Eastman is the person who inspired me to become a scientist. She taught me how to keep a lab notebook, make solutions, design experiments, and be excited about hypotheses and building molecular models. I am grateful for all of her advice and training, in particular for her suggestion that I apply to the MCB program at UW/Fred Hutch for graduate school.

My thesis advisor, Sue Biggins, has been an incredible mentor. She has encouraged me throughout my PhD, even when I was feeling discouraged, is a great role model, and runs her lab with integrity and scientific vision. I have learned so much while in her lab, from designing projects, public speaking, and writing grants and papers, to the importance of communicating with the public about science. I am also grateful to all of my colleagues in the Biggins lab, both past and present, who have given me valuable advice and comments on my project and career through the years. In particular, I would like to acknowledge the contributions made to this thesis by Gary Deyter and Adrienne Barber.

My support networks in the UW MCB program and the Fred Hutch Basic Sciences Division have been fantastic. I am thankful to Jeff Delrow and Ryan Basom from the Fred Hutch Genomics Shared Resource and Jerry Davison from the Fred Hutch Computational Biology Shared Resource for their assistance and training as I learned genomics techniques and analysis.

In addition, the Fred Hutch Basic Sciences IT specialists Pat Heath and Luna Yu are incredibly helpful. The Fred Hutch and MCB administrators: Michele Karantsavelos, MaryEllin Robinson, Maia Low, Marci Burden, Maria Sanders, Nomi Odano, Diane Darling, and Donna Modrell, make it so much easier to figure out program requirements, funding applications, and so many other problems that I've needed their help with. The MCB directors: Michael Emerman, Dave Raible, Katie Peichel, Rich Gardner, and Nina Salama, are also always helpful and have been wonderful sources of advice through the years. Thank you to my committee members, Toshi Tsukiyama, Steve Henikoff, Linda Wordeman, and Rich Gardner, for your helpful comments and advice about my project.

Thank you most of all to my parents and family. My parents encouraged me to explore and learn about nature and science from a young age, and their philosophy of knowledge and careers – that we should focus on the things that we are really excited about, and become experts in those fields – has greatly influenced my choices. As I have tried to figure out what interests me most, and to learn as much as I can about that topic, my parents have always been willing to listen to me, give me wonderful advice, and have been there for me at all times. Your support and love are so important to me. I am also grateful to my brother, who is always up for a discussion about science, life, or anything else. My grandparents, aunts and uncles, and the rest of my extended family have also been so helpful and supportive through my education, I couldn't have done this without all of you. Finally, thank you to my boyfriend, Chris, for your encouragement and understanding as we have gone through graduate school together. This has been a difficult but rewarding journey, and I couldn't have picked a better person to do this with than you.

INTRODUCTION

1.1 CHROMATIN

1.1.1 *DNA is packaged into chromatin*

The primary unit of chromatin is the nucleosome, which consists of 147 bp of DNA wrapped around an octameric histone core (**Figure 1.1**) (*1-3*). Most nucleosomes contain two copies each of the canonical histones, H2A, H2B, H3, and H4. Nucleosomes are arranged in a primary "beads on a string" structure (**Figure 1.1**), which is then further organized into higher order structures, giving rise to interphase chromosome domains and condensed mitotic chromosomes, depending on the stage of the cell cycle (*2*). The secondary structure of chromatin has been proposed to be a 30nm fiber, which has been observed *in vitro* (*4*). However, it is unclear if this actually occurs *in vivo* (*4, 5*). In addition, other types of secondary and tertiary structure have recently been identified *in vivo* using high-throughput sequencing based chromosome conformation mapping techniques, including gene loops, topologically associated domains (TADs), and nuclear compartments (*6-8*) (**Figure 1.1**).

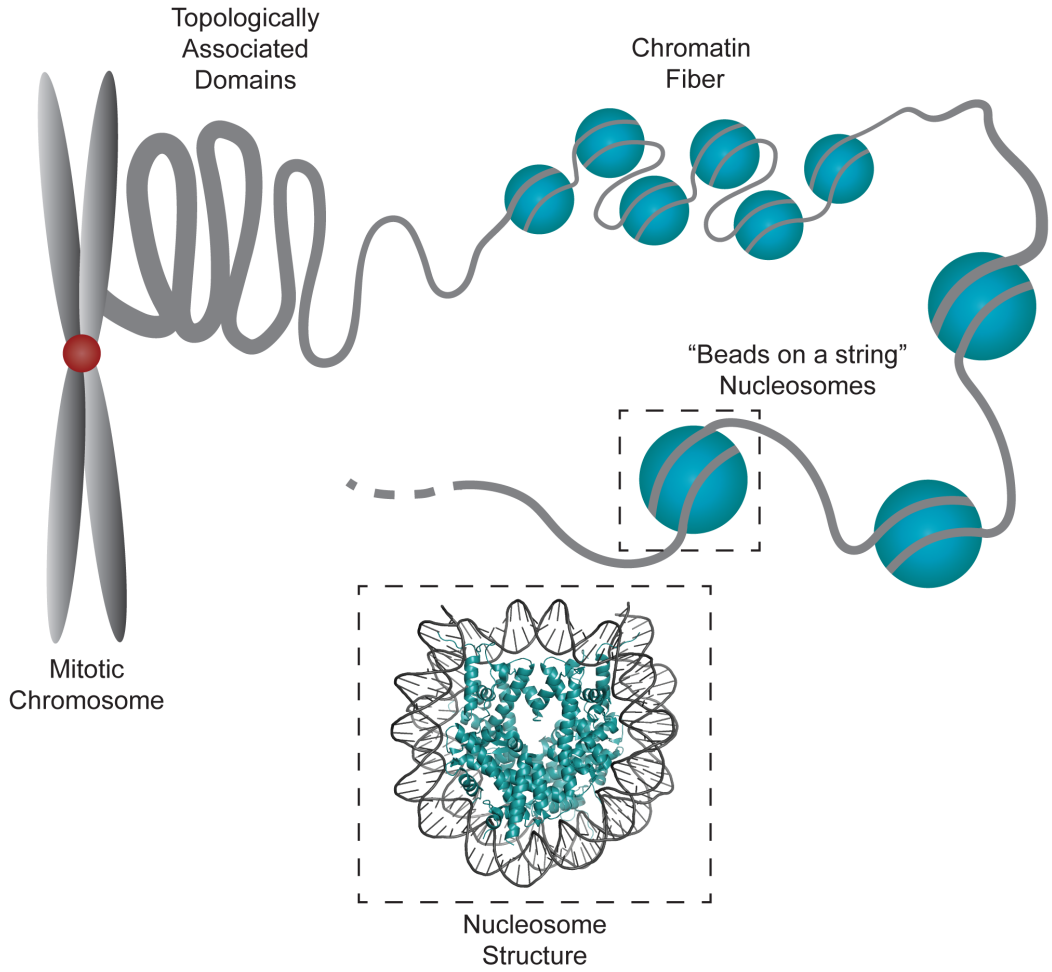

Figure 1.1. Chromatin structure
DNA (grey) is wrapped around histone proteins (blue) to form nucleosomes, which are organized into higher order structures, including "beads on a string", chromatin fibers, topologically associated domains, and interphase and mitotic chromosomes. Red circle indicates the centromere. Nucleosome structure is PDB ID 1ID3 (*9*)

The main functions of chromatin are two-fold. First, the organization of DNA around histone proteins to form nucleosomes allows for organized packing of the DNA into the nucleus. It has been proposed that the nucleosomes of each chromosome are packed into a fractal globule structure to allow each section to remain accessible as needed, without becoming tangled (*8*). Secondly, some DNA in each nucleosome becomes inaccessible to binding by other proteins, such as transcription factors, due to occlusion by the histone proteins themselves (*2*). This creates

an additional layer of regulation for chromatin functions, beyond DNA sequence, that depends on the location, occupancy, and composition of nucleosomes (*10*).

As most eukaryotic DNA is bound to histone proteins, chromatin is the main platform for all nuclear processes. This means that in a eukaryotic cell, transcription, replication, and chromosome segregation all occur in the context of chromatin, not on free DNA (*2, 11, 12*). The cell regulates how chromatin affects these processes through the use of epigenetic marks. These include histone modifications and composition, as well as nucleosome occupancy and localization (*2, 13-16*). Because these marks are epigenetic, they do not depend on the underlying DNA sequence, but are instead a separate layer of regulation (*2*). Some chromatin marks are highly dynamic, while others persist through generations (*17, 18*).

1.1.2 *Epigenetic marks consist of histone variant composition and post-translational modifications of nucleosomes*

One type of epigenetic mark that affects chromatin accessibility and function is the incorporation of histone variants into specific nucleosomes. There are only two histone variants in budding yeast, H2A.Z^{Htz1}, a variant of H2A, and CENP-A^{Cse4}, a variant of H3 (*19*). Other organisms such as humans have multiple variants of both H2A and H3, however, variants of H2B and H4 are much less common (*14, 19, 20*). H2A.Z^{Htz1} is found at promoter nucleosomes, at the -1 and +1 positions relative to transcription start sites (TSS) (**Figure 1.2**) (*14, 21, 22*). H2A.Z^{Htz1} regulates transcriptional activity, but in different ways, depending on the context (*23*). H2A.Z^{Htz1} is often found at promoters of repressed genes, and is thought to set up a "poised" transcriptional state, which is ready to be activated quickly upon a cellular signal (*24-26*). Conversely, H2A.Z^{Htz1} containing nucleosomes are also found at promoters of many active genes, and are thought to decrease the nucleosomal barrier to transcription by reducing RNA polymerase pausing at

promoters (*25, 27*). Interestingly, in human cells, H2A.Z is anti-correlated with H3-H4 turnover, and it has been suggested that this is due to increased H2A.Z-H2B dimer displacement, which allows RNA polymerase to travel through the gene without causing turnover of the entire nucleosome (*27*). However, in budding yeast there is a positive correlation between H3 turnover and H2A.Z^{Htz1} containing nucleosomes, so the mechanism of how H2A.Z controls transcription may not be completely conserved between yeast and humans (*28*). H2A.Z^{Htz1} is also found at nucleosomes flanking the centromere, and has been suggested to be a barrier element that insulates different epigenetic states (*21*).

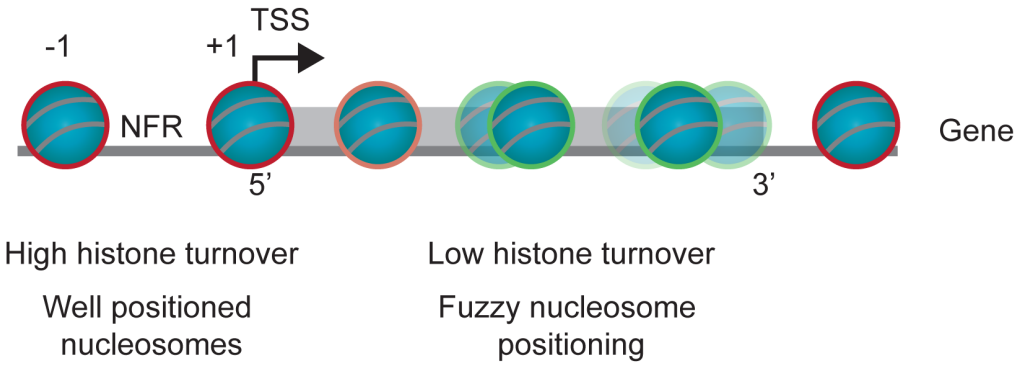

Figure 1.2. Nucleosome positioning and turnover at promoters and genes in budding yeast
Color of nucleosome outline indicates turnover rate (red = high, orange = medium, green = low). Transparency indicates positioning, opaque nucleosomes are well positioned, while more transparent nucleosomes have fuzzy positioning.

The only other histone variant in budding yeast is CENP-A^{Cse4} (also called CenH3), which is the centromeric histone H3 variant (*29, 30*). The centromeric H3 variant is highly conserved across species, and the budding yeast CENP-A^{Cse4} protein has been reported to complement RNAi depletion of the human CENP-A protein in cell culture (*31-33*). In wild-type (WT) cells, CENP-A^{Cse4} only binds to centromeric DNA, where it is required for the assembly of the kinetochore, a large proteinaceous structure that links sister chromatids with spindle microtubules to allow for chromosome segregation during mitosis (*34*). While the centromere is

genetically defined in budding yeast, and may also have genetic elements in other eukaryotes such as humans, CENP-A^{Cse4} is thought to be the main epigenetic mark of the centromere (*35*). In humans, there are cases of chromosomes with neocentromeres where there is CENP-A but no underlying centromeric sequence, and these are able to form kinetochores and support cell division (*36*). In budding yeast, both the centromeric DNA and CENP-A^{Cse4} are essential for kinetochore assembly and chromosome segregation (*30*). There is only one CENP-A^{Cse4} nucleosome bound per centromere in budding yeast, and this stoichiometry is necessary for correct cell division (*37*). To ensure that all sister chromatids contain a centromeric nucleosome, a dedicated chaperone, Scm3, incorporates CENP-A^{Cse4} at the centromere (*38-40*). The human ortholog is the CENP-A chaperone HJURP (*41*). In addition, CENP-A^{Cse4} is regulated by proteolysis to prevent multiple centromeric nucleosomes from being incorporated on one sister chromatid (*42-44*). These processes will be discussed in more detail below in Section 1.2: Control of Centromeric Histone Localization.

Besides the histone variant composition of nucleosomes, post-translational modifications of histones tails, such as phosphorylation, methylation, acetylation, and ubiquitylation, are the other main form of epigenetic regulation in eukaryotes (*26*). Histone modifications can recruit specific proteins to modulate the compaction of chromatin, can bind to or be deposited by transcription machinery, and may also lead to changes in DNA-histone or histone-histone interactions, which could affect nucleosome stability (*2*). In general, histone acetylation is associated with actively transcribed genes, while histone methylation is more varied. For example, in budding yeast H3K79 methylation is mainly found at silent chromatin, but H3K4 and H3K36 methylation occur over actively transcribed genes (*26, 45*).

1.1.3 *Histone chaperones incorporate histones into nucleosomes*

Histones are incorporated into or removed from nucleosomes by histone chaperones (*46*). These are proteins and protein complexes that prevent nonspecific binding of the positively charged histones to each other, to prevent aggregation and to assist incorporation of histones into nucleosomes (*46*). Histones are generally found as dimers, either H2A-H2B or H3-H4, or tetramers, $(H3\text{-}H4)_2$, when not incorporated into nucleosomes, and these are the complexes that are bound by various chaperones (*46*). In addition, some chaperones regulate the incorporation of nucleosomes at specific cell cycle stages or particular regions of the chromatin (*46, 47*). Some histone chaperones are specific for certain histone variants or histones with certain posttranslational modifications, while others can incorporate many different forms of histone proteins (*46*). Replication-coupled nucleosome assembly is the major pathway that incorporates histones into chromatin every cell cycle (*47*). This occurs during S-phase, and is important for reassembling chromatin after passage of the replication fork. Replication-coupled histone chaperones for H3-H4 include Asf1 and the CAF-1 complex, which are thought to work together to incorporate newly synthesized H3-H4 following the replication fork, and Rtt106 which works in a parallel pathway (*48*). There is also replication-independent nucleosome assembly for H3-H4, mediated by Asf1, Hir1, Rtt106, and Spt6 (*48*). It is thought that for this replication-independent assembly, the histone chaperones interact with transcription and chromatin remodeling machinery to regulate gene expression (*48*). FACT (Facilitates Chromatin Transcription/Transactions) and Nap1 are H2A-H2B specific, and are involved in both replication-coupled and replication-independent turnover (*46*). The rate of turnover of H3-H4 is generally slower than the turnover rate of H2A-H2B (*2*). The centromeric histone variant CENP-A^{Cse4} has a specific histone chaperone, Scm3, that incorporates it only at the centromere (*38-40*).

In addition, there is cross talk between some histone modifications and nucleosome assembly. Acetylation of newly synthesized histones H3 and H4 is involved with replication-coupled nucleosome assembly, and is highly conserved (*48*). These are H4 acetylations on lysines 5 and 12, which are mediated by the histone acetyl-transferase Hat1, and H3 lysine 56 acetylation, which is performed by the Rtt109-Vps75 complex, and requires the histone chaperone Asf1 to be bound to the H3-H4 dimers (*48, 49*). H3-K56 acetylation is important for regulating replication-coupled histone deposition and increasing the binding of H3-H4 to histone chaperones CAF-1 and Rtt106. This mark is removed later in the cell cycle by NAD dependent deacetylases Hst2 and Hst4 (*48*).

1.1.4 *Chromatin remodelers regulate nucleosome position and occupancy*

Nucleosome localization and occupancy are dynamic, and chromatin-remodeling complexes are an additional layer of regulation on these features. There are stereotypical nucleosome positions at genes, with well-positioned nucleosomes at promoters and the start of genes, surrounding a nucleosome-free region (NFR, also called a nucleosome-depleted region, or NDR), and phased nucleosomes following the +1 nucleosome through the gene body, with positioning becoming more fuzzy towards the 3' ends of genes (*2, 13, 50*) (**Figure 1.2**). In addition, nucleosomes flanking centromeres and origins of replication are also well positioned (*51-53*). The position of each nucleosome is defined by a combination of factors, including sequence intrinsic positioning, statistical positioning, or the packing of nucleosomes between nearby well-positioned nucleosomes, and sliding of nucleosomes to less thermodynamically favorable positions by chromatin remodelers using ATP (*13*).

There are four classes of chromatin remodelers, the SWI/SNF, ISWI, CHD and INO80 families (*10*). All chromatin remodelers contain a conserved SWI2/SNF2-family ATPase domain, but the different families have other distinct domains (*10*). Some chromatin remodelers can act on any nucleosome, while others act on only specific histone variants or nucleosomes with certain posttranslational modifications (*10*). Chromatin remodelers are required to shift nucleosomes as needed to regulate access to DNA motifs that are targets of DNA binding proteins. By changing nucleosome position or the way that DNA is wrapped around a nucleosome, chromatin remodelers can occlude or reveal different regions of the DNA to affect transcription and replication machinery access (*10*).

Chromatin remodelers can also regulate the histone variant composition of nucleosomes. In budding yeast, the SWR-C chromatin-remodeling complex incorporates H2A.Z^{Htz1} into nucleosomes through a two-step process, with a heterotypic H2A-H2A.Z^{Htz1} nucleosome intermediate (*22, 54-56*). Histone chaperones Chz1, Nap1, and FACT bind to H2A.Z^{Htz1}-H2B dimers, and H2A.Z^{Htz1}-H2B from all of these complexes can be incorporated into chromatin by the SWR-C complex (*22, 57*). SWR-C preferentially adds H2A.Z^{Htz1} to nucleosomes with longer flanking linker regions, such as those at promoters next to NFRs (*58*). The reverse reaction is thought to be carried out by the INO80 complex (INO80-C), which is a chromatin-remodeling complex in the same family as SWR-C and has multiple functions (*59*). INO80-C has been shown to remove H2A.Z^{Htz1} from nucleosomes by promoting full nucleosome turnover of H2A.Z^{Htz1}-containing nucleosomes, which can then be replaced by H2A-containing nucleosomes (*59, 60*). However, there is some controversy about whether this reverse reaction occurs *in vitro* (*61*). In addition, INO80-C can slide nucleosomes to center them on a DNA template and acts as a nucleosome spacing factor on multi-nucleosome templates *in vitro* (*62*).

1.1.5 *Histone turnover dynamics are modulated by both histone chaperones and chromatin remodelers*

Replication-independent nucleosome turnover dynamics are another way that chromatin processes are regulated (*28, 48*). The rate of turnover varies throughout the genome, and is also different between species. In budding yeast, promoters tend to have high histone turnover, while intragenic regions have lower turnover (*28*). Histone chaperones such as Hir1 and CAF-1 are required for the high turnover at promoters (*63*). In addition, not all histone proteins have the same dynamics. Histones H3 and H4 tend to be replaced less frequently than H2A and H2B, and the localization of histone variant H2A.Z^{Htz1} is correlated with the highest rate of H3 turnover in budding yeast (*28, 48*). This is in contrast to recent results in human cells, where H2A.Z is localized to promoter nucleosomes with lower H3-H4 turnover, and may allow increased removal of the H2A.Z-H2B dimers during transcription to allow RNA polymerase to move through the nucleosome without completely disrupting the $(H3\text{-}H4)_2$ tetramer (*27*). In addition, biochemical analysis of nucleosomes containing histone H2A.Z^{Htz1} suggests that these are less stable than H2A containing nucleosomes (*64*). In budding yeast, there are only two versions of H3, the canonical H3.3-like version and the centromeric histone variant (*28*). The H3.3 variant is used for both replication-coupled and replication-independent nucleosome assembly throughout the euchromatin. This is in contrast to some other eukaryotes, such as humans, where H3.1 is the replication-coupled variant, while H3.3 is only incorporated in a replication-independent manner (*48*).

Chromatin remodelers can also affect histone turnover. For example, SWR-C and INO80-C have been shown to have opposite effects on turnover of nucleosomes containing histone H2A.Z^{Htz1} (*60*). When SWR-C is bound to these nucleosomes following incorporation of

H2A.Z^{Htz1}, the nucleosomes are more stable. This is in contrast to INO80-C binding, which promotes full nucleosome turnover, evicting both H2A.Z^{Htz1} and the other histone proteins, to allow an H2A containing nucleosome to be assembled (*59, 60*).

1.1.6 *Chromosome segregation*

Mitosis is defined as the division of the nucleus, and is an essential part of the cell cycle. For cells to pass on their genetic material to the next generation, each pair of sister chromatids must be correctly segregated, so that one copy goes into each daughter cell (*34*). In budding yeast, there is a closed mitosis, meaning that the nuclear envelope does not break down, as it does in other eukaryotes (*65*). In addition, the spindle is formed early in the cell cycle, and the chromosome segregation machinery is present and ready as soon as the DNA is replicated (*65*). Budding yeast have 16 chromosomes in a haploid state, and each of these chromosomes attaches to just one kinetochore microtubule during mitosis (*65*).

1.1.7 *Centromeric chromatin*

Centromeres in budding yeast are genetically defined, and are only 120 bp in length, in contrast to the repetitive multi-megabase centromeres found in other eukaryotes (*66-68*). There are three regions of each yeast centromere, CDE (Centromere DNA Element) I, CDEII, and CDEIII. CDEI and CDEIII are 8 and 26 bp consensus sequences, respectively, while CDEII is a 78-86bp AT rich region (*69*). Cbf1 binds to CDEI, CBF3 binds to CDEIII, and CENP-A^{Cse4} binds to CDEII (*30, 70*). Only one centromeric CENP-A^{Cse4} containing nucleosome is incorporated at each budding yeast "point" centromere, and this serves as the platform for the kinetochore, which links sister chromatids to spindle microtubules (*37, 67*). The centromere and CENP-A^{Cse4} are essential for chromosome segregation during mitosis (*29, 30, 68*).

Surrounding the centromere is the pericentromere, a region of each chromosome that is important for biorientation of kinetochores (*71*). The protein complexes cohesin and condensin bind to the pericentromere, and these are essential for the biorientation function. Cohesin holds sister chromatids together until anaphase and condensin compacts chromosomes into mitotic structures (*72-74*). In addition, the pericentromere forms loops, which act as a chromatin spring to transduce force from the kinetochores to the rest of the chromosome (*67*). This is thought to be important for tension sensing, to signal to the kinetochore that it is correctly attached to microtubules from opposite poles (*74*). In budding yeast, pericentric chromatin is enriched for H2A.Z^{Htz1} and is hypoacetylated on histone H4 lysine 16 (*21, 75, 76*). H4-K16 hypoacetylation may help control localization of CENP-A^{Cse4} to the centromere (*75, 76*). In humans, the centromeric and pericentric chromatin is very different than in budding yeast. While CENP-A is found at both types of centromeres, in humans the region of CENP-A binding is much larger, and CENP-A nucleosomes are interspersed with H3 nucleosomes (*77*). These regional centromeres also connect to multiple microtubules each, in contrast to the budding yeast "point" centromeres, which only connect to one microtubule per sister chromatid (*67*).

1.2 Control of Centromeric Histone Localization

1.2.1 *Centromeric nucleosome assembly*

In budding yeast, the most upstream kinetochore component is the CBF3 complex, consisting of the Ndc10, Cep3, Ctf13, and Skp1 proteins (*78-82*). CBF3 binds in a sequence specific manner to the CDEIII region of centromeric DNA, and is essential for kinetochore assembly and chromosome segregation (*79, 80*). The Ndc10 subunit of CBF3 is a binding partner for Scm3, the CENP-A^{Cse4} chaperone (*40, 83*). Scm3 interacts with the CENP-A Targeting Domain (CATD) of

CENP-A^{Cse4} and also binds to both Ndc10 and directly to the AT rich CDEII region of centromeric DNA, and in this way brings CENP-A^{Cse4}-H4 to the centromere (*84-86*). The timing of centromeric nucleosome assembly is directly following S-phase, and the rest of the kinetochore forms soon after, since budding yeast have a very short G2-phase before the onset of mitosis (*78*).

The structure of the centromeric nucleosome is controversial. There is evidence for both an octameric CENP-A^{Cse4} containing nucleosome, similar to a canonical H3 containing nucleosome, as well as for a hemisome structure containing just one copy each of the histone proteins (*87*). Evidence for a hemisome includes the ability of CENP-A^{Cse4} nucleosomes to form positive supercoils on plasmid DNA, as well as the length of the centromeric DNA available to be wrapped around the nucleosome at the centromere, which is only 80bp, shorter than the usual 147bp required for an octameric nucleosome, and H4S47C cleavage mapping (*87-90*). Both hemisomes and octameric nucleosomes have been reconstituted *in vitro* with CENP-A^{Cse4}, although only hemisomes form stably on CDEII DNA (*91*). However, there is also evidence for an octameric nucleosome based on counting of fluorescently labeled CENP-A^{Cse4} *in vivo*, which showed that there are enough CENP-A^{Cse4} molecules per kinetochore cluster for two CENP-A^{Cse4} at each centromere, although it is unclear whether all CENP-A^{Cse4} in the kinetochore cluster are incorporated into centromeric DNA (*92, 93*). This fluorescence microscopy study also showed that the number of CENP-A^{Cse4} molecules at the centromere does not oscillate throughout the cell cycle (*92, 94, 95*). While the structure of the centromeric nucleosome is debated, it is generally accepted that mislocalized CENP-A^{Cse4} containing nucleosomes on chromosome arms are octameric, and protect a similar length of DNA from MNase digestion to H3 octameric nucleosomes (*87, 88*). After the centromeric nucleosome assembles, inner kinetochore proteins

Mif2 and other COMA complex components are the next to bind, and these recruit the microtubule binding proteins of the kinetochore to assemble (*78*).

Chromatin remodeling factors are also important for assembling the centromeric chromatin. The SWI/SNF-like chromatin-remodeling factor Fun30 is required for budding yeast centromere function. Fun30 is essential for setting up the correct H2A.Z^{Htz1} nucleosome phasing surrounding the centromeric nucleosome (*96*). INO80-C has also been shown to have a role at centromeres, and deletion of the Ino80 subunit leads to defective chromosome segregation, through problems with the pericentromere (*97*). RSC appears to have a similar role, as it associates with the centromere and pericentromere and is required for maintaining chromatin structure at these regions (*98*). In fission yeast, the histone chaperone FACT is another chromatin factor that is involved with setting up correct chromatin structure at the centromere (*99, 100*).

1.2.2 *The ubiquitin-proteasome pathway controls CENP-A^{Cse4} levels*

CENP-A^{Cse4} levels are regulated by ubiquitin-mediated proteolysis. When translation is inhibited, WT CENP-A^{Cse4} is quickly degraded, in a proteasome dependent manner (*42*). Ubiquitin is a small protein that can be covalently linked to lysines in other proteins (*101*). Ubiquitin is transferred to target proteins through E1, E2, and E3 enzymes (**Figure 1.3**). The E1, or ubiquitin-activating enzyme, uses ATP to form a high-energy thioester bond with the terminal glycine residue in ubiquitin (*101*). There is only one E1 enzyme in budding yeast, called Uba1 (*101*). Next, this activated ubiquitin is transferred to an E2, or ubiquitin-conjugating enzyme via transesterification (*101*). There are 13 known E2 enzymes in budding yeast, the Ubc proteins (*101*). The last step of the ubiquitin pathway is transfer of the ubiquitin molecule to the substrate, which is catalyzed by the E3 enzymes, the ubiquitin ligases. Generally ubiquitin is conjugated to

lysine residues in the target proteins by formation of an isopeptide bond between the activated carboxyl group on ubiquitin and the ε-amino groups on lysine residues (*101*). The E3s are the largest family of enzymes, with 60-100 found in budding yeast. Ubiquitin ligases are responsible for substrate specificity, and multiple E3s can work with each E2 (*101*). The two main families of E3 ligases are HECT (Homologous to E6-AP Carboxy Terminus) and RING (Really Interesting New Domain) domain containing proteins. For HECT E3 ligases, ubiquitin is transferred from the E2 to the E3 enzyme, and the E3 directly ubiquitylates the substrate. This is in contrast to RING E3s, which serve as an adapter to bring the E2 protein conjugated to ubiquitin in close proximity to the substrate, without an E3 conjugated step (*101*). Target proteins can be monoubiquitylated, multiubiquitylated, or polyubiquitylated. In general, polyubiquitylated proteins are targeted for degradation at the proteasome, while mono- and multiubiquitylation lead to outcomes such as changes in localization or function of the target protein (*101*). The most well studied effect of ubiquitylation is to signal that the target protein should be degraded by the proteasome. This is mainly mediated through K48 linked polyubiquitin chains, although recent studies have suggested that other unconventional linkages can also lead to degradation (*101*).

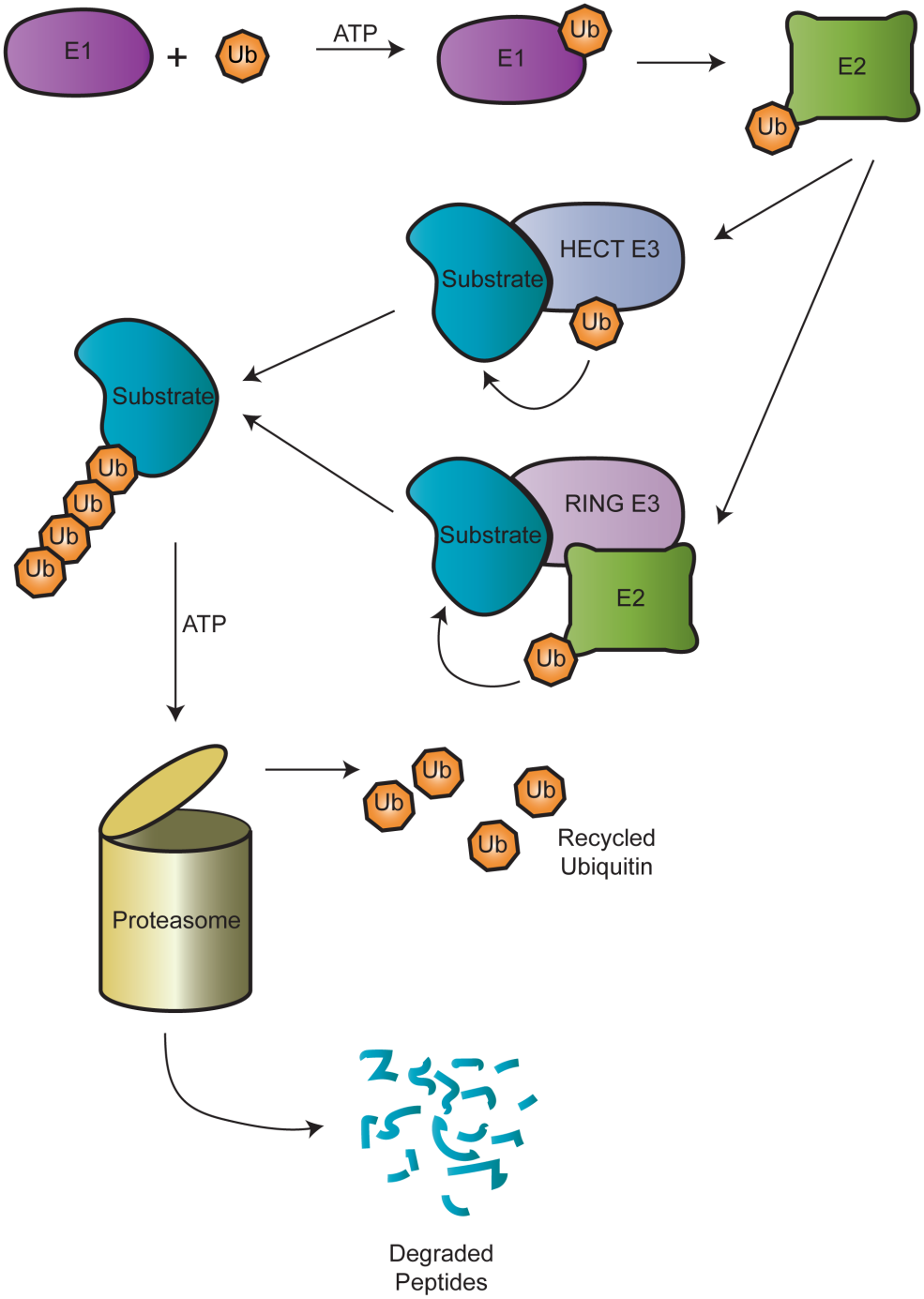

Figure 1.3. The ubiquitin-proteasome system
Ubiquitin is conjugated to the E1 in an ATP dependent step. The E1 then transfers ubiquitin to the E2 enzyme, which either transfers the ubiquitin to an E3 (HECT), or binds to an E3 (RING) to transfer the ubiquitin to the substrate protein. Polyubiquitylated substrates are targeted to the proteasome for degradation. Unfolding of the substrate before proteolysis requires ATP. Ubiquitin is removed from substrate before substrate degradation by deubiquitinases on the proteasome lid, and ubiquitin is recycled for subsequent use.

The proteasome is a large protein complex made up of the regulatory particle, consisting of a base and a lid, and the core particle, a barrel shaped structure (*101*). Polyubiquitylated proteins are recognized by the regulatory particle, which binds to ubiquitin chains (*101*). Substrates are unfolded by the AAA+ ATPases in the regulatory particle, and are then fed into the lumen of the core particle, which contains the proteolytic active sites (*101*). Ubiquitin is removed before proteolysis by deubiquitinases on the lid of the proteasome, so that it can then be recycled in the cell (*101*). Besides ubiquitin, there are other small proteins that can be covalently linked to target proteins or other molecules. In budding yeast, these include Smt3 (SUMOylation), Rub1 (NEDDylation), Urm1 (urmylation), and the autophagy factors Atg8 and Atg12 (*101*). These follow a similar conjugation process to ubiquitylation, but use separate machinery, and can have quite different consequences, such as signaling or transport to certain cellular compartments (*101*).

The first E3 ubiquitin ligase shown to affect CENP-A^{Cse4} turnover was Psh1, a RING family E3 ligase (*43, 44*). Psh1 mediates CENP-A^{Cse4} ubiquitylation and degradation in budding yeast, and is activated by Casein Kinase 2 (Cka2) phosphorylation (*43, 44, 102*). However, deletion of Psh1 does not completely stabilize CENP-A^{Cse4}, suggesting that other mechanisms are also involved (*43, 44*). Subsequent publications have identified multiple other proteins that also regulate CENP-A^{Cse4} stability. One of these is Doa1, which mediates ubiquitin recycling in the cell, and is required for ubiquitylation of the N-terminus of CENP-A^{Cse4} (*103*). In addition, the F-box protein Rcy1 was recently implicated in CENP-A^{Cse4} turnover (*104*). It is currently unclear if these E3s have redundant functions or instead ubiquitylate different pools of CENP-A^{Cse4}, and this would be an interesting topic for future study. CENP-A^{Cse4} is more stable in *rcy1*Δ *psh1*Δ double mutants than in either single mutant, suggesting that these pathways act in

parallel pathways (*104*). Analysis of the regions of CENP-A^{Cse4} ubiquitylated by these different pathways suggests some specificity. Psh1 requires the CATD within the C-terminal histone fold domain (HFD) of CENP-A^{Cse4} to bind to CENP-A^{Cse4} and mediate its ubiquitylation (*43*). In addition, mass spectrometry analysis showed that the C-terminal lysine residues K131, 155, 163, and 172 are the main targets of Psh1 mediated ubiquitylation *in vitro* (*44*). Conversely, the N-terminal CENP-A^{Cse4} tail is sufficient for the ubiquitylation that requires Doa1 (*103*).

There is also evidence that other post-translational modifications affect CENP-A^{Cse4} stability. Proline isomerization by the peptidyl prolyl *cis-trans* isomerase Fpr3 is required for Psh1-mediated CENP-A^{Cse4} ubiquitylation and degradation (*105*). The Fpr3 protein is required for the interaction between CENP-A^{Cse4} and Psh1, potentially through structural changes in CENP-A^{Cse4} due to *cis-trans* isomerization of CENP-A^{Cse4} proline 134 (*105*). CENP-A^{Cse4} is also SUMOylated by the SUMO E3 ligases Siz1 and Siz2, and this targets it for SUMO-targeted ubiquitin ligase (STUbL) Slx5 mediated ubiquitylation and proteolysis (*106*). Slx5 acts on CENP-A^{Cse4} in a Psh1 independent fashion (*106*). It is not yet known how the Slx5 directed degradation pathway interacts with Rcy1 or Doa1 mediated degradation of CENP-A^{Cse4}, or if there are any connections between SUMOylation of CENP-A^{Cse4} and proline isomerization by Fpr3.

Surprisingly, the E3 ubiquitin ligase Psh1 has been found to localize to the centromere and kinetochore, even though CENP-A^{Cse4} at the kinetochore is stable (*42, 44, 107*). There have been multiple mechanisms identified that may be active in this region to protect CENP-A^{Cse4} from degradation. One example is the deubiquitinase Ubp8, which has been shown to oppose Psh1 mediated CENP-A^{Cse4} degradation by removing short poly-ubiquitin chains, although unexpectedly, *ubp8*Δ strains also show increased CENP-A^{Cse4} mislocalization to telomere and

rDNA loci (*108*). In addition, both Pat1, an inner kinetochore protein, and Scm3, the CENP-A^{Cse4} chaperone, have been shown to protect centromeric CENP-A^{Cse4} from degradation (*44, 109*). Alternatively, Psh1 at the centromere may have a positive role, perhaps by protecting against extra CENP-A^{Cse4} nucleosomes forming in the region. Fluorescence microscopy experiments have measured increased CENP-A^{Cse4} at kinetochore foci in *psh1*Δ cells. However it is unclear if these molecules are incorporated into nucleosomes, or represent soluble CENP-A^{Cse4} (*110*). Proteolysis of the centromeric histone variant is a conserved process, although the specific E3 ligases may not be conserved. In *Drosophila melanogaster*, F-box protein Partner of Paired (Ppa) has been shown to bind to and mediate proteasomal degradation of CENP-A^{CID} to prevent mislocalization (*111, 112*). Conversely, CUL3/RDX also mediates CENP-A^{CID} ubiquitylation in *D. melanogaster*, but this ubiquitylation leads to a more stable centromeric nucleosome (*113*). While human CENP-A is degraded in senescent cells and in certain viral infections, it is currently unknown if there is an endogenous E3 ubiquitin ligase that targets CENP-A in human cells as a part of normal homeostasis (*114-116*).

1.2.3 *Protection against CENP-A^{Cse4} euchromatic localization by histone chaperones and chromatin remodelers*

Deletion of histone chaperones CAF-1 and Hir1 leads to mislocalization of CENP-A^{Cse4} to promoters (*63, 117*). This double mutant also has decreased H3 turnover throughout the genome, which was suggested to contribute to the CENP-A^{Cse4} localization defect (*63*). Conversely, moderate overexpression of CENP-A^{Cse4} has been shown to cause mislocalization of CENP-A^{Cse4} to promoter regions in WT cells. These regions have the highest histone turnover in budding yeast (*88*). The other histone chaperone that has been shown to control CENP-A^{Cse4} mislocalization is FACT, which is required for Psh1 recognition of CENP-A^{Cse4} *in vivo* (*118*).

The yeast SWI/SNF complex is one chromatin-remodeling factor that destabilizes mislocalized CENP-A^{Cse4} to prevent ectopic incorporation (*119*). In fission yeast, mechanisms that promote H3 chromatin integrity such as FACT and Clr6-CII histone deacetylase activity have also been shown to defend against ectopic CENP-A^{Cnp1} deposition (*99*). It is not known how mislocalized CENP-A^{Cse4} becomes incorporated into nucleosomes in budding yeast, but in human cells the histone chaperone DAXX (which does not have a homolog in budding yeast) is required for CENP-A mislocalization to occur (*120*).

1.2.4 *Previously observed centromeric histone mislocalization patterns*

In budding yeast, moderate overexpression of CENP-A^{Cse4} was shown to result in mislocalization to promoter nucleosomes, and it was suggested that this was due to high histone turnover in these areas (*88*). A separate genome-wide analysis of an epitope tagged CENP-A^{Cse4} protein in budding yeast suggested that there was higher mislocalization at genes that are very highly transcribed, and to centromere like regions (CLRs) (*121, 122*). However, subsequent work suggested that this may be an artifact of the ChIP-seq protocol used in that study (*123*). ChIP-qPCR of the CENP-A^{Cse4}-K16R mutant showed no enrichment for CLRs (*121*). In the CAF-1/Hir1 study, CENP-A^{Cse4} was found to mislocalize to -1 and +1 nucleosomes at promoters and to be depleted from intragenic regions in a *cac1*Δ *hir1*Δ double mutant (*63*).

In *D. melanogaster*, overexpressed CENP-A^{CID} becomes mislocalized to regions near telomeres and pericentric heterochromatin, particularly to silent intergenic regions on heterochromatin boundaries (*124, 125*). Fission yeast show a similar mislocalization pattern in the absence of FACT, where CENP-A^{Cnp1} becomes mislocalized to pericentric regions, and is excluded from highly transcribed genes (*99*). In addition, overexpression of CENP-A^{Cnp1} leads to

incorporation at telomeric repeats, near rDNA, and at pericentric regions (*126*). When the endogenous centromere is deleted from a chromosome, CENP-A^{Cnp1} forms stable neocentromeres only at regions of low H2A.Z^{Htz1}, including pericentric and subtelomeric regions (*127*). Overexpression of human CENP-A in HeLa cells results in mislocalization to active promoters and enhancers, transcription factor binding sites, and CTCF binding sites (*120*). Overall, mislocalized CENP-A is enriched at nucleosomes with higher turnover, such as those containing H2A.Z and H3.3 (*120*). CENP-A is also recruited to sites of double strand breaks in human cells (*128*). While many studies have investigated the localization of CENP-A in different organisms, none had tested the genome-wide localization pattern in the absence of proteolysis before this work.

1.2.5 *Consequences of mislocalization of the centromeric nucleosome*

In budding yeast, cells die when CENP-A^{Cse4} is overexpressed in the absence of Psh1, and this is correlated with mislocalization to the euchromatin (*43, 44*). The mechanism of death in this condition is currently unknown. One possibility is that the mislocalized CENP-A^{Cse4} could be recruiting other kinetochore proteins, leading to chromosome missegregation or chromosome breaks due to multicentric chromosomes. This is supported by work in other organisms, as mislocalization of CENP-A^{CID} is sufficient to form ectopic kinetochores in *D. melanogaster* (*124, 125*). In budding yeast, a ChIP-seq study identified regions of ectopic kinetochore protein binding with mislocalized CENP-A^{Cse4}. While the level of binding was much lower than at the endogenous centromeres, this can not be formally ruled out as a mechanism of cell death (*121*). Chromosome spread assays do not show any increase in other kinetochore protein mislocalization when CENP-A^{Cse4} is mislocalized, however this could be hard to detect due to

clustering of functional kinetochores (*78*). Alternatively, extra CENP-A^{Cse4} could be pulling kinetochore proteins away from the endogenous centromeres, leading to death due to a lack of kinetochore proteins at the centromeres. Another possibility is that replacing H3 with CENP-A^{Cse4} at euchromatic nucleosomes could lead to problems with interphase chromatin functions such as transcription or DNA replication. A study in human cells found a slight change in transcription with CENP-A mislocalization, but until my work, this had not been tested in budding yeast (*120*). Understanding the mechanism of the cell death associated with mislocalized CENP-A^{Cse4} may be useful for understanding the development and potential treatment of some human cancers, as there are cancer cell lines with increased CENP-A levels and ectopic localization, although it is not yet known if this is a causal factor in cancer development (*120, 129*).

1.3 Research Questions

1.3.1 *Where in the genome does mislocalized CENP-A^{Cse4} accumulate?*

In Chapter 2, I first address the question of where CENP-A^{Cse4} becomes mislocalized in the absence of Psh1 mediated proteolysis using a genomics approach. I performed ChIP-seq on Flag epitope tagged CENP-A^{Cse4} from WT or *psh1*Δ budding yeast cells, with or without CENP-A^{Cse4} overexpression. Using a combination of custom R scripts and published software packages to analyze the ChIP-seq data, I found that CENP-A^{Cse4} is mislocalized to promoter nucleosomes in *psh1*Δ with overexpressed CENP-A^{Cse4}. Additionally, mislocalized CENP-A^{Cse4} is found at nucleosomes that contain the histone variant H2A.Z^{Htz1} in WT cells. I also explore the impact of transcription level and direction on CENP-A^{Cse4} mislocalization.

1.3.2 *What additional chromatin-based mechanisms regulate ectopic CENP-A^{Cse4}?*

Using the CENP-A^{Cse4} mislocalization data from the ChIP-seq experiment described above, I investigated whether the regions of observed CENP-A^{Cse4} mislocalization were important for understanding the mechanism of its mislocalization. Since CENP-A^{Cse4} mislocalized to H2A.Z^{Htz1} containing nucleosomes, I was curious if H2A.Z^{Htz1} or the chromatin remodeling complexes that normally act on H2A.Z^{Htz1} had any effect on CENP-A^{Cse4} mislocalization. I found that while H2A.Z^{Htz1} was not required for mislocalization of CENP-A^{Cse4} to promoters, INO80-C, which normally removes H2A.Z^{Htz1} from nucleosomes, was partially responsible for CENP-A^{Cse4} mislocalization to euchromatin. In a deletion mutant of the INO80-C subunit *NHP10*, growth of overexpressed CENP-A^{Cse4} with *psh1*Δ was partially rescued and there was a decrease in the mislocalization to euchromatin.

1.3.3 *What are the consequences of CENP-A^{Cse4} mislocalization?*

The pattern of CENP-A^{Cse4} mislocalization to promoter nucleosomes in *psh1*Δ with overexpressed CENP-A^{Cse4} made me curious about the effect of CENP-A^{Cse4} on transcription. To test if mislocalization of the centromeric histone variant to promoters disrupted transcription of downstream genes, I performed RNA-seq from WT, *psh1*Δ, overexpressed CENP-A^{Cse4} and *psh1*Δ with overexpressed CENP-A^{Cse4} strains. I found that almost 300 genes were misregulated in the *psh1*Δ with overexpressed CENP-A^{Cse4} strain, with almost no changes in the other strains. This suggests that mislocalization of CENP-A^{Cse4} to promoters may cause misregulation of transcription of a subset of genes. These changes in transcription may be responsible for the observed cell death, either alone or along with other unknown factors.

1.3.4 *Do other histone proteins contribute to CENP-A^{Cse4} localization?*

In Chapter 3, I investigate whether other histone proteins contribute to controlling CENP-A^{Cse4} localization. This work was done in collaboration with Gary Deyter with help from Adrienne Barber. To start this project, we performed a genetic screen of overexpressed CENP-A^{Cse4} in an H4 mutant library, and found that H4-R36A is sensitive to overexpression of CENP-A^{Cse4}, and that CENP-A^{Cse4} becomes stabilized and mislocalized to the euchromatin in this mutant. As H4-R36A has been published to affect the localization of FACT, which is important for CENP-A^{Cse4} degradation by Psh1, we tested whether there was a change in the Psh1-CENP-A^{Cse4} interaction in this mutant (*118, 130*). We found that the Psh1-CENP-A^{Cse4} interaction was decreased, and that Psh1 was mislocalized to 3' ends of genes, likely contributing to the mislocalization of CENP-A^{Cse4} in the H4-R36A strain.

Chapter 2. REGULATION OF BUDDING YEAST CENP-A LEVELS PREVENTS MISINCORPORATION AT PROMOTER NUCLEOSOMES AND TRANSCRIPTIONAL DEFECTS

*Modified from an article of the same title published in PLoS Genetics (*131*)

(Running title: Mislocalization of CENP-A^{Cse4} affects transcription)

Erica M Hildebrand[1,2], and Sue Biggins[1*]

[1]Howard Hughes Medical Institute, Division of Basic Sciences, Fred Hutchinson Cancer Research Center, Seattle, Washington, United States of America

[2]Molecular and Cellular Biology Program, University of Washington, Seattle, Washington, United States of America

*Corresponding author

E-mail: sbiggins@fredhutch.org (SB)

2.1 SUMMARY

The exclusive localization of the histone H3 variant CENP-A to centromeres is essential for accurate chromosome segregation. Ubiquitin-mediated proteolysis helps to ensure that CENP-A does not mislocalize to euchromatin, which can lead to genomic instability. Consistent with this, overexpression of the budding yeast CENP-A^{Cse4} is lethal in cells lacking Psh1, the E3 ubiquitin ligase that targets CENP-A^{Cse4} for degradation. To identify additional mechanisms that prevent CENP-A^{Cse4} misincorporation and lethality, we analyzed the genome-wide mislocalization pattern of overexpressed CENP-A^{Cse4} in the presence and absence of Psh1 by chromatin immunoprecipitation followed by high throughput sequencing. We found that ectopic CENP-A^{Cse4} is enriched at promoters that contain histone H2A.Z^{Htz1} nucleosomes, but that H2A.Z^{Htz1} is not required for CENP-A^{Cse4} mislocalization. Instead, the INO80 complex, which removes H2A.Z^{Htz1} from nucleosomes, promotes the ectopic deposition of CENP-A^{Cse4}. Transcriptional profiling revealed gene expression changes in the *psh1*Δ cells overexpressing CENP-A^{Cse4}. The down-regulated genes are enriched for CENP-A^{Cse4} mislocalization to promoters, while the up-regulated genes correlate with those that are also transcriptionally up-regulated in an *htz1*Δ strain. Together, these data show that regulating centromeric nucleosome localization is not only critical for maintaining centromere function, but also for ensuring accurate promoter function and transcriptional regulation.

2.2 INTRODUCTION

The eukaryotic genome is packaged into chromatin, which consists of 147 bp repeating units of DNA wrapped around histone proteins to form nucleosomes (*3*). Chromatin is important not only for packaging and protecting DNA, but also for regulating access to genes and other DNA

elements by nuclear proteins involved in processes such as transcription, replication, and chromosome segregation. Most nucleosomes are composed of the canonical histone proteins, H2A, H2B, H3, and H4 (*2*). However, the behavior and functions of nucleosomes can be altered both by chemically modifying canonical histones through post-translational modifications and by exchanging canonical histones for histone variants that alter nucleosome composition (*2*). For example, H2A.Z is a variant of histone H2A and is found at promoter nucleosomes genome-wide where it regulates transcription (*2, 21, 132*). In contrast, the conserved CENP-A variant (also called CenH3) replaces H3 in nucleosomes exclusively at the centromere where it regulates chromosome segregation (*29, 37, 133*). Because changes in nucleosome composition can have a major impact on the underlying functions of the genome, it is critical to understand the mechanisms that control the localization of histone modifications and variants.

The genomic incorporation of the budding yeast H2A.Z^{Htz1} (SGD ID: S000005372) histone variant is regulated by the SWR1 (SWR-C) and INO80 (INO80-C) chromatin remodeling complexes (*134*). H2A.Z^{Htz1} localizes to intergenic regions, specifically near transcription start sites (TSS) at the +1 and -1 nucleosomes surrounding nucleosome-depleted regions (NDRs) (*21-23, 132, 135, 136*). In budding yeast, H2A.Z^{Htz1} nucleosomes are correlated with high nucleosome turnover (*28*), which is proposed to assist transcriptional initiation or rapid changes between transcriptional states (*27, 137, 138*). SWR-C incorporates H2A.Z^{Htz1} into nucleosomes by exchanging H2A-H2B dimers for H2A.Z^{Htz1}-H2B dimers (*54, 60, 139*). In contrast, the mechanism of H2A.Z^{Htz1} removal from nucleosomes by INO80-C is less well understood because it has two reported activities that both lead to H2A.Z^{Htz1} exchange, either by swapping H2A.Z^{Htz1}-H2B dimers for H2A-H2B dimers (*59*) or by promoting turnover of the entire nucleosome (*60, 134*).

The localization of the CENP-A variant is regulated by the histone chaperone HJURP (Scm3 in budding yeast), which is targeted specifically to centromeres (*38-41, 140*). Centromeric sequence and size are highly variable throughout eukaryotes and can be specified by either an underlying sequence or through epigenetic inheritance (*68, 141*). Despite the diversity of centromeres, CENP-A is a conserved hallmark of all centromeres. The presence of CENP-A directs the formation of the kinetochore, a large protein complex that mediates attachments between the microtubules of the mitotic spindle and the chromosome during cell division (*32, 68, 142*). CENP-A mislocalization to euchromatin through overexpression or tethering can lead to ectopic kinetochore formation and genomic instability (*124, 143, 144*). However, CENP-A mislocalization has not been reported to disrupt other genomic processes (*120, 145*).

Multiple mechanisms ensure that CENP-A does not mislocalize to euchromatin. A number of chromatin remodelers and histone chaperones are reported to help maintain centromeric chromatin or prevent CENP-A mislocalization, including Fun30, RSC, INO80-C, CAF-1, HIR, FACT, and RbAp48 and SWI/SNF (*63, 96, 97, 99, 117, 119, 146*). In addition, ubiquitin-mediated proteolysis prevents ectopic CENP-A localization by controlling total CENP-A protein levels (*42, 111, 114, 116*). In budding yeast, proteolysis of CENP-A^{Cse4} (SGD ID: S000001532) is mediated by an E3 ubiquitin ligase called Psh1 (SGD ID: S000005415) (*43, 44*). When CENP-A^{Cse4} is overexpressed in the absence of Psh1-mediated proteolysis (*42-44, 147*), cells accumulate high levels of CENP-A^{Cse4} in euchromatin. This also results in lethality, although the underlying cause has not been determined (*42-44*).

Similar to CENP-A, H2A.Z also contributes to chromosome segregation. In human cells, H2A.Z is found at pericentric regions, where it is incorporated at the inner centromere between the CENP-A nucleosome domains, and helps to establish centromeric heterochromatin (*148,*

149). Similarly, H2A.Z^{Htz1} is also a component of pericentric chromatin in budding yeast, where it localizes to nucleosomes flanking the CENP-A^{Cse4} nucleosome and is important for chromosome segregation through unknown mechanisms (*21, 150, 151*). However, it is unclear whether there is a connection between the localization of the histone variants. In human cells, overexpressed CENP-A was found to mislocalize to regions enriched for H2A.Z, although no physical interaction was detected between these two histone variants (*120*). In contrast, studies in *S. pombe* have shown that CENP-A^{Cnp1} tends to mislocalize to ectopic regions that are depleted of H2A.Z^{Htz1} (*127*).

We set out to determine whether there are features of euchromatin that normally prevent budding yeast CENP-A misincorporation as well as to identify the functional consequences of CENP-A mislocalization to euchromatin. The identification of euchromatic sites that strongly misincorporate CENP-A may also shed light on the underlying cause of the lethality. To address these questions, we performed the first genome-wide analysis of CENP-A overexpression in the absence of ubiquitin-mediated degradation. We found that overexpressed CENP-A^{Cse4} mislocalizes to promoters that are enriched for NDRs flanked by H2A.Z^{Htz1}, and this mislocalization is dramatically enhanced in cells that cannot degrade CENP-A^{Cse4}. This localization pattern appears to be due in part to co-opting of INO80-C to incorporate excess CENP-A^{Cse4} into promoter nucleosomes that normally contain H2A.Z^{Htz1}. Consistent with this, there was a significant correlation between transcripts that were misregulated in cells lacking H2A.Z^{Htz1} and those with high levels of CENP-A^{Cse4} mislocalization. We also found that a subset of promoters that misincorporate CENP-A^{Cse4} have decreased transcription, which may be the underlying cause of lethality. Together, these data suggest that it is essential that cells regulate

CENP-A^{Cse4} localization not only to ensure proper chromosome segregation, but also to protect cells from promoter nucleosome disruption and transcriptional misregulation.

2.3 RESULTS

2.3.1 *Excess CENP-A^{Cse4} mislocalizes to intergenic regions of the genome*

To identify the precise genomic sites of CENP-A^{Cse4} mislocalization in budding yeast, we performed ChIP-seq on endogenous and overexpressed CENP-A^{Cse4} in the presence and absence of Psh1-mediated proteolysis. All strains contained a fully functional ectopic *3Flag-CSE4* gene integrated at the *URA3* locus under the endogenous promoter and were deleted for the endogenous *CSE4* gene. Cells overexpressing CENP-A^{Cse4} contained an additional copy under the control of the *GAL* promoter (*pGAL-3Flag-CSE4*). As seen previously, CENP-A^{Cse4} overexpression inhibited the growth of WT cells and resulted in lethality in *psh1*Δ cells (**Supplemental Figure 2.1A**) (*43, 44*). The growth inhibition correlated with the total amount of chromatin-bound CENP-A^{Cse4} protein (**Figure 2.1.A, Supplemental Figure 2.1B**).

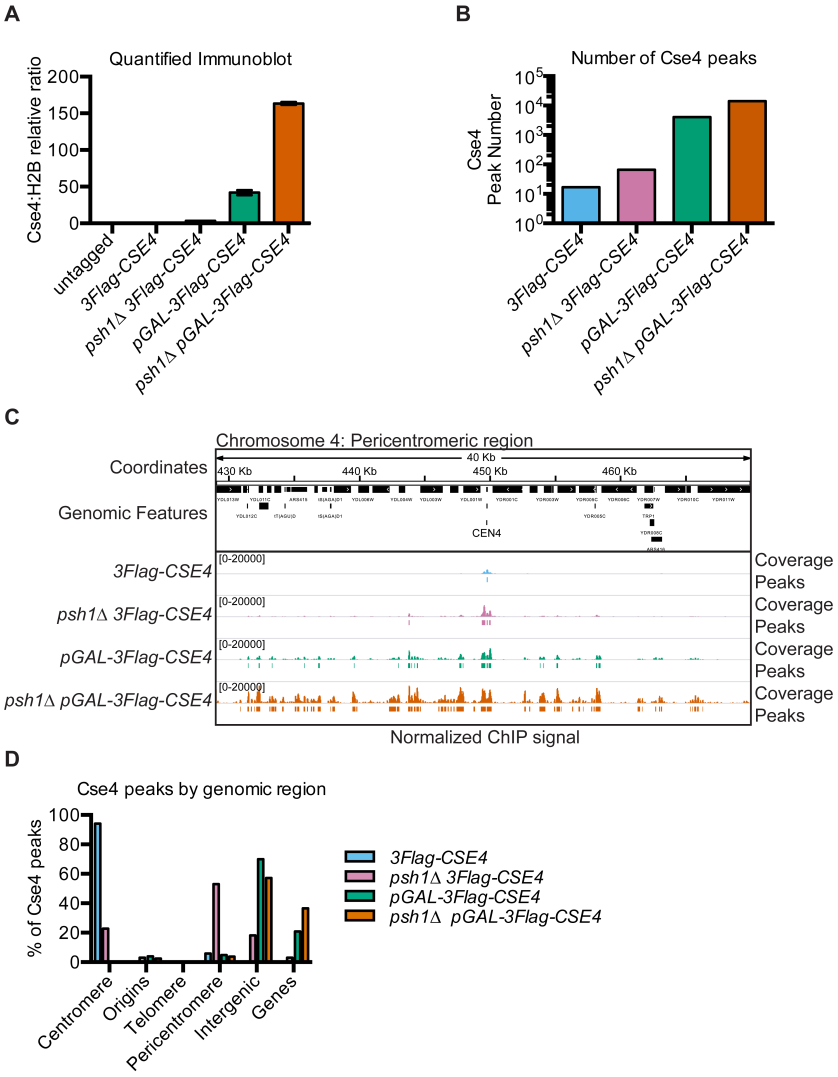

Figure 2.1. Intergenic regions are the major sites of overexpressed CENP-A^{Cse4} mislocalization.
(A) Quantification of CENP-A^{Cse4} levels in MNase-digested chromatin in untagged (SBY3, black), *3Flag-CSE4* (SBY10419, blue), *psh1Δ 3Flag-CSE4* (SBY10484, pink), *pGAL-3Flag-CSE4* (SBY10425, green) and *psh1Δ pGAL-3Flag-Cse4* (SBY10483, orange) strains. The ratio of CENP-A^{Cse4}:H2B in the chromatin in each strain was quantified relative to the CENP-A^{Cse4}:H2B ratio from the *3Flag-CSE4* (SBY10419) strain. Quantification is based on two biological replicates. Error bars are +/- 1 standard error of the mean (SEM) of the two biological replicates. (B) The total number of CENP-A^{Cse4} peaks called in the indicated strains: *3Flag-CSE4* (SBY10419, blue), *psh1Δ 3Flag-CSE4* (SBY10484, pink), *pGAL-3Flag-CSE4* (SBY10425, green) and *psh1Δ pGAL-3Flag-CSE4* (SBY10483, orange). (C) A representative region of the CENP-A^{Cse4} ChIP-seq coverage on Chromosome 4 between 429,000 base pairs (bp) and 470,000 bp is shown. The CENP-A^{Cse4} ChIP-seq coverage for the strains in (B) is normalized to the coverage at the centromeres after subtracting the input. Peaks are shown as lines below each coverage signal (the cutoff is the average minimum coverage at the centromere in the *3Flag-CSE4* strain). The scale of the normalized coverage is from 0-20,000 for all strains. (D) The percentage of CENP-A^{Cse4} peak centers in each type of genomic region is graphed for each strain, as in (B). The percentage of each feature in the genome is: genes (68.23%), intergenic (27.04%), pericentromeres (2.62%), telomeres (1.16%), origins (0.92%) and centromeres (0.02%).

To analyze CENP-A^{Cse4} localization, cells were crosslinked with formaldehyde and the chromatin was isolated and subsequently digested with Micrococcal nuclease (MNase), which cuts linker DNA between nucleosomes. The CENP-A^{Cse4} nucleosomes were purified from the MNase-treated chromatin by immunoprecipitation of 3Flag-Cse4. The amount of CENP-A^{Cse4} recovered in the ChIP samples reflected the starting levels in the chromatin (**Supplemental Figure 2.1C**). The input samples (MNase-digested chromatin) and ChIP samples (3Flag-Cse4-bound chromatin after immunoprecipitation) were made into paired-end sequencing libraries using a modified Solexa library preparation protocol that captures DNA particles down to ~25 bp (**Supplemental Figure 2.1D**) (*88, 152*). Paired-end sequencing resulted in greater than 1.5 million reads/sample, with an average read length ranging from 147-164 bp (**Supplemental Table 2.1**). The mononucleosome-sized sequencing reads from the input and ChIP samples for each strain were mapped to the *S. cerevisiae* reference genome version *SacCer3* (*153*).

The peaks of CENP-A^{Cse4} enrichment genome-wide correlated with the levels of chromatin-bound CENP-A^{Cse4} (**Figure 2.1B**, **Table 2.1**). Seventeen peaks were identified for the *3Flag-CSE4* strain, representing the sixteen centromeres as well as a peak 150 bp from *CEN9*. A small amount of CENP-A^{Cse4} mislocalization was seen starting in the *psh1*Δ strain with 66 peaks, and was further increased in cells overexpressing CENP-A^{Cse4} with 4043 peaks. The greatest enrichment in the euchromatin was detected in the *psh1*Δ cells overexpressing CENP-A^{Cse4} with 14,199 peaks. An example of the coverage data and corresponding peaks for a representative region around Centromere 4 shows a single centromere peak for the WT strain and additional peaks around the centromere in the other strains (**Figure 2.1C**). The increased CENP-A^{Cse4} mislocalization in surrounding euchromatin is especially apparent in the *pGAL-3Flag-CSE4* and *psh1*Δ *pGAL-3Flag-CSE4* strains that have the highest levels of CENP-A^{Cse4}. We independently

confirmed the CENP-A^{Cse4} enrichment at *CEN4* and at other representative peaks by ChIP-qPCR (**Supplemental Figure 2.2A**). Our initial analysis also identified a CENP-A^{Cse4} peak at the rDNA locus in all strains. This did not show significant enrichment in the *3Flag-CSE4* strain by ChIP-qPCR but did in the cells with overexpressed CENP-A^{Cse4}, similar to previously reported data (*44, 154*) (**Supplemental Figure 2.2A**). However, due to the difficulty in analyzing this repetitive region by standard mapping algorithms, ChIP coverage of this region was excluded from further computational analyses.

Table 2.1. CENP-A^{Cse4} peak information

Strain	Peak calling threshold	Average coverage (rDNA removed)	Number of Peaks	Number (and %) of genes with Cse4 peaks in promoter	Number (and %) of genes with Cse4 peaks in 3' end
3Flag-CSE4 (SBY10419)	3263	15.3	17	7 (0.106%)	15 (0.228%)
psh1Δ 3Flag-CSE4 (SBY10484)	3263	122	66	21 (0.319%)	37 (0.563%)
pGAL-3Flag-CSE4 (SBY10425)	3263	387	4043	3058 (46.5%)	2638 (40.1%)
psh1Δ pGAL-3Flag-CSE4 (SBY10483)	3263	1696	14199	5921 (90.0%)	5175 (78.7%)

To determine if mislocalized CENP-A^{Cse4} favors certain genomic regions, we analyzed the percentage of CENP-A^{Cse4} peaks in various functional regions of the genome, including centromeres, pericentromeres, telomeres, replication origins, genes, and intergenic regions (**Figure 2.1D**). We defined pericentromeres as 20 Kilobases (Kb) flanking each centromere, consistent with the 20-50 Kb size of cohesin enrichment around each centromere in budding yeast (*155, 156*). As expected, the majority of CENP-A^{Cse4} peaks in WT cells were at centromeres, with an increase in pericentric peaks in the *psh1*Δ mutant. However, the majority of

peaks in the strains overexpressing CENP-A^{Cse4} were in the intergenic regions, with a smaller percentage within genes. As intergenic regions make up less than 30% of the entire genome, these data indicate a strong enrichment of CENP-A^{Cse4} in intergenic regions in cells overexpressing CENP-A^{Cse4}.

We next asked whether the intergenic enrichment correlates with features known to be associated with centromeres. ChIP-seq of mildly overexpressed CENP-A^{Cse4} previously identified 23 centromere-like regions (CLRs) on chromosome arms that are enriched for mislocalized CENP-A^{Cse4} and other kinetochore proteins (*121*). These CLRs share characteristics with centromeric sequences such as having a high AT% and conferring stability to plasmid DNA. As expected, most of the CLRs have CENP-A^{Cse4} peaks in the *psh1*Δ *pGAL-3Flag-CSE4* strain (**Supplemental Figure 2.2B**). However, CENP-A^{Cse4} was overexpressed to much higher levels in our study (150-fold compared to 3-fold), so the CLRs are a small fraction of the total peaks. Consistent with this, there was also enrichment in low confidence negative control regions (LCNCRs), indicating there is no preference for CLR localization. We also analyzed the AT content of the DNA bound by mislocalized CENP-A^{Cse4}, as this is a defining characteristic of centromeric DNA in budding yeast. As expected, CENP-A^{Cse4} peaks were highly enriched for AT nucleotides in the WT strain. However there was only a moderate increase in AT% in the *psh1*Δ strain compared to the input nucleosomes, and almost no AT bias in the strains with overexpressed CENP-A^{Cse4} (**Supplemental Figure 2.2C-F**). Together, these data indicate that the mislocalization of CENP-A^{Cse4} is due to a more widespread effect than just centromere-like characteristics.

2.3.2 *Mislocalized CENP-A^{Cse4} is enriched in promoters but is not correlated with basal transcription levels*

We next asked whether the intergenic enrichment of overexpressed CENP-A^{Cse4} was specific to either promoters (defined as 500 bp upstream of the transcription start site (TSS)) or transcription terminators (defined as 500 bp downstream of the transcription termination site (TTS)) by calculating the number of these regions with CENP-A^{Cse4} peaks (**Table 2.1**). CENP-A^{Cse4} was enriched in both regions when overexpressed, so we more precisely analyzed the pattern by plotting the average coverage in 10 bp windows for regions 500 bp upstream and downstream of all TSS or TTS (the TSS or TTS is plotted at position 0 based on previously reported RNA-seq transcription start positions (*157*)). In the *psh1*Δ cells overexpressing CENP-A^{Cse4}, there was enrichment -200 bp from the TSS and directly over the TSS, which correspond to the -1 and +1 nucleosomes respectively (**Figure 2.2A**). At the TTS, CENP-A^{Cse4} was enriched in the nucleosome just after the termination site, and was shifted slightly into the NDR compared to the WT nucleosomes. Although the level of CENP-A^{Cse4} enrichment in the other three strains was much lower overall, the trend is similar in the cells with increased CENP-A^{Cse4}. This pattern is reminiscent of the pattern of CENP-A^{Cse4} mislocalization upon deletion of *CAC1* and *HIR1*, which leads to ectopic CENP-A^{Cse4} enrichment at promoters in the presence of Psh1 (*63*).

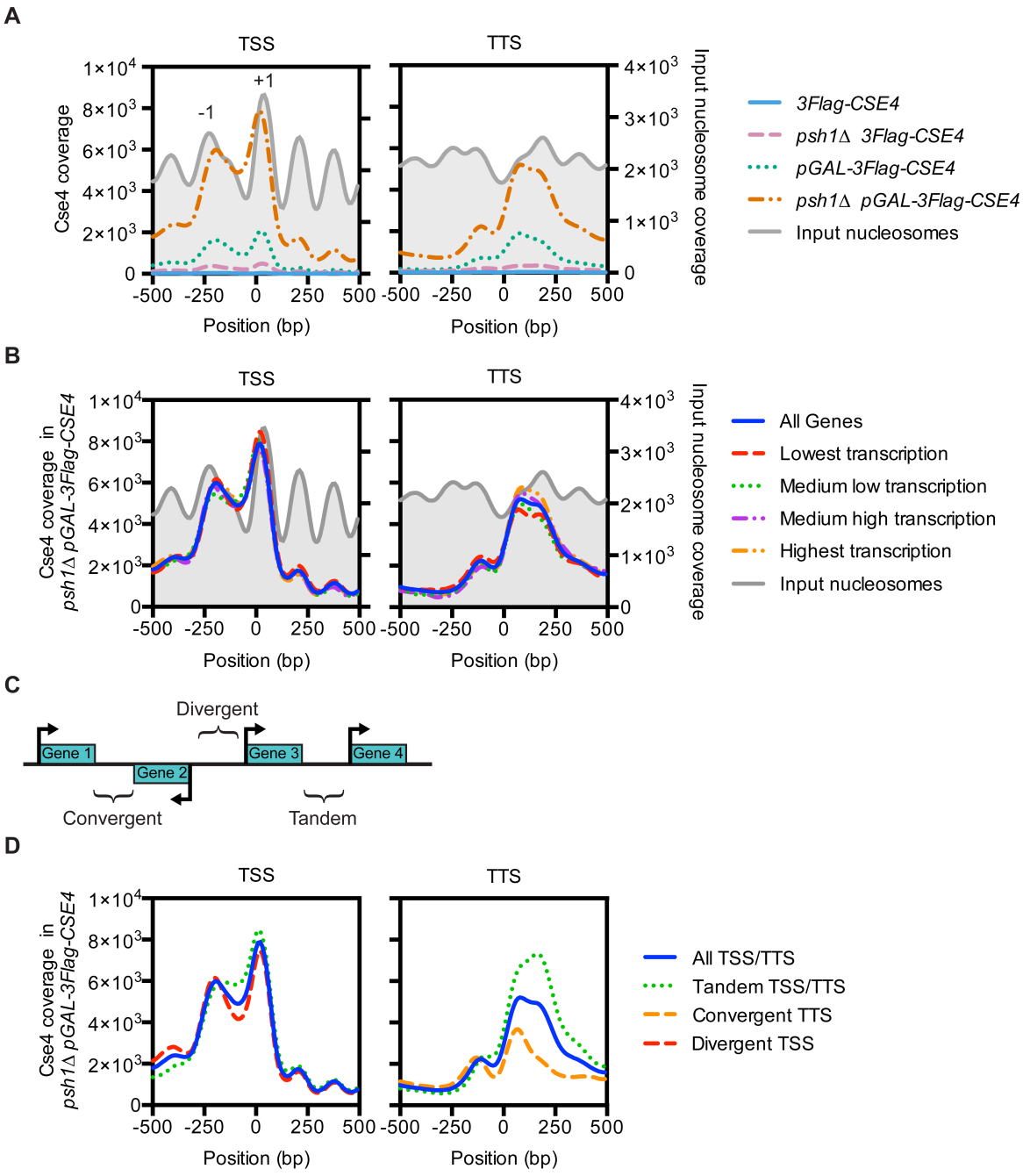

Figure 2.2. Overexpressed CENP-A^{Cse4} mislocalizes to promoters
(A) Mean CENP-A^{Cse4} ChIP coverage 500 bp upstream and downstream of all transcription start sites (TSS) or transcription termination sites (TTS), for *3Flag-CSE4* (SBY10419, blue), *psh1Δ 3Flag-CSE4* (SBY10484, pink), *pGAL-3Flag-Cse4* (SBY10425, green) and *psh1Δ pGAL-3Flag-Cse4* (SBY10483, orange). The input nucleosome positions are from the input MNase-seq data from the *3Flag-CSE4* strain (SBY10419) and are plotted in grey. (B) Mean CENP-A^{Cse4} ChIP coverage for the *psh1Δ pGAL-3Flag-CSE4* (SBY10483) strain separated by transcription levels of the corresponding genes (*158*). (C) Diagram of the classification of the different types of intergenic regions based on the direction of transcription of the flanking genes. (D) Mean CENP-A^{Cse4} ChIP coverage for the *psh1Δ pGAL-3Flag-CSE4* strain (SBY10483) separated by the direction of transcription for the corresponding TSS or TTS.

We next asked whether the accumulation of CENP-A^{Cse4} in promoters and terminators is associated with the basal level of transcription in WT cells. We plotted CENP-A^{Cse4} enrichment at the TSS and TTS of genes binned into quartiles by the published transcription levels in a WT strain, ranked from lowest transcription to highest transcription (*158*). However, there was no correlation between CENP-A^{Cse4} enrichment and the different transcription levels (**Figure 2.2B**, **Supplemental Figure 2.3**). Therefore, the CENP-A^{Cse4} localization to promoters in the *psh1*Δ *pGAL-3Flag-CSE4* strain was not an artifact of increased chromatin accessibility in areas of high transcription, such as was found in the previously reported CENP-A^{Cse4} ChIP-seq for slightly overexpressed or hypomorphic CENP-A^{Cse4} (*123*). We also analyzed whether CENP-A^{Cse4} mislocalization correlated with the direction of transcription of the surrounding genes, since this has been shown for cohesin localization, which is specifically enriched in convergent intergenic regions outside of the pericentromere (*155, 159*). We classified the intergenic regions as tandem (between two genes transcribed in the same direction), convergent (between two genes transcribed towards each other), or divergent (between two genes transcribed away from each other) (**Figure 2.2C**). In promoters, CENP-A^{Cse4} was enriched at the tandem and divergent genes (**Figure 2.2D**, **Supplemental Figure 2.4**). At the terminators, CENP-A^{Cse4} was enriched at the tandem TTS and depleted at the convergent TTS. Because convergent regions lack promoters, these data are consistent with the enrichment of CENP-A^{Cse4} to promoter regions.

2.3.3 *Mislocalized CENP-A^{Cse4} is found at H2A.Z^{Htz1}-enriched nucleosomes flanking NDRs*

Since CENP-A^{Cse4} mislocalization to promoters was not correlated with transcription levels, we looked for another chromatin feature specific to promoters that might enhance CENP-A^{Cse4} incorporation. One characteristic of promoters that is less commonly found at the 3' ends of

genes is the NDR between the -1 and +1 nucleosomes at the TSS (*160*). We therefore compared CENP-A^{Cse4} profiles centered on all NDRs and found a strong CENP-A^{Cse4} enrichment in the nucleosomes flanking the NDRs in the *psh1*Δ *pGAL-3Flag-CSE4* strain (**Figure 2.3A**). Because NDRs vary in length up to 557 bp, we asked whether there was a specific NDR length that correlated with CENP-A^{Cse4} mislocalization and found the highest enrichment in NDRs longer than 65 bp (**Figure 2.3B**). We obtained similar results when the analysis was centered on the TSS instead of the NDR, consistent with the enrichment of CENP-A^{Cse4} in NDR containing promoters (**Supplemental Figure 2.5A-D**).

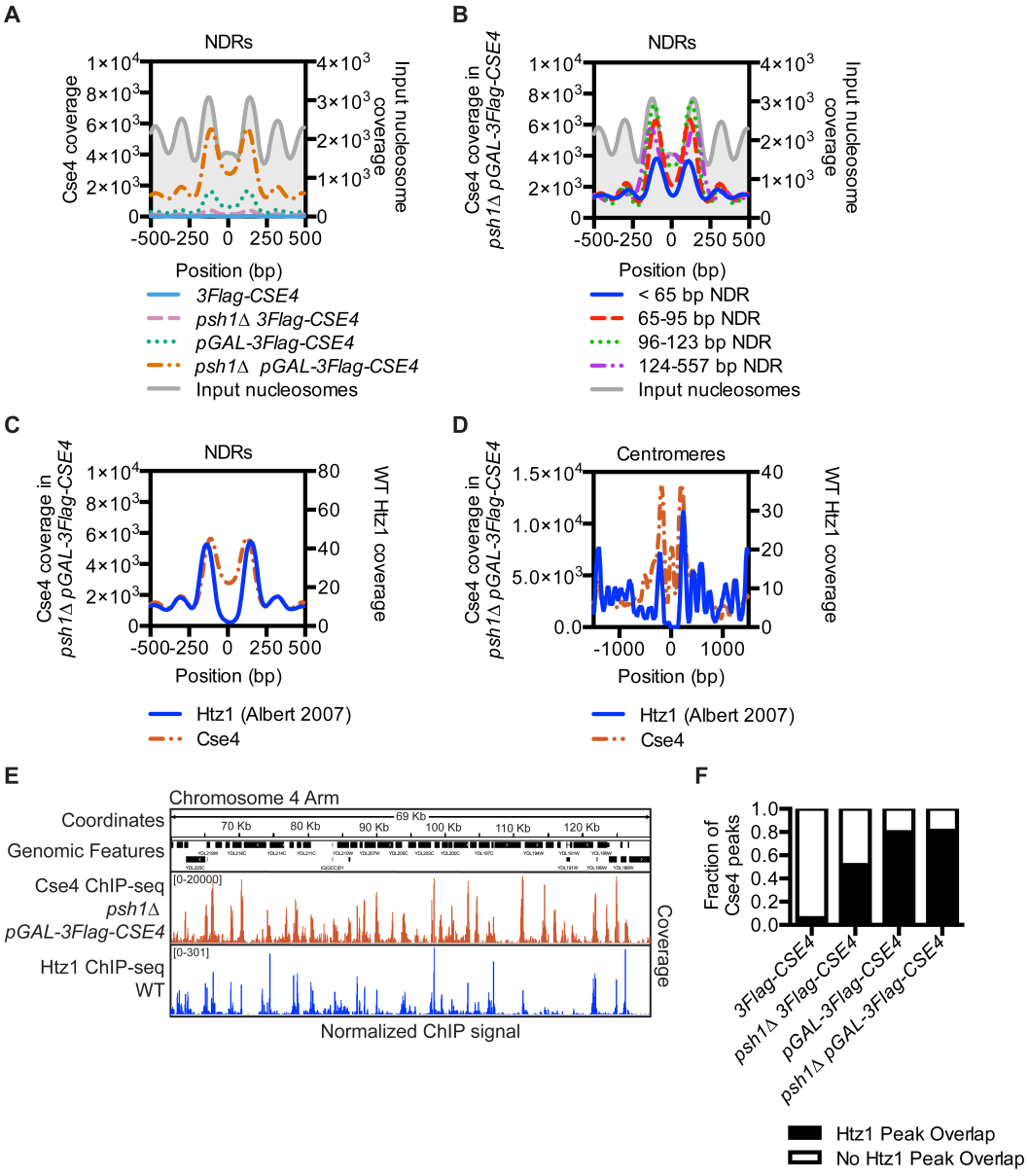

Figure 2.3. CENP-A^{Cse4} mislocalizes to regions that are enriched for the histone variant H2A.Z^{Htz1}. (A) Mean CENP-A^{Cse4} ChIP coverage for the *3Flag-CSE4* (SBY10419, blue), *psh1Δ 3Flag-CSE4* (SBY10484, pink), *pGAL-3Flag-CSE4* (SBY10425, green) and *psh1Δ pGAL-3Flag-CSE4* (SBY10483, orange) strains centered on annotated NDRs (*160*). (B) Mean CENP-A^{Cse4} ChIP coverage for the *psh1Δ pGAL-3Flag-CSE4* (SBY10483) strain centered on annotated NDRs, binned by NDR length (*160*). (C) Mean CENP-A^{Cse4} ChIP coverage for the *psh1Δ pGAL-3Flag-CSE4* (SBY10483, orange) strain (left y axis) vs. mean H2A.Z^{Htz1} ChIP coverage (*21*) (blue) (right y axis) at all NDRs. (D) Mean CENP-A^{Cse4} ChIP coverage for the *psh1Δ pGAL-3Flag-CSE4* (SBY10483, orange) strain (left y axis) vs. mean normalized H2A.Z^{Htz1} ChIP coverage (*21*) (blue) (right y axis) at all centromeres. (E) CENP-A^{Cse4} ChIP coverage for the *psh1Δ pGAL-3Flag-CSE4* (SBY10483, orange) strain and WT H2A.Z^{Htz1} coverage (*21*) (blue) on the chromosome 4 arm between 60,000 bp and 130,000 bp. The scale of the normalized coverage is from 0-20,000 for the CENP-A^{Cse4} ChIP-seq and from 0-301 for the H2A.Z^{Htz1} ChIP-seq. (F) Overlap between CENP-A^{Cse4} peaks in *3Flag-CSE4* (SBY10419), *psh1Δ 3Flag-CSE4* (SBY10484), *pGAL-3Flag-CSE4* (SBY10425) or *psh1Δ pGAL-3Flag-CSE4* (SBY10483) compared to WT H2A.Z^{Htz1} nucleosomes (*21*).

The localization of CENP-A^{Cse4} to the nucleosomes flanking the NDRs is similar to H2A.Z^{Htz1}, the only other histone variant in budding yeast (*21*). In addition, the SWR-C chromatin-remodeling complex that incorporates H2A.Z^{Htz1} preferentially binds to NDRs greater than 50 bp (*58*), similar to the length of NDRs that have the highest CENP-A^{Cse4} enrichment (greater than 65 bp) (**Figure 2.3B**). We therefore investigated the relationship between previously reported H2A.Z^{Htz1} localization (*21*) and the mislocalization of overexpressed CENP-A^{Cse4} in *psh1*Δ cells. There was a striking similarity in their enrichment at NDRs (**Figure 2.3C**), as well as a similar trend of co-enrichment in the nucleosomes flanking replication origins (**Supplemental Figure 2.5E, F**) and centromeres (**Figure 2.3D, Supplemental Figure 2.5G**). The CENP-A^{Cse4} coverage at the TSS was also similar to H2A.Z^{Htz1} coverage, while at the TTS CENP-A^{Cse4} was shifted more into the 3' NDR than H2A.Z^{Htz1} (**Supplemental Figure 2.6A, B**). The histone variants exhibited a genome-wide trend to co-localize, as seen in a representative region of the arm of Chromosome 4 (**Figure 2.3E, Supplemental Figure 2.6C**). There was a high coincidence of overlap between CENP-A^{Cse4} peaks in the experimental strains with H2A.Z^{Htz1} peaks in WT cells, although they were not specifically enriched in any of the genomic features correlated with CENP-A^{Cse4} mislocalization (**Figure 2.3F, Supplemental Figure 2.6D, E**). Together, these data indicate a significant enrichment of misincorporated CENP-A^{Cse4} at sites where H2A.Z^{Htz1} nucleosomes are normally located genome-wide in *psh1*Δ cells overexpressing CENP-A^{Cse4}.

2.3.4 *CENP-A^{Cse4} accumulation in chromatin does not depend on H2A.Z^{Htz1}*

The co-localization of the histone variants led us to further analyze their relationship. First, we tested whether H2A.Z^{Htz1} promotes CENP-A^{Cse4} localization by performing ChIP on WT, *psh1*Δ, and *psh1*Δ *htz1*Δ cells overexpressing CENP-A^{Cse4}. *htz1*Δ cells are defective in induction from

the *GAL* promoter (*161*), so we used a tetracycline promoter to control *CSE4* levels. Overexpressed CENP-A^{Cse4} bound to promoter regions in the *psh1*Δ *htz1*Δ double mutant, at levels similar to or even higher than the *psh1*Δ strain (**Figure 2.4A**). These data indicate that H2A.Z^{Htz1} is not required for CENP-A^{Cse4} mislocalization, so we next asked whether the H2A.Z^{Htz1} incorporation machinery is involved. Swr1 (SGD ID: S000002742) is the Swi/Snf family ATPase in SWR-C that deposits H2A.Z^{Htz1} into nucleosomes (*22, 55, 60*), so we measured the levels of chromatin-bound CENP-A^{Cse4} in *swr1*Δ cells. We confirmed that H2A.Z^{Htz1} was reduced at a previously reported promoter nucleosome locus by ChIP-PCR (**Figure 2.4B**) (*54-56*). However, bulk H2A.Z^{Htz1} was not depleted in the chromatin fraction in *swr1*Δ (**Supplemental Figure 2.7A, B**). Similar to our findings with the *htz1*Δ mutant, CENP-A^{Cse4} chromatin levels were somewhat higher in the *swr1*Δ *psh1*Δ cells compared to *psh1*Δ (**Figure 2.4C**). In addition, there was no change in CENP-A^{Cse4} stability in *swr1*Δ cells (**Supplemental Figure 2.7C**). We also tested whether CENP-A^{Cse4} overexpression in the *psh1*Δ mutant affects H2A.Z^{Htz1} promoter occupancy, but did not detect an effect at the loci analyzed (**Supplemental Figure 2.7D**). However, given that H2A.Z^{Htz1} is estimated to occupy only a small proportion of nucleosomes at any given locus in the population, it may be difficult to detect a significant difference (*22, 60*). Together, our data suggest that although ectopic CENP-A^{Cse4} and WT H2A.Z^{Htz1} localize to similar sites, the H2A.Z^{Htz1} incorporation machinery does not promote CENP-A^{Cse4} mislocalization and may instead help to prevent CENP-A^{Cse4} promoter incorporation.

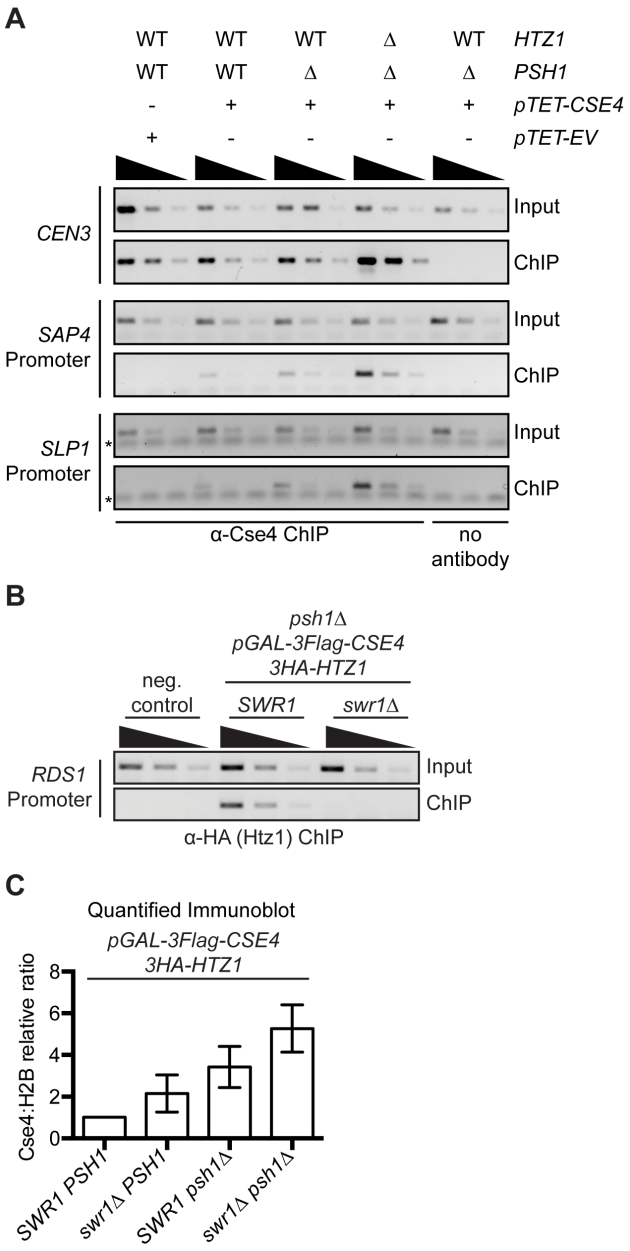

Figure 2.4. CENP-A^{Cse4} mislocalization does not depend on H2A.Z^{Htz1} incorporation.
(A) ChIP was performed with anti-Cse4 antibody on negative control cells (SBY15924), as well as *pTET-CSE4* (SBY15903), *psh1*Δ *pTET-CSE4* (SBY15904) and *psh1*Δ *htz1*Δ *pTET-CSE4* (SBY15906) cells overexpressing CENP-A^{Cse4} for six hours. As a control, we also performed a ChIP experiment with no antibody in *psh1*Δ *pTET-CSE4* cells. Input dilutions are 1:100, 1:300, 1:100 and ChIP dilutions are 1x, 1:3, 1:9. (B) ChIP-PCR of 3HA-Htz1 at the *RDS1* promoter. Strains used: negative (neg.) control (SBY3), *psh1*Δ *pGAL-3Flag-CSE4 3HA-HTZ1* (SBY12833), *psh1*Δ *pGAL-3Flag-CSE4, 3HA-HTZ1 swr1*Δ (SBY12924). Input dilutions: 1:100, 1:300, 1:900. ChIP dilutions: 1:3, 1:9, 1:21. (C) Relative CENP-A^{Cse4} levels were measured by quantifying the mean chromatin CENP-A^{Cse4}:H2B fold change vs. *pGAL-3Flag-CSE4 HA-HTZ1* +/- 1 SEM using quantitative immunoblots of chromatin fraction (n = 3), p = 0.0204 (paired t-test comparing the Cse4:H2B relative ratio in *psh1*Δ *pGAL-3Flag-CSE4* to *swr1*Δ *psh1*Δ *pGAL-3Flag-CSE4*). Strains used were *pGAL-3Flag-CSE4 3HA-HTZ1* (SBY12832), *swr1*Δ *pGAL-3Flag-CSE4 3HA-HTZ1* (SBY12956), *psh1*Δ *pGAL-3Flag-CSE4 3HA-HTZ1* (SBY12833) and *swr1*Δ *psh1*Δ *pGAL-3Flag-CSE4 3HA-HTZ1* (SBY12924).

2.3.5 *INO80-C contributes to CENP-A^{Cse4} mislocalization in psh1Δ cells*

Since the ectopic localization of CENP-A^{Cse4} does not depend on H2A.Z^{Htz1} incorporation, we asked whether chromatin remodelers that remove H2A.Z^{Htz1} are involved. INO80-C has been reported to act preferentially on H2A.Z^{Htz1}-containing +1 nucleosomes and to promote full nucleosome turnover (*59, 60*). We therefore hypothesized that CENP-A^{Cse4} might be incorporated into chromatin when canonical H3 is removed by INO80-C-mediated nucleosome turnover. Previous work showed that deletion of the ATPase Ino80 (SGD ID: S000003118) leads to a global alteration of H2A.Z^{Htz1} localization patterns genome-wide without affecting the overall levels of H2A.Z^{Htz1} incorporation in the genome (*59, 162*). However, this deletion mutant is not viable in the strain background we used in this study (*163*). We therefore used a deletion of *NHP10* (SGD ID: S000002160), a non-essential INO80-C subunit that facilitates binding to nucleosomes and DNA, but that does not affect catalytic activity *in vitro* (*164-166*). To analyze CENP-A^{Cse4} levels, we performed chromatin fractionation in WT and *nhp10*Δ cells overexpressing CENP-A^{Cse4}. Similar to previously reported work, we did not detect a change in total H2A.Z^{Htz1} levels in the chromatin in the *nhp10*Δ strain (**Supplemental Figure 2.8A, B**) (*59, 162*). However, CENP-A^{Cse4} chromatin levels were somewhat reduced when *NHP10* was deleted (**Figure 2.5A, Supplemental Figure 2.8B**), suggesting that INO80-C histone exchange activity contributes to CENP-A^{Cse4} misincorporation. To more directly test this possibility, we asked whether Ino80 associates with CENP-A^{Cse4} *in vivo*. CENP-A^{Cse4} co-immunoprecipitated with Ino80 (**Figure 2.5B**), and this interaction increased in the absence of Psh1. To determine how this affects cell viability, we also analyzed the growth of *nhp10*Δ mutant cells overexpressing CENP-A^{Cse4}. Although strong CENP-A^{Cse4} overexpression is lethal to *psh1*Δ cells regardless of the presence of *NHP10* (**Supplemental Figure 2.8C**), a deletion of *NHP10* improved the growth of

*psh1*Δ mutant cells that were moderately overexpressing CENP-A^{Cse4} (**Figure 2.5C**). We confirmed these effects were not due to altered levels or stability of CENP-A^{Cse4} in *nhp10*Δ mutant cells (**Supplemental Figure 2.8D, E**). Together, these data suggest that at least some of the ectopic CENP-A^{Cse4} deposition is likely coupled to the chromatin remodeling activity of INO80-C.

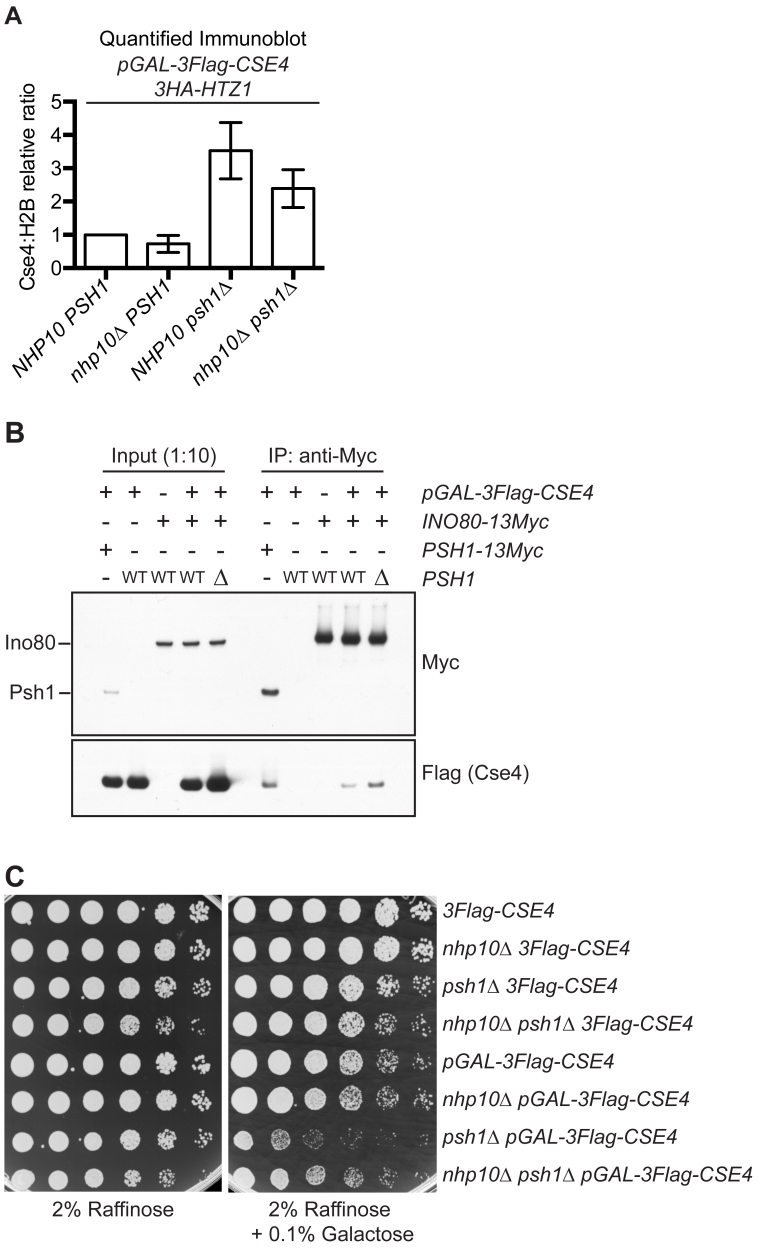

Figure 2.5. INO80-C contributes to CENP-A^{Cse4} misincorporation.
(A) Mean chromatin CENP-A^{Cse4}:H2B fold change vs. *pGAL-3Flag-CSE4 HA-HTZ1* strain +/- 1 SEM from quantitative immunoblots of the chromatin fraction. Strains used: *pGAL-3Flag-CSE4 HA-HTZ1* (SBY12832), *nhp10*Δ *pGAL-3Flag-CSE4 3HA-HTZ1* (SBY12930), *psh1*Δ *pGAL-3Flag-CSE4 3HA-HTZ1* (SBY12833), and *nhp10*Δ *psh1*Δ *pGAL-3Flag-CSE4 3HA-HTZ1* (SBY12959). (n = 3). p = 0.0593 (paired t-test comparing the Cse4:H2B relative ratio in *psh1*Δ *pGAL-3Flag-CSE4* to *nhp10*Δ *psh1*Δ *pGAL-3Flag-CSE4*). (B) Co-Immunoprecipitation (co-IP) of overexpressed 3Flag-Cse4 with either Psh1-13Myc or Ino80-13Myc from the following strains: *PSH1-13Myc pGAL-3Flag-CSE4* (SBY14482), *pGAL-3Flag-CSE4* (SBY9540), *INO80-13Myc* (SBY14527), *INO80-13Myc pGAL-3Flag-CSE4* (SBY14526), *INO80-13Myc psh1*Δ *pGAL-3Flag-CSE4* (SBY14515). (C) Five-fold serial dilutions of strains *3Flag-CSE4* (SBY10419), *nhp10*Δ *3Flag-CSE4* (SBY12958), *psh1*Δ *3Flag-CSE4* (SBY10484), *nhp10*Δ *psh1*Δ *3Flag-CSE4* (SBY12928), *pGAL-3Flag-CSE4* (SBY10425), *nhp10*Δ *pGAL-3Flag-CSE4* (SBY12930), *psh1*Δ *pGAL-3Flag-CSE4* (SBY10484), and *nhp10*Δ *psh1*Δ *pGAL-3Flag-CSE4* (SBY12959) were plated on indicated media.

2.3.6 *Mislocalized CENP-A^{Cse4} perturbs transcription in the absence of Psh1*

The mislocalization of CENP-A^{Cse4} to promoters suggested that it could lead to transcriptional changes in the downstream genes. In addition, the relationship between CENP-A^{Cse4} incorporation and H2A.Z^{Htz1} removal by INO80-C suggested that any transcriptional changes might correlate with those in *htz1*Δ cells. We therefore performed RNA-seq on WT, *psh1*Δ, *pGAL-3Flag-CSE4*, *psh1*Δ *pGAL-3Flag-CSE4* and *htz1*Δ strains that were treated with galactose for two hours. As a control, we also included a *pGAL-H3* strain to ensure any effects were specific to CENP-A^{Cse4} overexpression and not just an effect of increased histone turnover. Cells containing just a *PSH1* deletion or overexpressing CENP-A^{Cse4} or H3 had very little change in transcription (**Figure 2.6A, B**). However, a large number of genes were misregulated in *psh1*Δ cells overexpressing CENP-A^{Cse4}, as well as in *htz1*Δ cells as previously described (*167, 168*). We confirmed that these gene expression changes were not due to an indirect effect of CENP-A^{Cse4} mislocalization to the rDNA by measuring the rDNA copy number and rRNA transcript levels, which were not significantly different between the strains (**Supplemental Figure 2.9A, B**). We also confirmed that the differentially transcribed genes in the *psh1*Δ *pGAL-3Flag-CSE4* strain are not a consequence of altered cell cycle progression (*43, 169*) (**Supplemental Figure 2.9C**).

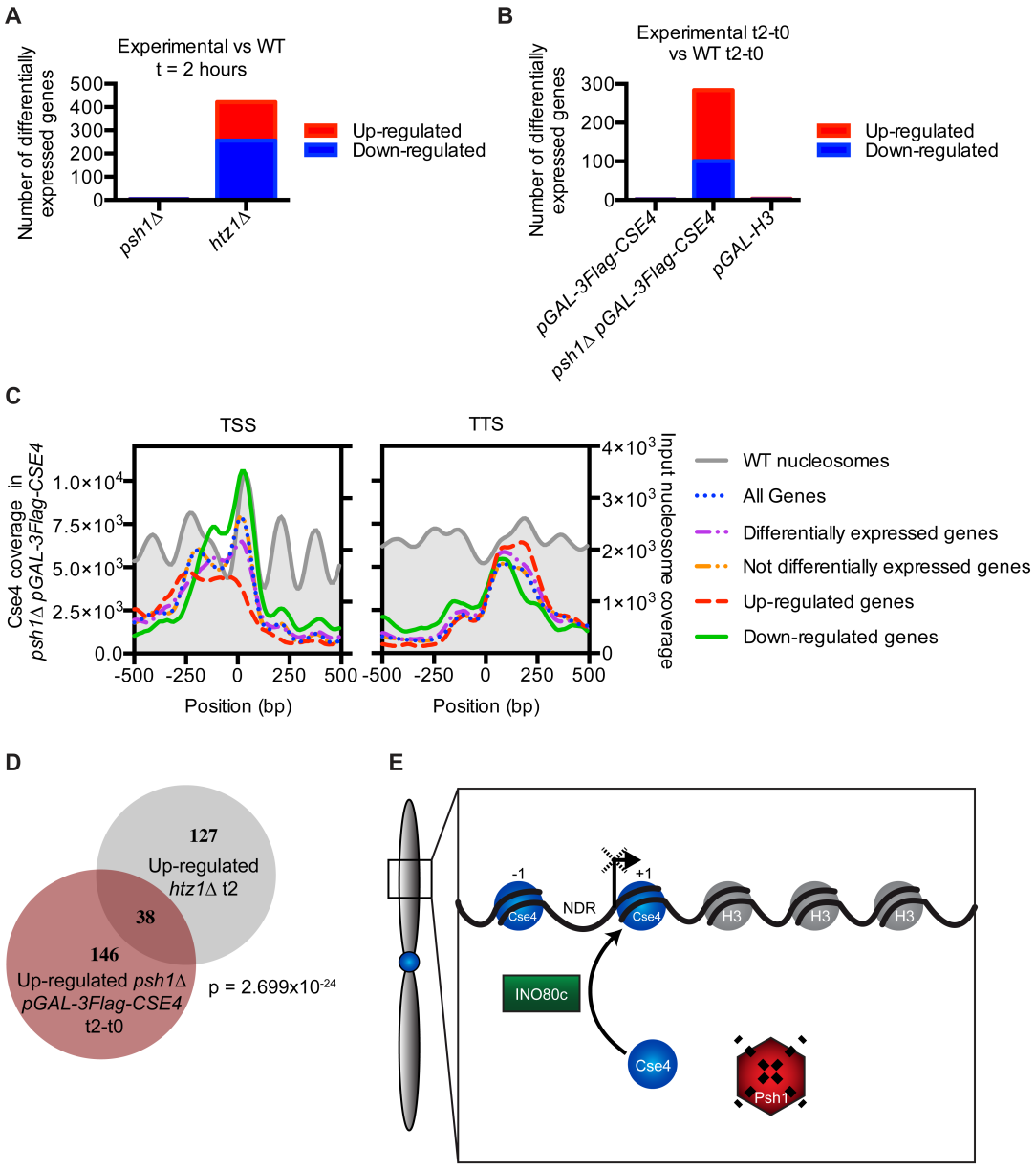

Figure 2.6. CENP-A^{Cse4} mislocalization to promoters alters transcription.
(A) Graph of the number of transcripts significantly increased or decreased compared to the WT strain by RNA-seq of *psh1*Δ and *htz1*Δ cells at t=2 hours. Differential expression analysis statistics were performed using edgeR (*170*). (B) Graph of the number of transcripts significantly increased or decreased at t=2 hours compared to t=0 in *pGAL-3Flag-CSE4*, *psh1*Δ *pGAL-3Flag-CSE4*, and *pGAL-H3* that are not also changed at t=2 hours compared to t=0 in the WT strain. (C) TSS and TTS profiles of CENP-A^{Cse4} enrichment based on the measured transcriptional changes by RNA-seq in the *psh1*Δ *pGAL-3Flag-CSE4* strain. (D) Proportional Venn diagram of genes up-regulated in *psh1*Δ *pGAL-3Flag-CSE4* at t=2 hours and genes up-regulated in *htz1*Δ at t=2 hours. p = 2.699x10^{-24} (p-value from a cumulative hypergeometric distribution test, which represents the probability of the number of genes overlapped or greater between the two strains.) (E) Model: At chromosome arms, INO80-C-mediated full nucleosome turnover may lead to CENP-A^{Cse4} deposition and H2A.Z^{Htz1} removal. Psh1 blocks stable CENP-A^{Cse4} promoter incorporation by ubiquitylating mislocalized CENP-A^{Cse4} and targeting it for degradation. Mislocalization of CENP-A^{Cse4} to promoters leads to misregulation of a subset of downstream genes, which could affect survival of these cells.

To determine whether CENP-A^{Cse4} mislocalization to promoters correlates with transcriptional misregulation of downstream genes, we compared the promoters with CENP-A^{Cse4} peaks to the genes showing altered transcription in the *psh1*Δ strain overexpressing CENP-A^{Cse4}. While there was a significant overlap ($p = 0.0009$, hypergeometric distribution) between the down-regulated genes and those with promoter CENP-A^{Cse4} peaks (**Supplemental Figure 2.9D**), the vast majority of genes with CENP-A^{Cse4} promoter peaks do not have changes in transcription. This is similar to the relationship between H2A.Z^{Htz1} peaks and the genes that are differentially regulated in *htz1*Δ (*23*), confirming that changes in the histone composition of promoters does not always lead to direct transcriptional effects. However, the downregulated genes have much higher CENP-A^{Cse4} coverage at the +1 nucleosome compared to other promoters, suggesting that both the amount and position of CENP-A^{Cse4} misincorporation may determine which downstream genes become misregulated (**Figure 2.6C**). Analysis of transcription factor binding sites enriched at promoters of the downregulated genes with CENP-A^{Cse4} promoter peaks identified Cse2 (SGDID: S000005293) as the most significantly enriched transcription factor (Supplemental File 2.2). Cse2 is a subunit of the RNA Polymerase II Mediator complex, and has also been shown to be required for chromosome segregation (*171, 172*), leading to the possibility that the transcriptional defects are correlated with altered Cse2 function.

Given the relationship between CENP-A^{Cse4} and H2A.Z^{Htz1} localization, we also asked whether there was a correlation between the transcriptional changes in *psh1*Δ *pGAL-3Flag-CSE4* and *htz1*Δ mutant cells. Interestingly, there was a significant overlap between the genes that increased transcription in both strains (**Figure 2.6D**), and these were also enriched for CENP-A^{Cse4} in the NDR (**Supplemental Figure 2.9E**). We analyzed the promoters of the affected genes for common transcription factors and found 24 that are enriched at the promoters of these genes

(Supplemental File 2.2), so the underlying mechanism for the misregulation is not clearly associated with one factor. However, these data are consistent with the relationship between CENP-A^{Cse4} mislocalization and the INO80-C chromatin remodeling machinery that controls H2A.Z^{Htz1}.

2.4 DISCUSSION

In this study, we performed the first genome-wide localization of the centromeric histone variant CENP-A^{Cse4} in the absence of Psh1-mediated proteolysis and found that it mislocalizes to intergenic regions when overexpressed. There was a significant correlation between the sites of CENP-A^{Cse4} mislocalization and nucleosomes that normally incorporate the H2A.Z^{Htz1} variant. Consistent with this, we found that INO80-C, which acts on H2A.Z^{Htz1} nucleosomes, also contributes to the ectopic localization of CENP-A^{Cse4}, identifying another mechanism that promotes CENP-A^{Cse4} mislocalization. We also found that the number of CENP-A^{Cse4} ectopic peaks is significantly enhanced and leads to transcriptional defects when Psh1 is absent, underscoring the importance of proteolysis in maintaining genome stability through the exclusive localization of the centromeric histone variant.

The intergenic mislocalization of CENP-A^{Cse4} is similar to what has been observed with mild CENP-A^{Cse4} overexpression (*88, 121*) although we found that the mislocalization of overexpressed CENP-A^{Cse4} is much stronger in the absence of proteolysis. In human cells, CENP-A overexpression misincorporates at CTCF binding sites, which are associated with the histone variants H2A.Z and H3.3 and have high levels of histone turnover (*120*). In budding yeast, the connection between histone turnover and CENP-A^{Cse4} mislocalization is less clear. High histone turnover and more open chromatin have been shown to be permissive for CENP-

A^{Cse4} mislocalization (*88, 121*). This is consistent with our results, as promoters have a higher level of turnover than intragenic regions (*28*). However, a *caf1*Δ *hir1*Δ double mutant that decreases histone turnover genome-wide still mislocalizes even endogenous levels of CENP-A^{Cse4} to promoters (*63*). Therefore, histone turnover is not strictly required for CENP-A^{Cse4} mislocalization and there must be additional mechanisms that promote the ectopic deposition of CENP-A^{Cse4}.

2.4.1 *INO80-C promotes CENP-A^{Cse4} mislocalization*

We identified a strong similarity between H2A.Z^{Htz1} localization and CENP-A^{Cse4} mislocalization in nucleosomes flanking NDRs, such as replication origins, centromeres, and +1 nucleosomes at promoters. We also found that INO80-C contributes to CENP-A^{Cse4} mislocalization. CENP-A^{Cse4} co-immunoprecipitates with INO80-C, and this interaction is increased in the *psh1*Δ mutant where there are higher levels of CENP-A^{Cse4}. Consistent with this, an *nhp10*Δ mutant reduced the ectopic localization and partially rescued the growth defect of the *psh1*Δ mutant when CENP-A^{Cse4} was overexpressed. However, *nhp10*Δ does not fully rescue the lethality or ectopic deposition, so additional chromatin remodelers or histone chaperones must also contribute to ectopic CENP-A^{Cse4} incorporation. In humans, the chaperone activity of DAXX is involved in CENP-A deposition in euchromatin (*120*), but there is no ortholog of this protein in budding yeast.

H2A.Z^{Htz1} localization to nucleosomes flanking NDRs requires SWR-C binding, and SWR-C enrichment is increased with longer NDRs *in vivo* (*58*). Similarly, we found that CENP-A^{Cse4} is enriched at longer NDRs. However, we determined that H2A.Z^{Htz1} and SWR-C are not required for CENP-A^{Cse4} deposition. Our work is instead consistent with the possibility that the

two yeast histone variants could have an antagonistic relationship, such that they are found at the same places in the genome, but never at the same time. This is reminiscent of the relationship between CENP-A^{Cnp1} and H2A.Z^{Htz1} in fission yeast, where CENP-A^{Cnp1} forms neocentromeres in regions with low H2A.Z^{Htz1} when the endogenous centromere is deleted (*127*). However, we detect CENP-A^{Cse4} mislocalization at nucleosomes that normally have high H2A.Z^{Htz1} enrichment. We speculate that this is due to different mechanisms leading to ectopic deposition. In fission yeast, the ectopic CENP-A^{Cnp1} localization to neocentromeres depended on the centromeric chaperone (*127*), while our data suggests a role for INO80-C in the ectopic deposition of highly expressed CENP-A^{Cse4}. Given that INO80-C acts in opposition to SWR-C to remove H2A.Z^{Htz1} from nucleosomes, we propose that the full nucleosome turnover activity of INO80-C leads to the removal of H3 and the incorporation of CENP-A^{Cse4} into promoter nucleosomes (**Figure 2.6E**). This model explains both the co-localization of the histone variants and the potentially antagonistic relationship between H2A.Z^{Htz1} and CENP-A^{Cse4} in the chromatin.

2.4.2 *Psh1 acts on CENP-A^{Cse4} throughout the euchromatin*

Although there is a significantly higher level of euchromatic CENP-A^{Cse4} in the absence of Psh1, the locations of the ectopic nucleosome positions are similar regardless of Psh1 activity. In both cases, overexpressed CENP-A^{Cse4} is enriched intergenically, suggesting that Psh1 does not have preferential sites of action genome-wide. However, CENP-A^{Cse4} was not significantly incorporated into genes even in the absence of Psh1, suggesting that additional mechanisms control its localization. We previously showed that the FACT complex, which was recently demonstrated to remove H2A.Z^{Htz1} from genes, interacts with Psh1 to facilitate CENP-A^{Cse4}

degradation (*43, 118, 162*). However, FACT does not interact with CENP-A^{Cse4} in the absence of Psh1 (*43*). One possibility is that FACT could indirectly antagonize CENP-A^{Cse4} mislocalization into genes by ensuring that H3 is quickly reincorporated into nucleosomes following transcription, similar to its role in fission yeast (*99*). In the future, it will be important to understand how intragenic regions are protected from CENP-A^{Cse4} deposition.

2.4.3 *CENP-A^{Cse4} mislocalization causes defects in transcription*

For the first time in any organism, we detected large-scale changes in transcription when CENP-A mislocalized to euchromatin. This only occurred in cells lacking Psh1, and the downregulated genes had very high levels of CENP-A^{Cse4} in their promoters. This suggests that strong misincorporation of CENP-A^{Cse4} at a promoter may be required to cause transcriptional defects, and may explain why this has not been previously observed. The levels of CENP-A^{Cse4} overexpression achieved in the absence of proteolysis are much higher than previous studies that have analyzed CENP-A^{Cse4} mislocalization. It is not clear whether mislocalization of CENP-A^{Cse4} at a given promoter is sufficient to directly decrease transcription. We found a significant enrichment of the Cse2 transcription factor in the promoters of the downregulated genes, leading to the intriguing possibility that CENP-A^{Cse4} incorporation alters Cse2 function at a subset of genes to inhibit transcription. It is interesting to note that Cse2 and Cse4 were identified in the same genetic screen for mutants in chromosome segregation (*29, 171*), and it will be important to further explore their relationship in the future.

We also identified genes that increased transcription when CENP-A^{Cse4} was mislocalized, and these significantly overlap with those altered in *htz1*Δ mutant cells. This further confirms the potential antagonistic relationship between the yeast histone variants, and suggests that high

levels of CENP-A^{Cse4} may lead to similar chromatin changes at a subset of promoters as cells lacking H2A.Z^{Htz1}. The underlying mechanism for why only a fraction of promoters that contain H2A.Z^{Htz1} are transcriptionally up-regulated in its absence is not known. We speculate that a change in nucleosome positioning or stability occurs at these promoters that facilitates the access of transcriptional machinery. Consistent with this, we found that the up-regulated gene promoters have CENP-A^{Cse4} enrichment within rather than flanking the NDR and lack strong +1 enrichment.

2.4.4 *Conclusions*

We found that regulating the levels and localization of the centromeric histone variant is critical to prevent transcriptional misregulation in budding yeast. Although CENP-A mislocalization leads to the formation of ectopic kinetochores in other organisms, we have not been able to determine whether this occurs in budding yeast due to the difficulty of detecting ectopic kinetochores (*43*). Our work suggests the possibility that transcriptional defects due to the mislocalization of CENP-A^{Cse4} in the absence of proteolysis may be the underlying cause of lethality in these cells. These data highlight the need to accurately regulate the localization of the centromeric histone variant CENP-A^{Cse4} to both ensure genomic stability through its centromeric functions, as well as to prevent the disruption of euchromatic functions.

2.5 MATERIALS AND METHODS

2.5.1 *Yeast strain construction and microbial techniques*

Microbial techniques and media were as described (*173, 174*). For all experiments involving induction of *pGAL-3Flag-CSE4* or *pGAL-H3*, budding yeast cells of indicated strains were

grown to log phase (OD 0.55-0.8, Bio-Rad SmartSpec^{TM} 3000) in lactic acid media at 23 ^{o}C and induced for 2 hours with 2% galactose. Yeast strains were constructed using standard genetic techniques. Epitope-tagged proteins were constructed using either a PCR integration technique (*175*) or by the integration of plasmids after restriction digestion. Specific plasmids and yeast strains used in this study are described in **Supplemental Table 2.2** and **Supplemental Table 2.3.**

2.5.2 *General protein techniques*

Protein extracts to check total CENP-A^{Cse4} levels were prepared as described (*176*). Immunoblots using chemiluminescence were performed as previously described (*176*). For all immunoblots, the antibody dilutions were as follows: Mouse anti-Pgk1 monoclonal antibodies (Invitrogen Catalog # 459250) at a 1:10,000 dilution were used as a loading control. Mouse anti-Flag M2 monoclonal antibodies (Sigma-Aldrich Catalog # F3165) were used at a 1:3000 dilution, Mouse anti-HA 12CA5 monoclonal antibodies (Roche Catalog # 1-583-816) were used at a 1:10,000 dilution, and rabbit anti-H2B polyclonal antibodies (Active Motif Catalog # 39237) were used at a 1:3,000 dilution. Mouse anti-Myc 9E10 monoclonal antibodies were used at a 1:10,000 dilution (Covance Catalog # MMS-150R). Co-IP experiments were performed as previously described (*118*) for Psh1-Myc and Ino80-Myc strains using 5ul Protein G Dynabeads conjugated with 1.5ul anti-Myc (A-14, SC-789) and run on a gradient SDS-PAGE gel. Quantitative immunoblots were carried out according to (*177*) with the modification of using 4% non-fat milk in PBS as the blocking agent for the anti-Flag immunoblot. Briefly, IRDye anti-mouse and anti-rabbit secondary antibodies from LI-COR were used at a 1:15,000 dilution. The immunoblots were imaged on a LI-COR imaging system, and the protein levels were quantified using Image Studio^{TM} Lite.

2.5.3 *Chromatin fractionation assay*

Chromatin fractionation assays were performed as described (*118*), followed by quantitative immunoblots. The mean and SEM of three independent experiments is reported. anti-PGK1 was used as a marker and loading control for the soluble fraction, and anti-H2B was used as a marker and loading control for the chromatin fraction. The Cse4:H2B and H2A.Z:H2B ratios were normalized to the *pGAL-3Flag-CSE4* strain. Note that the levels of H2A.Z^{Htz1} and H2B are somewhat variable between strains. This may be due to differential susceptibility of the cell wall to zymolyase digestion during the chromatin fractionation procedure, which seems to vary between strains. To control for this, we used H2B to determine the level of total chromatin in each condition.

2.5.4 *ChIP-seq*

3Flag-Cse4-containing nucleosomes were isolated by ChIP of 3Flag-Cse4 using monoclonal anti-Flag M2 antibodies (Sigma-Aldrich Catalog # F3165). ChIPs were performed with Micrococcal nuclease (MNase, Worthington Biochemical Corporation Catalog # LS004798)-treated chromatin as described (*152*) with the following addition. Before nuclei isolation, proteins were crosslinked to DNA with 1% formaldehyde for 15 minutes. Crosslinks were then reversed before DNA extraction by the addition of 1% SDS and an overnight incubation at 65 ^{o}C (*178*). DNA was extracted using phenol:chloroform extraction and ethanol precipitation, and was treated with RNAse and purified using a Qiagen Reaction Clean-up kit before library construction. Paired-end sequencing libraries of both input DNA from MNase-digested chromatin and 3Flag-Cse4 ChIP DNA were prepared using a modified Solexa library preparation protocol that captures DNA particles down to ~25 bp (*152*). Cluster generation, followed by 25

cycles of paired-end sequencing on an Illumina HiSeq 2000, was performed by the Fred Hutchinson Cancer Research Center Genomics Shared Resource facility, resulting in 24 bp paired end reads. Base calling was performed using Illumina's Real Time Analysis software v1.13.48.0. Raw FASTQ sequence files were deposited in the NCBI GEO Series GSE69696.

2.5.5 *Identification of CENP-A^{Cse4}-enriched loci from ChIP-seq data*

Raw reads (passing Solexa quality test) were mapped to the *S. cerevisiae* reference genome version SacCer3 (*Saccharomyces* Genome Database (SGD)/UCSC) using the Burrows-Wheeler Aligner (BWA) (*179*). The resulting Binary Sequence Alignment/Map (BAM) files were filtered for proper pairs with a mapping score >= 30 using samtools (*180*). Mononucleosomes were identified as paired-end reads with insert sizes between 50 bp and 240 bp using R Bioconductor packages GenomicRanges, rtracklayer, Rsamtools, nucleR, and the UCSC SacCer3 reference genome (*153, 181-183*). ChIP reads were compared to the input reads for each strain using the Dynamic Analysis of Nucleosome and Protein Occupancy by Sequencing, version 2 (DANPOS2) function Dpos with background subtraction (*184*), and the background-subtracted ChIP signal was normalized to the coverage at centromeric regions for each strain, which contains a CENP-A^{Cse4} nucleosome throughout the cell cycle (*178*), and smoothed using the default DANPOS2 Dpos smoothing parameters (*184*). The resulting normalized coverage data was visualized using the Integrated Genomics Viewer (IGV) (*185, 186*). Wiggle track format (WIG) files of the normalized coverage for each sample in 10 bp steps are available under NCBI GEO Series GSE69696.

To identify genomic loci enriched for CENP-A^{Cse4}, we analyzed the coverage relative to the centromere. Although CENP-A^{Cse4} is constitutively localized to the centromere (*187*), its

coverage at the centromere is under-represented relative to other genomic regions. This effect is likely due to the decreased solubility of the centromere to MNase digestion due to kinetochore protein binding, which makes it possible for other genomic regions to appear enriched above its occupancy at the centromere (*88*). We called peaks of CENP-A^{Cse4} occupancy in each strain as any region where the CENP-A^{Cse4} enrichment was above the threshold of the minimum average coverage at any centromere in the *3Flag-CSE4* strain using R Bioconductor packages Genomic Ranges, rtracklayer, and the UCSC SacCer3 reference genome (*153, 181-183*) and the DANPOS2 function Dtriple to call peaks without any further normalization or smoothing (*184*). rDNA ChIP coverage was set to 0 before peak calling due to the high copy number of this region, and this locus was excluded from subsequent computational analyses. Input nucleosome peaks were also called using DANPOS2 (*184*). Browser Extensible Data (BED) files of the called peaks for each sample are available at NCBI GEO Series GSE69696.

2.5.6 *Overlap of CENP-A^{Cse4} peaks with genomic regions*

Genomic regions were annotated using the following strategy: *Saccharomyces* Genome Database (SGD) annotations of the SacCer3 genome were used to call regions of centromeres, pericentromeres, telomeres, origins of replication, genes, and intergenic regions in that order, such that each base was assigned to only the first overlapping region type. To analyze the percentage of peaks from each strain in each genomic region, 1 bp regions at the center of each CENP-A^{Cse4} peak were overlapped with each region so that each peak was counted only once using R Bioconductor packages Genomic Ranges, rtracklayer, and UCSC SacCer3 (*153, 181-183*). The same analysis was performed with CENP-A^{Cse4} peaks that either did or did not overlap WT H2A.Z^{Htz1} peaks.

2.5.7 *Meta-analysis of CENP-A^{Cse4} and H2A.Z^{Htz1} enrichment at gene ends and other genomic loci*

We analyzed mean CENP-A^{Cse4} and H2A.Z^{Htz1} enrichment at the starts and ends of genes as well as centered on NDRs, origins of replication, or centromeres using the DANPOS2 profile function (*160, 184*). H2A.Z^{Htz1} ChIP data is from (*21*). H2A.Z^{Htz1} coverage was calculated from the mapped reads with greater than 90% identity using the DANPOS2 function dpos with the default parameters (*184*), after lifting over the coordinates to the SacCer3 genome using R Bioconductor packages Genomic Ranges, rtracklayer, and UCSC SacCer3 (*153, 181-183*). For the analysis of the transcription start sites (TSS) and transcription termination sites (TTS), the mean CENP-A^{Cse4} or H2A.Z^{Htz1} coverage in 10 bp windows was calculated for 500 bp upstream and downstream of 3987 transcripts using custom gene files modified to use experimentally derived TSS data instead of open reading frame (ORF) start sites from Nagalakshmi et al, 2008 (GSE11209) (*157*). For the analysis of specific groups of genes, the gene file was divided into the specified bins using R Bioconductor packages before using the DANPOS2 function. For NDRs, origins, and centromeres, DANPOS2 profile was run centered on the genomic features using bed files containing either each NDR (*160*), origin (from SacCer3 annotation) or centromere (from SacCer3 annotation). All plots were made using GraphPad Prism version 6.0 for OSX, GraphPad Software, La Jolla California USA, www.graphpad.com.

2.5.8 *Comparison of CENP-A^{Cse4} and H2A.Z^{Htz1} nucleosome localization*

Coverage data was visualized using IGV (*185, 186*). The fraction of overlap between CENP-A^{Cse4} peaks for each strain and reported H2A.Z^{Htz1} peaks (coarse grain nucleosome positions)

from wild-type (WT) cells (*21*) was calculated using R Bioconductor packages GenomicRanges and rtracklayer (*181-183*).

2.5.9 *ChIP-PCR with sonication for H2A.Z^{Htz1} and pTet-CSE4*

ChIP was performed from 50 ml formaldehyde-crosslinked cultures as described (*71*). Chromatin was fragmented by sonication to approximately 500 bp fragments. For HA-Htz1 ChIP, 3HA-Htz1 was immunoprecipitated using anti-HA (12CA5) antibodies (Roche). 3-fold serial dilutions of the Input (1:100, 1:300, 1:900) and ChIP (1:3, 1:9, 1:27) DNA were used for PCR reactions to detect the amount of DNA pulled down with 3HA-Htz1 in each strain (*71*) and were analyzed on 1.4% agarose gels. Primers for the *RDS1* promoter are from (*56*) and are listed in **Supplemental Table 2.4.** For CENP-A^{Cse4} ChIP, CENP-A^{Cse4} was immunoprecipitated using anti-Cse4 (235N) antibodies (*37*) from strains with CENP-A^{Cse4} expression induced from an inducible tetracycline repressed promoter (*188*) after a 6-hour washout of doxycycline (5ug/ml) in YC-URA media. 3-fold serial dilutions of the Input (1:100, 1:300, 1:900) and ChIP (1x, 1:3, 1:9) DNA were used for PCR reactions at *CEN3* (*178*), the *SAP4* promoter and the *SLP1* promoter.

2.5.10 *RNA-seq*

Total RNA was extracted from each sample using a hot acid phenol extraction protocol (*189*), followed by DNAse I treatment (Invitrogen Amplification Grade) phenol:chloroform extraction, and ethanol precipitation. Two or three independent biological replicates of each genotype were used. Total RNA integrity was checked using an Agilent 2200 TapeStation (Agilent Technologies, Inc., Santa Clara, CA) and quantified using a Trinean DropSense96 spectrophotometer (Caliper Life Sciences, Hopkinton, MA). RNA-seq libraries were prepared

from total RNA using the TruSeq RNA Sample Prep v2 Kit (Illumina, Inc., San Diego, CA, USA) and a Sciclone NGSx Workstation (PerkinElmer, Waltham, MA, USA). Library size distributions were validated using an Agilent 2200 TapeStation (Agilent Technologies, Santa Clara, CA, USA). Additional library QC, blending of pooled indexed libraries, and cluster optimization were performed using Life Technologies' Invitrogen Qubit® 2.0 Fluorometer (Life Technologies-Invitrogen, Carlsbad, CA, USA).

RNA-seq libraries were pooled (18-plex) and clustered onto a flow cell lane. Sequencing was performed using an Illumina HiSeq 2500 in "rapid run" mode employing a single-read, 50 base read length (SR50) sequencing strategy. Image analysis and base calling was performed using Illumina's Real Time Analysis v1.18 software, followed by 'demultiplexing' of indexed reads and generation of FASTQ files, using Illumina's bcl2fastq Conversion Software v1.8.4 (http://support.illumina.com/downloads/bcl2fastq_conversion_software_184.html). Reads of low quality were filtered prior to alignment to the reference genome (UCSC SacCer3 assembly) using TopHat v2.1.0(*190*). Counts were generated from TopHat alignments for each gene using the Python package HTSeq v0.6.1(*191*). Genes with low counts across all samples were removed, prior to identification of differentially expressed genes using the Bioconductor package edgeR v3.12.0(*170*). A false discovery rate (FDR) method was employed to correct for multiple testing(*192*). Differential expression was defined as $|\log_2 (\text{ratio})| \geq 0.585$ (± 1.5-fold) with the FDR set to 5%. Normalized differential expression data are available as excel files (Supplemental File 2.1) and raw data is available under NCBI GEO Series GSE69696.

2.5.11 *Comparison of transcriptional changes with htz1Δ*

The overlap between lists of genes with significantly changed transcription compared to WT yeast in *htz1Δ* at t=2 hours, and *psh1Δ pGAL-3Flag-CSE4* at t=2 hours – t=0 vs. WT t=2 hours – t=0 was found using the Whitehead Institute Compare Two Lists tool (http://jura.wi.mit.edu/bioc/tools/compare.php). The number of significantly up or down regulated transcripts overlapped between the genotypes was compared using the hypergeometric distribution (p-value is probability of getting more than the observed number of successes) using the total number of genes in the edgeR result files as the total population, using the GeneProf hypergeometric distribution calculator (*193*).

2.5.12 *ChIP-qPCR to validate CENP-A^{Cse4} peaks*

ChIP DNA samples prepared for ChIP-seq were analyzed by quantitative real-time PCR (qPCR) (7900HT, ABI Prism) to validate CENP-A^{Cse4} peaks as described (*177*) with the following modifications to the data analysis. A standard curve of input DNA was run for each primer set, and the replication efficiency of each primer set was calculated based on these values. The percent input was then calculated using the efficiency calibrated ΔCt method (*194*) for each ChIP sample taking into account the dilutions of both the input and ChIP samples for each strain. Oligo sequences are listed in **Supplemental Table 2.4.**

2.5.13 *Comparison of CENP-A^{Cse4} peaks to CLRs and LCNCRs*

CLR and LCNCR coordinates (*121*) were lifted over from the UCSC SacCer2 to the UCSC SacCer3 genome before comparing to the CENP-A^{Cse4} peaks from this study. The proportions of CLRs or LCNCRs that overlap CENP-A^{Cse4} ChIP-seq peaks in this study were calculated using

R Bioconductor packages rtracklayer, Rsamtools, and BSgenome.Scerevisiae.UCSC.sacCer3 (*153, 181-183, 195*). Graph showing proportions was made using GraphPad Prism version 6.0 for OSX, Graphpad Software, La Jolla California USA, www.graphpad.com.

2.5.14 *% AT calculation*

% AT/CENP-A^{Cse4} or input nucleosome peak for each strain was calculated in R using Bioconductor packages rtracklayer, Rsamtools, and BSgenome.Scerevisiae.UCSC.sacCer3 (*153, 181-183, 195*) Boxplots of the distributions of %AT/peak were plotted using GraphPad Prism version 6.0 for OSX, Graphpad Software, La Jolla California USA, www.graphpad.com.

2.5.15 *H2A.Z^{Htz1} score distributions*

Boxplots of the distribution of the H2A.Z^{Htz1} score for either H2A.Z^{Htz1} peaks that overlap CENP-A^{Cse4} peaks or those that do not overlap CENP-A^{Cse4} peaks in all CENP-A^{Cse4} ChIP-seq strains were made using R Bioconductor packages GenomicRanges and rtracklayer (*181-183*) and GraphPad Prism version 6.0 for OSX, Graphpad Software, La Jolla California USA, www.graphpad.com.

2.5.16 *CENP-A^{Cse4} stability assay*

CENP-A^{Cse4} stability assays were performed as previously described (*43*), with the following modifications. Yeast were grown at 23 ^{o}C throughout the experiment. The (-) sample for each strain was taken before inducing *pGAL-3Flag-CSE4* overexpression. After taking the (-) sample, all strains were induced with 2% galactose for 2 hours before adding 2% glucose and 50ug/ml cyclohexamide to begin the stability assay time course.

2.5.17 *qPCR measurement of rDNA copy number ratio*

Genomic DNA was extracted using phenol:chloroform extraction with bead beating followed by ethanol precipitation (*174*). The genomic DNA was RNAse A treated, phenol:chloroform extracted and then ethanol precipitated. rDNA and *UTH1* copy number were analyzed by quantitative real-time PCR (qPCR) (7900HT, ABI Prism) as described (*177*) with the following modifications to the data analysis. A standard curve of input DNA was run for each primer set, and the replication efficiency of each primer set was calculated based on these values. The rDNA:*UTH1* ratio was calculated for each experimental strain relative to a WT strain (SBY3) using the efficiency calibrated ΔCt method (*194*). Oligo sequences are listed in **Supplemental Table 2.4.** Graphs were made using GraphPad Prism version 6.0 for OSX, Graphpad Software, La Jolla California USA, www.graphpad.com.

2.5.18 *qPCR measurement of rRNA transcript level*

0.5 ug samples of the DNAse-treated RNA that was used for the RNA-seq experiment were made into cDNA using the iScript™ Reverse Transcription Supermix for RT-qPCR (Bio-Rad). rRNA and *ACT1* transcript levels were analyzed by quantitative real-time PCR (qPCR) (7900HT, ABI Prism) as described (*177*) with the following modifications to the data analysis. A standard curve of input DNA was run for each primer set, and the replication efficiency of each primer set was calculated based on these values. The rRNA:*ACT1* ratio was calculated for each experimental strain at t = 0 and t = 2 hours relative to a WT strain (SBY3) at t = 0 using the efficiency calibrated ΔCt method (*194*). Oligo sequences are listed in **Supplemental Table 2.4**. Graphs were made using GraphPad Prism version 6.0 for OSX, Graphpad Software, La Jolla California USA, www.graphpad.com.

2.5.19 *Comparison of transcriptional changes with cell cycle regulated genes*

Genes significantly up- or down-regulated in the *psh1*Δ *pGAL-3Flag-CSE4* strain at t2 compared to t0 were compared to a list of cell cycle regulated genes (*169*) using Microsoft Excel. Histograms were made of the cell cycle % where the expression of these genes peaked using GraphPad Prism version 6.0 for OSX, Graphpad Software, La Jolla California USA, www.graphpad.com. 1% cell cycle = M/G1, 100% cell cycle = the next M/G1.

2.5.20 *Comparison of transcriptional changes with mislocalized CENP-A^{Cse4} peaks*

The list of genes with significant changes in transcript level from the RNA-seq analysis were compared with the list of genes with CENP-A^{Cse4} peaks within their promoters (500 bp upstream of TSS) in the *psh1*Δ *pGAL-3Flag-CSE4* strain using the Whitehead Institute Compare Two Lists tool (http://jura.wi.mit.edu/bioc/tools/compare.php). Venn diagram was drawn using BioVenn (*196*). The number of significantly changed transcripts that overlapped between the strains was compared using the hypergeometric distribution (p-value is probability of getting more than the observed number of successes) using the total number of genes present in both the differential transcription and CENP-A^{Cse4} peak analysis as the total population, using the GeneProf hypergeometric distribution calculator (*193*).

2.5.21 *Transcription factor enrichment analysis*

Gene lists of all genes down-regulated in *psh1*Δ *pGAL-3Flag-CSE4* with promoter CENP-A^{Cse4} peaks and of all genes up-regulated in both *psh1*Δ *pGAL-3Flag-CSE4* and in *htz1*Δ were analyzed for transcription factor enrichment using YEASTRACT(*197-201*). Lists of enriched transcription factors are included in Supplemental File 2.2.

2.6 ACKNOWLEDGEMENTS

We thank the Henikoff, Tsukiyama, and Wu labs for primer sequences and Jerry Davison, Jorja Henikoff, Christine Codomo, Adam Yadon, Jairo Rodriguez, Kristina Krassovsky, Sheila Teves, and Florian Steiner for assistance with ChIP-seq library preparation and analysis. We are also grateful to Eric Alcid, Jeff Delrow, Ryan Basom, Alyssa Dawson, and the FHCRC Genomic Resource for RNA purification assistance, RNA-seq library preparation, Illumina sequencing, and RNA-seq analysis, and Adrienne Barber for technical assistance. We also thank members of the Biggins, Tsukiyama, and Henikoff labs for helpful discussions and generous gifts of strains, and Toshio Tsukiyama, Geert Kops and the Biggins lab for critical comments on the manuscript.

2.7 SUPPLEMENTAL FIGURES

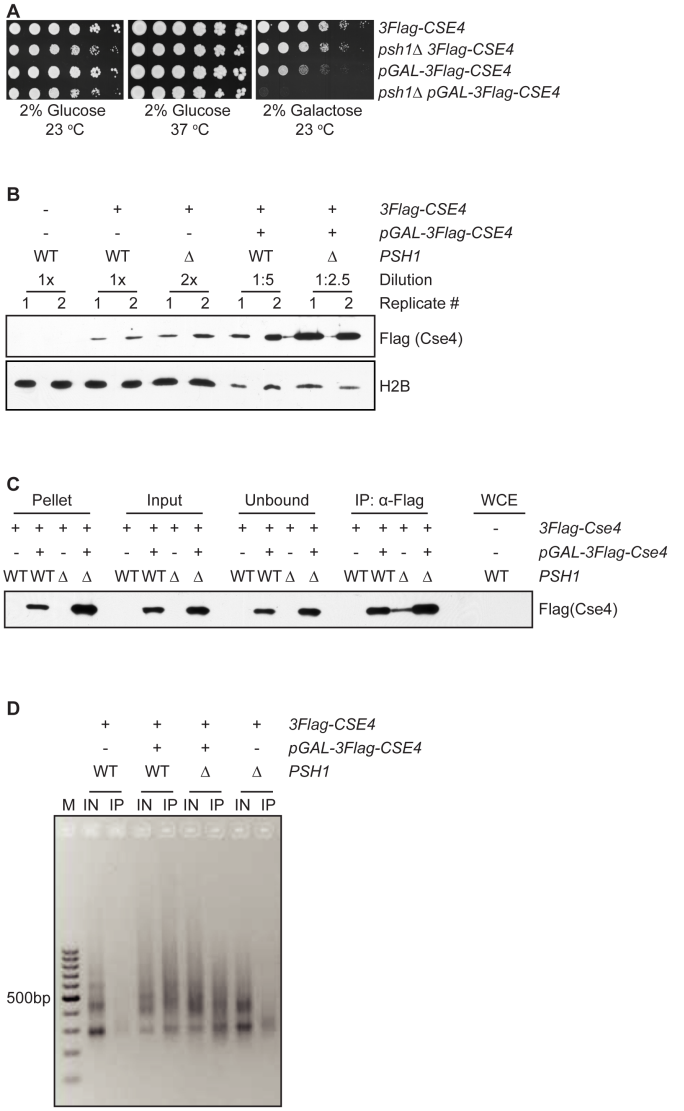

Supplemental Figure 2.1. Characterization of ChIP-seq strains
(A) 5-fold serial dilutions of ChIP-seq strains (*3Flag-CSE4* (SBY10419), *psh1*Δ *3Flag-CSE4* (SBY10484), *pGAL-3Flag-CSE4* (SBY10425) and *psh1*Δ *pGAL-3Flag-CSE4* (SBY10483)) grown on the indicated media at the indicated temperatures. (B) Immunoblot of CENP-A^{Cse4} and H2B levels in MNase-treated. chromatin (input) in the following strains: untagged WT (SBY3), *3Flag-CSE4* (SBY10419), *psh1*Δ *3Flag-CSE4* (SBY10484), *pGAL-3Flag-CSE4* (SBY10425) and *psh1*Δ *pGAL-3Flag-CSE4* (SBY10483). (C) Immunoblot of samples from the ChIP-seq experiment showing 3Flag-Cse4 in the insoluble pellet (Pellet), the MNase-treated input chromatin (Input), the unbound material (after anti-FLAG IP) (Unbound), and the anti-FLAG IP for the following strains: *3Flag-CSE4* (SBY10419), *pGAL-3Flag-CSE4* (SBY10425), *psh1*Δ *3Flag-CSE4* (SBY10484), and *psh1*Δ *pGAL-3Flag-CSE4* (SBY10483). Whole cell extract (WCE) from an untagged strain (SBY3) is also shown as a comparison. (D) Prepared Solexa libraries before sequencing for *3Flag-CSE4* (SBY10419), *pGAL-3Flag-CSE4* (SBY10425), *psh1*Δ *pGAL-3Flag-CSE4* (SBY10483) and *psh1*Δ *3Flag-CSE4* (SBY10484), Both Input (IN) and IP are shown for each strain.

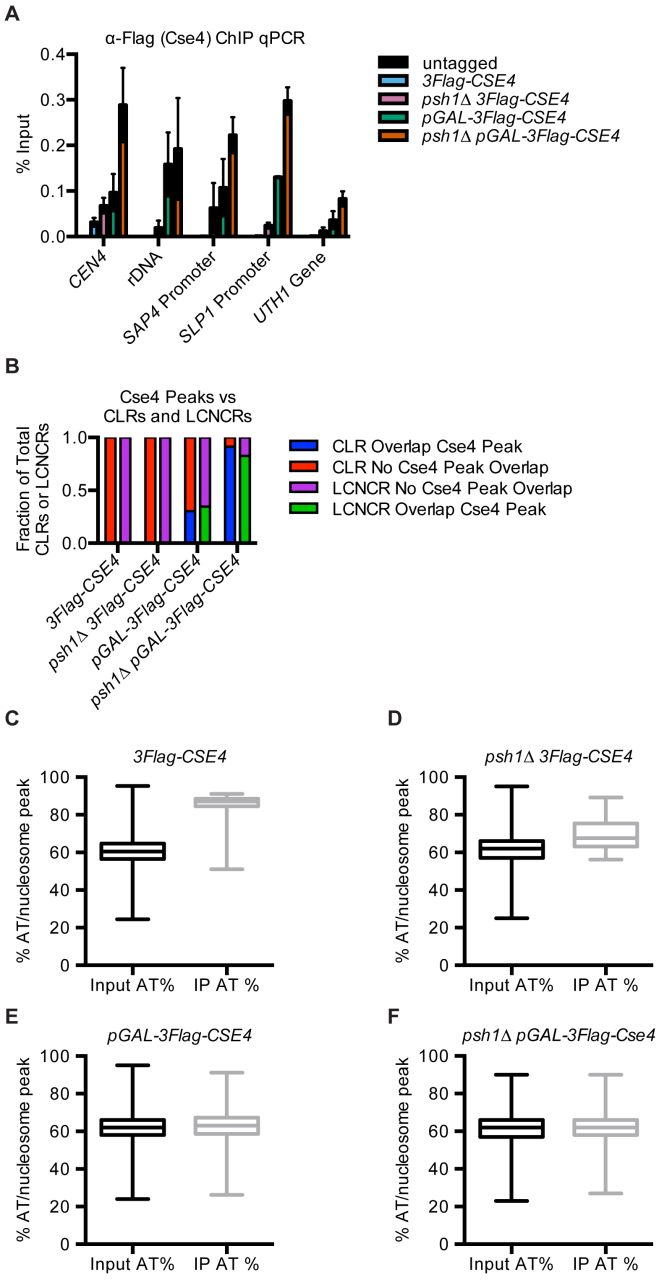

Supplemental Figure 2.2. Validation of ChIP-seq data
(A) ChIP-qPCR validation of CENP-A^{Cse4} centromeric peaks at *CEN4*, the rDNA locus, *SAP4* promoter, *SLP1* promoter, and the *UTH1* gene. % Input (means +/- 1 SEM) is shown for 2-4 biological replicates. Strains used were: untagged WT (SBY3, black), *3Flag-CSE4* (SBY10419, blue), *psh1Δ 3Flag-CSE4* (SBY10484, pink), *pGAL-3Flag-CSE4* (SBY10425, green) and *psh1Δ pGAL-3Flag-CSE4* (SBY10483, orange). (B) Fraction of total centromere like regions (CLRs) or low confidence negative control regions (LCNCRs) (*121*) that overlap CENP-A^{Cse4} ChIP-seq peaks in each strain. (C-F) AT% per CENP-A^{Cse4} ChIP or input nucleosome peak for the *3Flag-CSE4* strain (SBY10419), the *psh1Δ 3Flag-CSE4* strain (SBY10484), the *pGAL-3Flag-CSE4* strain (SBY10425), or the *psh1Δ pGAL-3Flag-CSE4* strain (SBY10483).

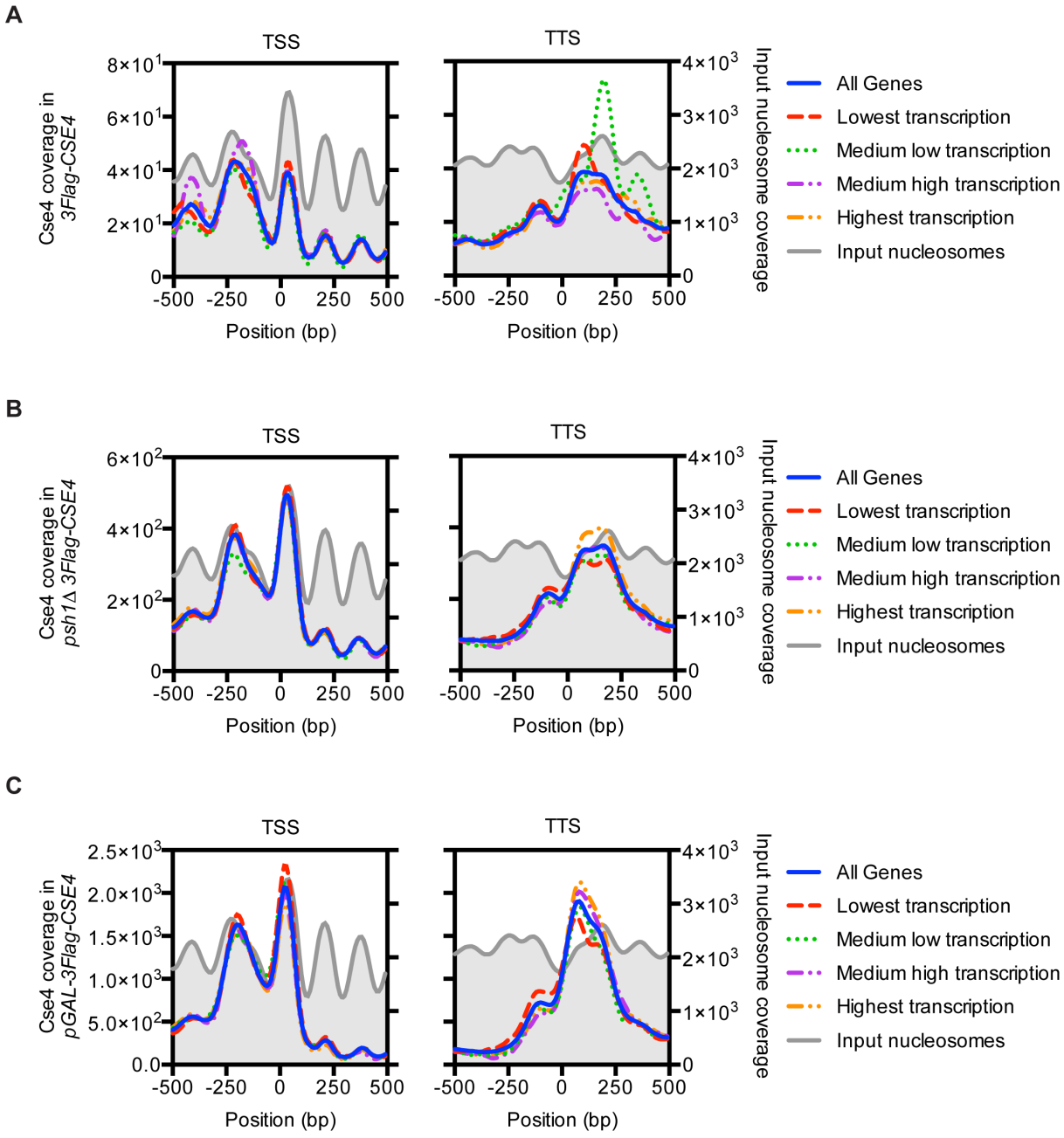

Supplemental Figure 2.3. Basal transcription levels are not correlated with CENP-A^{Cse4} mislocalization
(A-C) TSS and TTS profiles of CENP-A^{Cse4} ChIP compared to input nucleosome ChIP for *3Flag-CSE4* (SBY10419), *psh1*Δ *3Flag-CSE4* (SBY10484), or *pGAL-3Flag-CSE4* (SBY10425) strains. Genes are binned by basal transcription level (*157*).

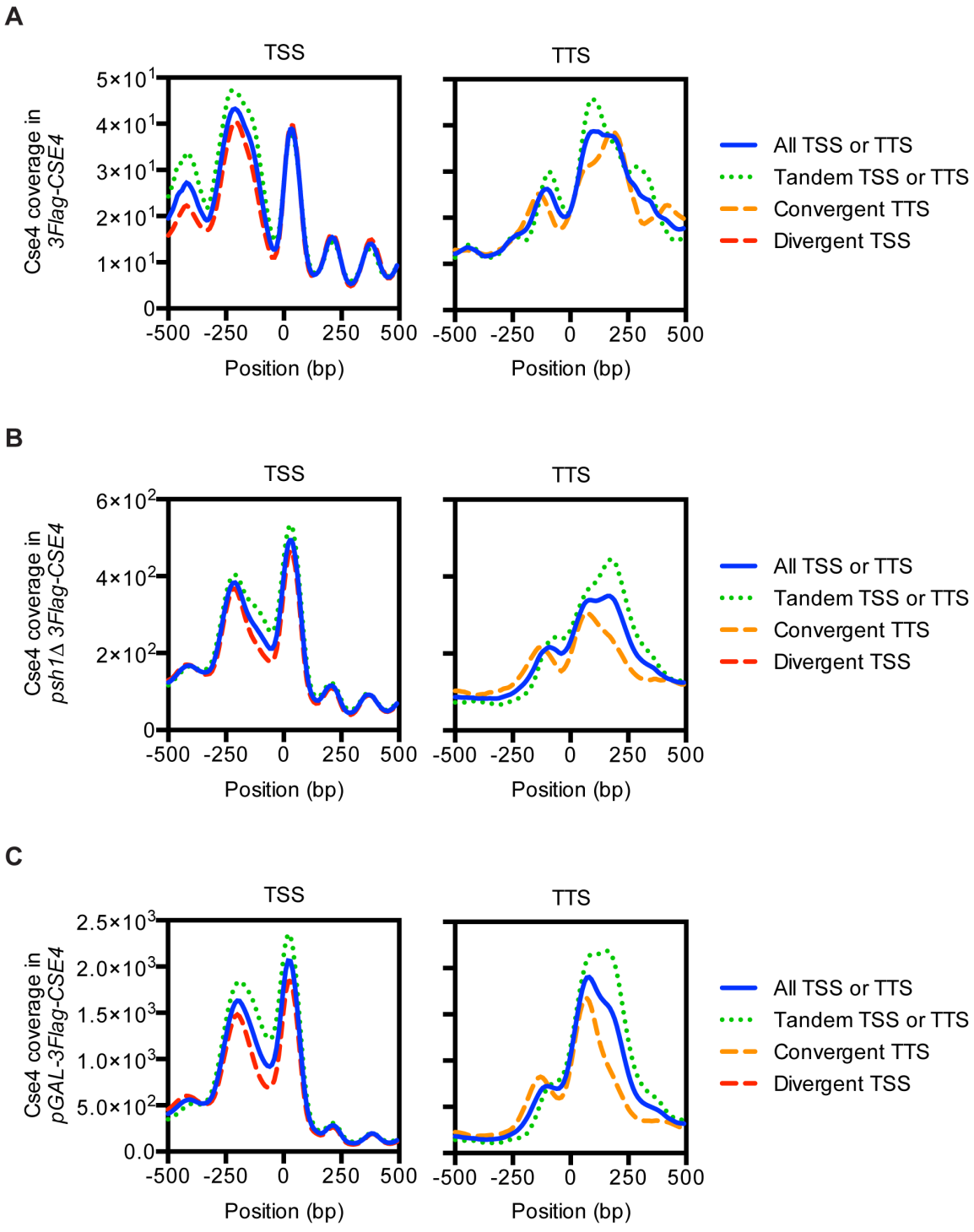

Supplemental Figure 2.4. Transcriptional direction is correlated with CENP-A^{Cse4} mislocalization
(A-C) TSS and TTS profiles of CENP-A^{Cse4} ChIP for *3Flag-CSE4* (SBY10419), *psh1Δ 3Flag-CSE4* (SBY10484), or *pGAL-3Flag-CSE4* (SBY10425) strains. The 5' and 3' ends of genes are binned by direction of upstream or downstream transcription.

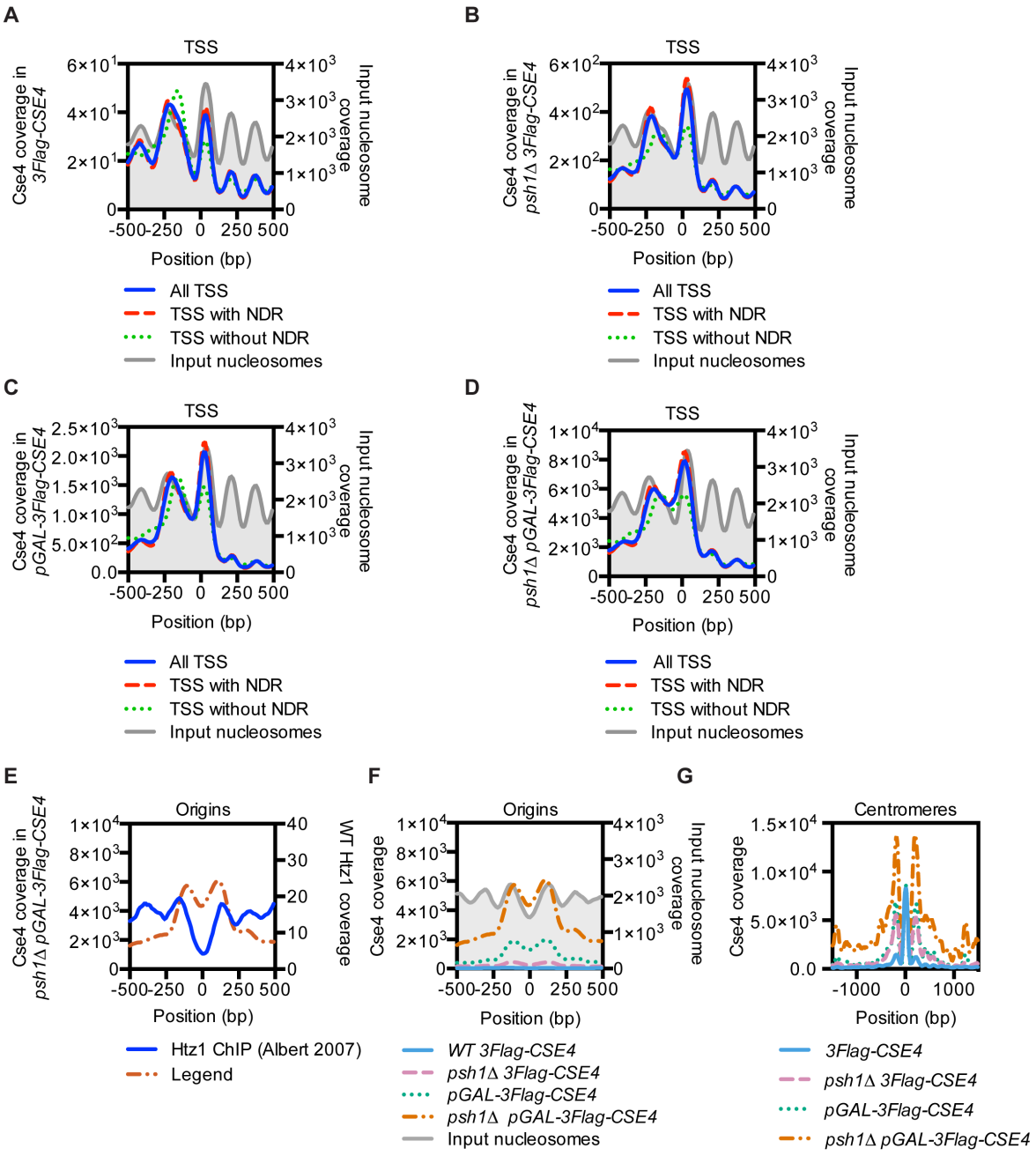

Supplemental Figure 2.5. CENP-A^{Cse4} is mislocalized to nucleosomes flanking NDRs, origins of replication, and centromeres

(A-D) Mean CENP-A^{Cse4} ChIP coverage 500 bp upstream and downstream of all transcription start sites (TSS), for *3Flag-CSE4* (SBY10419), *psh1Δ 3Flag-CSE4* (SBY10484), *pGAL-3Flag-CSE4* (SBY10425), and *psh1Δ pGAL-3Flag-CSE4* (SBY10483) strains separated by the presence of an annotated NDR (*160*) within the promoter. (E) Mean CENP-A^{Cse4} ChIP coverage for the *psh1Δ pGAL-3Flag-CSE4* (SBY10483) strain (left y axis) vs. mean H2A.Z^{Htz1} ChIP coverage (*21*) (right y axis) at all origins of replication. (F) Mean CENP-A^{Cse4} ChIP coverage for *3Flag-CSE4* (SBY10419), *psh1Δ 3Flag-CSE4* (SBY10484), *pGAL-3Flag-CSE4* (SBY10425), *psh1Δ pGAL-3Flag-CSE4* (SBY10483) strains at all origins. (G) Mean CENP-A^{Cse4} ChIP coverage for *3Flag-CSE4* (SBY10419), *psh1Δ 3Flag-CSE4* (SBY10484), *pGAL-3Flag-CSE4* (SBY10425), and *psh1Δ pGAL-3Flag-CSE4* (SBY10483) strains at all centromeres.

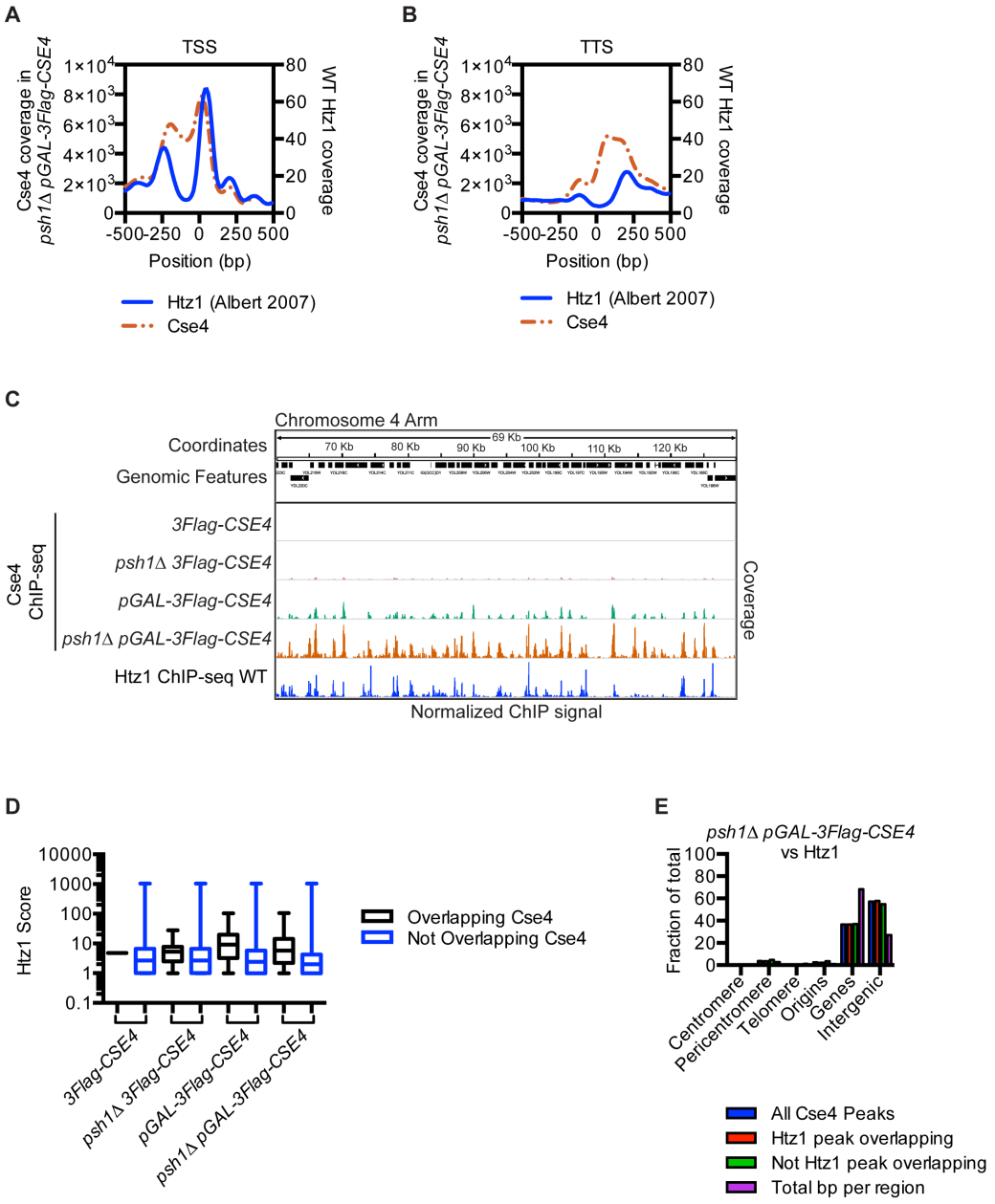

Supplemental Figure 2.6. CENP-A^{Cse4} localization to H2A.Z^{Htz1} nucleosomes
(A) Mean CENP-A^{Cse4} (from *psh1Δ pGAL-3Flag-CSE4* (SBY10483)) and H2A.Z^{Htz1} (from WT strain (*21*)) ChIP coverage 500 bp flanking all TSS. (B) Mean CENP-A^{Cse4} (from *psh1Δ pGAL-3Flag-CSE4* SBY10483) and H2A.Z^{Htz1} (from WT strain (*21*)) ChIP coverage 500 bp flanking all TTS. (C) CENP-A^{Cse4} ChIP coverage for the *3Flag-CSE4* (SBY10419, blue), *psh1Δ 3Flag-CSE4* (SBY10484, pink), *pGAL-3Flag-CSE4* (SBY10425, green), *psh1Δ pGAL-3Flag-CSE4* (SBY10483, orange) strain and WT H2A.Z^{Htz1} coverage (*21*) (blue) on the chromosome 4 arm between 60,000 bp and 130,000 bp. (D) Boxplot showing H2A.Z^{Htz1} score distributions for each H2A.Z^{Htz1} nucleosome with (black) or without (blue) overlapping CENP-A^{Cse4} peaks in the *3Flag-CSE4* (SBY10419), *psh1Δ pGAL-3Flag-CSE4* (SBY10484), *pGAL-3Flag-CSE4* (SBY10425) or *psh1Δ pGAL-3Flag-CSE4* (SBY10483) strains. (E) The percentage of CENP-A^{Cse4} peak centers separated by overlap with H2A.Z^{Htz1} peaks in each type of genomic region is graphed for the *psh1Δ pGAL-3Flag-CSE4* strain (SBY10483). See Figure 1B for the percentages of the total CENP-A^{Cse4} peaks in each genomic region.

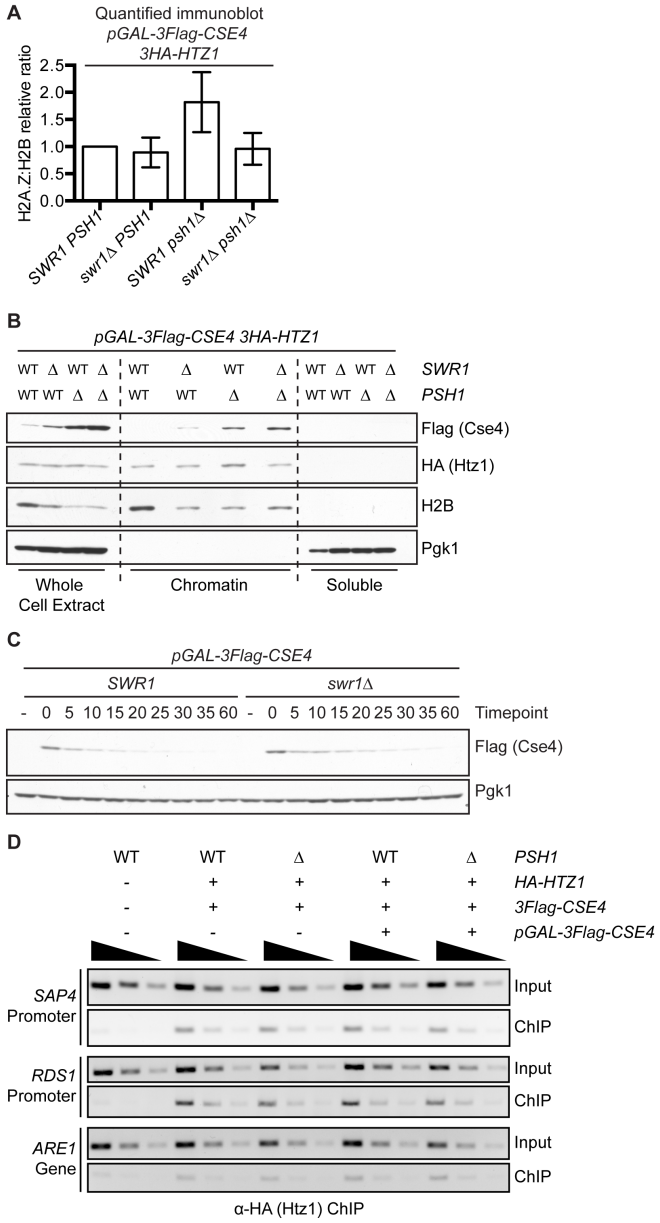

Supplemental Figure 2.7. The role of H2A.Z^{Htz1} and SWR-C in CENP-A^{Cse4} mislocalization
(A) Means +/- 1 SEM from quantitative immunoblots of chromatin fractionations measuring H2A.Z^{Htz1}:H2B fold change vs. the *pGAL-3Flag-CSE4* strain. Strains used: *pGAL-3Flag-CSE4 3HA-HTZ1* (SBY12832), *swr1*Δ *pGAL-3Flag-CSE4 3HA-HTZ1* (SBY12956), *psh1*Δ *pGAL-3Flag-CSE4 3HA-HTZ1* (SBY12833), and *swr1*Δ *psh1*Δ *pGAL-3Flag-CSE4 3HA-HTZ1* (SBY12924). n = 3. (B) Immunoblot of a chromatin fractionation experiment from strains as in (A). Pgk1 is a marker of the soluble fraction and H2B is a marker of the chromatin fraction. (C) Stability assay of *pGAL-3Flag-CSE4* in WT (SBY12332), vs. *swr1*Δ (SBY12333) background. (-) samples were taken before adding 2% galactose to induce *pGAL-3Flag-CSE4* overexpression. 0-60 minute timepoints were taken after adding 2% glucose and cyclohexamide (50ug/ml) to inhibit transcription and translation of *pGAL-3Flag-CSE4*. Pgk1 is shown as a loading control. (D) HA-Htz1 ChIP in untagged WT (SBY3), *3HA-HTZ1 3Flag-CSE4* (SBY12918), *psh1*Δ *3HA-HTZ1 3Flag-CSE4* (SBY13998), *3HA-HTZ1 pGAL-3Flag-CSE4* (SBY12832), *psh1*Δ *3HA-HTZ1 pGAL-3Flag-CSE4* (SBY12833) at the *SAP4* and *RDS1* promoters and within the *ARE1* gene.

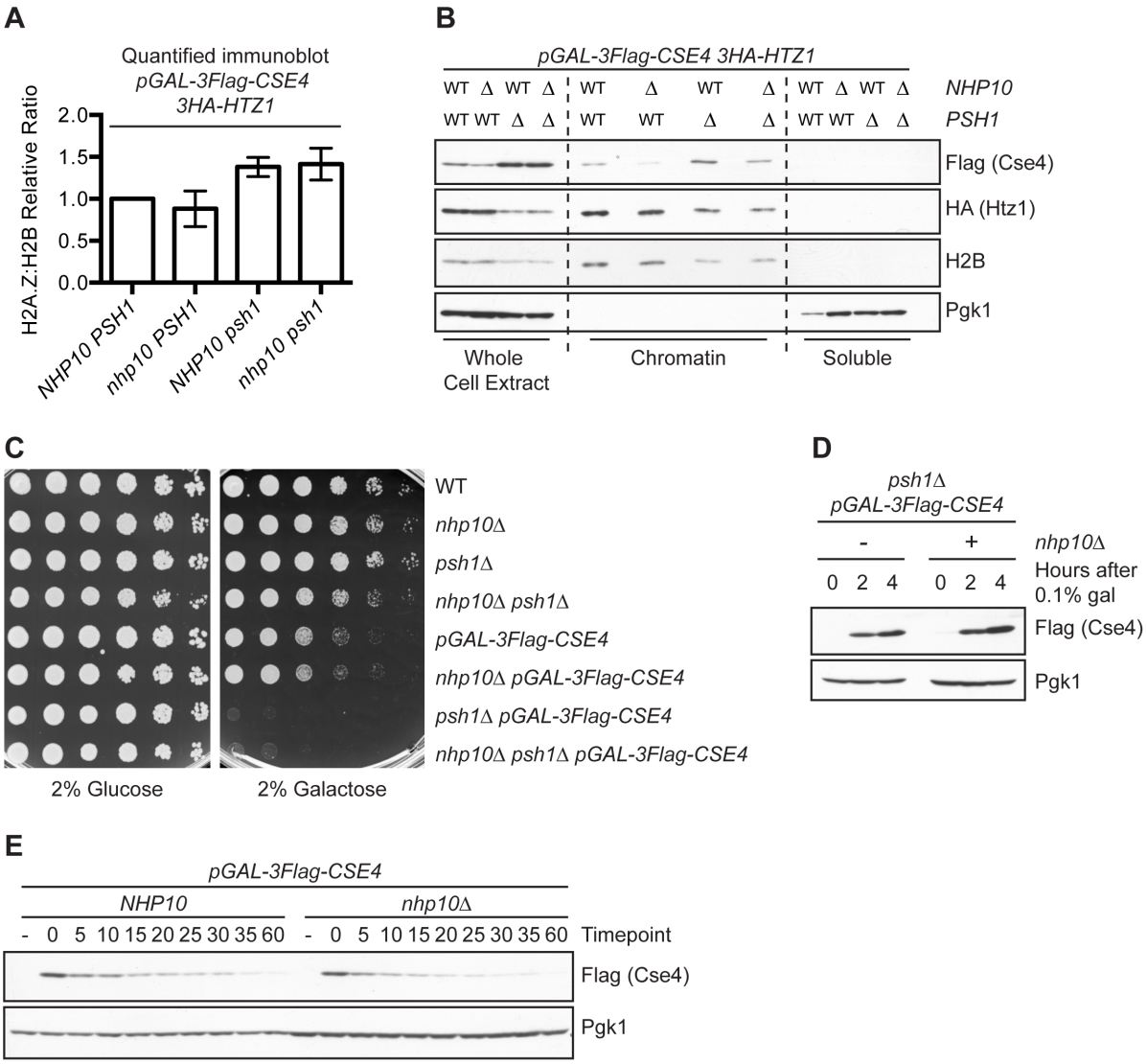

Supplemental Figure 2.8. The role of INO80-C in CENP-A^{Cse4} localization

(A) Mean +/- 1 SEM from quantitative immunoblots of chromatin fractionations measuring H2A.Z^{Htz1}:H2B fold change vs. *pGAL-3Flag-CSE4* strain. Strains used: *pGAL-3Flag-CSE4 HA-HTZ1* (SBY12832), *nhp10*Δ *pGAL-3Flag-CSE4 3HA-HTZ1* (SBY12930), *psh1*Δ *pGAL-3Flag-CSE4 3HA-HTZ1* (SBY12833), and *nhp10*Δ *psh1*Δ *pGAL-3Flag-CSE4 3HA-HTZ1* (SBY12959). n = 3. (B) Immunoblot of chromatin fractionation from the strains in (A). Pgk1 is a marker of the soluble fraction and H2B is a marker of the chromatin fraction. (C) 5-fold serial dilutions of WT (SBY3939), *nhp10*Δ (SBY11577), *psh1*Δ (SBY8336), *psh1*Δ *nhp10*Δ (SBY12346), *pGAL-3Flag-CSE4* (SBY12349), *nhp10*Δ *pGAL-3Flag-CSE4* (SBY12317), *psh1*Δ *pGAL-3Flag-CSE4* (SBY12350), *nhp10*Δ *psh1*Δ *pGAL-3Flag-CSE4* (SBY12348) strains on indicated media. (D) Immunoblot of CENP-A^{Cse4} levels when induced with low levels of galactose (0.1%) in *psh1*Δ *pGAL-3Flag-CSE4 3HA-HTZ1* (SBY12833) and *nhp10*Δ *psh1*Δ *pGAL-3Flag-CSE4 3HA-HTZ1* (SBY12959) cells. Pgk1 is shown as a loading control. (E) Stability assay of *pGAL-3Flag-CSE4* in wild-type (SBY12349) vs. *nhp10*Δ (SBY12317) background. (-) samples were taken before adding 2% galactose to induce *pGAL-3Flag-CSE4* overexpression. 0-60 minute timepoints were taken after adding 2% glucose and cyclohexamide (50ug/ml) to stop transcription and translation of *pGAL-3Flag-CSE4*. Pgk1 is shown as a loading control.

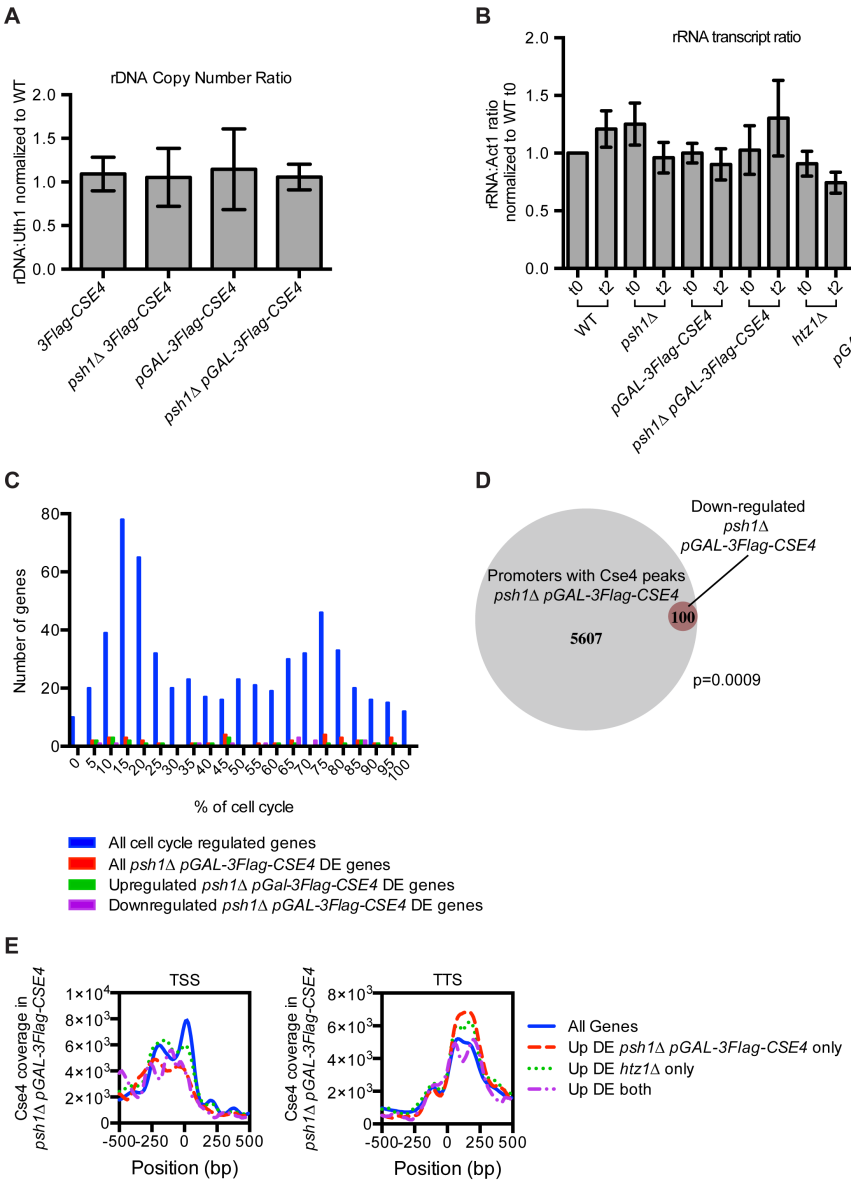

Supplemental Figure 2.9. Comparison of CENP-A^{Cse4} promoter mislocalization and changes in gene expression

(A) rDNA copy number ratio comparing the rDNA to *UTH1*, a single copy gene. Graph shows the mean ratio +/- 1 SEM for 3 biological replicates. Strains used were: *3Flag-CSE4* (SBY10419), *psh1Δ 3Flag-CSE4* (SBY10484), *pGAL-3Flag-CSE4* (SBY10425), *psh1Δ pGAL-3Flag-CSE4* (SBY10425). (B) rRNA expression analysis compared to *ACT1* at t0 and t2 for strains used in the RNA-seq experiment (see **Supplemental Table 2.5**). Graph shows mean ratio +/- 1 standard deviation. (n = 2-3) (C) Cell cycle distribution of cell cycle regulated genes differentially expressed (DE) at t2 in *psh1Δ pGAL-3Flag-CSE4*. (D) Proportional Venn diagram of genes upregulated in *psh1Δ pGAL-3Flag-CSE4* at t=2 hours and genes with CENP-A^{Cse4} peaks in their promoters in the *psh1Δ pGAL-3Flag-CSE4* strain. p = 0.009 from a cumulative hypergeometric distribution test. (E) TSS and TTS profiles of CENP-A^{Cse4} ChIP coverage in the *psh1Δ pGAL-3Flag-CSE4* (SBY10483) strain at all genes (blue), upregulated differentially expressed (DE) genes in *psh1Δ pGAL-3Flag-CSE4* only (red), upregulated DE genes in *htz1Δ* only (green), or upregulated DE genes in both *psh1Δ pGAL-3Flag-CSE4* and *htz1Δ* (purple).

2.8 SUPPLEMENTAL TABLES

Supplemental Table 2.1. ChIP-seq information

Strain	Input Correctly Mapped Mono-nucleosomal Read #	IP Correctly Mapped Mono-nucleosomal Read #	Input Average Read Length	IP Average Read Length	Average Mono-nucleosomal Read Depth/bp Input	Average Mono-nucleosomal Read Depth/bp IP
3Flag-CSE4 (SBY10419)	22462364	3016017	164	161	303	203
psh1Δ 3Flag-CSE4 (SBY10484)	19476982	1530412	148	147	238	88
pGAL-3Flag-CSE4 (SBY10425)	54398610	17742746	158	158	708	1145
psh1Δ pGAL-3Flag-CSE4 (SBY10483)	37815050	13220125	149	154	464	602

Supplemental Table 2.2. Yeast strains used in this chapter.

All strains are isogenic to W303

Strain	Genotype	Integrated and [replicating] plasmids	Source
SBY3	*MAT**a** ura3-1 leu2,3-112 his3-11 trp1-1 ade2-1 can1-100 bar1-1 bud4 rad5-535*		
SBY3939	*MAT**a** ura3-1 leu2,3-112 his3-11 trp1-1 ade2-1 can1-100 bar1-1 bud4 RAD5*		
SBY4471	*MAT**a** ura3-1 leu2,3-112 his3-11 trp1-1::pGAL-H3:TRP1 ade2-1 can1-100 bar1-1 bud4 RAD5*	*pSB893*	
SBY6183	*MAT**a** ura3-1 leu2,3-112 his3-11 trp1-1 ade2-1 can1-100 bar1-1 bud4 RAD5 htz1::HYG*		(*202*)
SBY9540	*MAT**a** ura3-1 leu2,3-112::pGAL-3Flag-CSE4::LEU2 his3-11 trp1-1 ade2-1 can1-100 bar1-1 bud4 rad5-535*	*pSB1729*	
SBY10419	*MAT**a** ura3-1::pCSE4-3Flag-CSE4::URA leu2,3-112 his3-11 trp1-1 ade2-1 can1-100 bar1-1 bud4 RAD5 cse4::KAN*	*pSB1067*	
SBY10425	*MAT**a** ura3-1::pCSE4-3Flag-CSE4::URA leu2,3-112::pGAL-3Flag-CSE4::LEU2 his3-11 trp1-1 ade2-1 can1-100 bar1-1 bud4 RAD5 cse4::KAN*	*pSB1067, pSB1729*	
SBY10483	*MAT**a** ura3-1::pCSE4-3Flag-CSE4::URA leu2,3-112::pGAL-3Flag-CSE4::LEU2 his3-11 trp1-1 ade2-1 can1-100 bar1-1 bud4 RAD5 cse4::KAN psh1::KAN*	*pSB1067, pSB1729*	
SBY10484	*MAT**a** ura3-1::pCSE4-3Flag-CSE4::URA leu2,3-112 his3-11 trp1-1 ade2-1 can1-100 bar1-1 bud4 RAD5 cse4::KAN psh1::KAN*	*pSB1067*	
SBY12317	*MAT**a** ura3-1 leu2,3-112::pGAL-3Flag-CSE4::LEU2 his3-11 trp1-1 ade2-1 can1-100 bar1-1 bud4 rad5-535 nhp10::HYG*	*pSB1729*	*nhp10::HYG* from (*203*)
SBY12332	*MAT**a** ura3-1 leu2,3-112::pGAL-3Flag-CSE4::LEU2 his3-11 trp1-1 ade2-1 can1-100 bar1-1 bud4 rad5-535*	*pSB1729*	
SBY12333	*MAT**a** ura3-1 leu2,3-112::pGAL-3Flag-CSE4::LEU2 his3-11 trp1-1 ade2-1 can1-100 bar1-1 bud4 rad5-535 swr1::HYG*	*pSB1729*	*swr1::HYG* from (*204*)
SBY12338	*MAT**a** ura3-1 leu2,3-112::pGAL-3Flag-CSE4::LEU2 his3-11 trp1-1 ade2-1 can1-100 bar1-1 bud4 RAD5 psh1::KAN*	*pSB1729*	
SBY12349	*MAT**a** ura3-1 leu2,3-112::pGAL-3Flag-CSE4::LEU2 his3-11 trp1-1 ade2-1 can1-100 bar1-1 bud4 RAD5*	*pSB1729*	
SBY12350	*MAT**a** ura3-1 leu2,3-112::pGAL-3Flag-CSE4::LEU2 his3-11 trp1-1 ade2-1 can1-100 bar1-1 bud4 RAD5 psh1::KAN*	*pSB1729*	
SBY12779	*MAT**a** ura3-1 leu2,3-112 his3-11 trp1-1 ade2-1 can1-100 bar1-1 bud5 RAD5 htz1::HYG::pHTZ1-3HA-HTZ1::TRP*	*pSB1072*	
SBY12832	*MAT**a** ura3-1::pCSE4-3Flag-CSE4::URA leu2,3-112::pGAL-3Flag-CSE4::LEU2 his3-11 trp1-1 ade2-1 can1-100 bar1-1 bud4 RAD5 htz1::HYG::pHTZ1-3HA-HTZ1::TRP cse4::KAN*	*pSB1067, pSB1072, pSB1729*	
SBY12833	*MAT**a** ura3-1::pCSE4-3Flag-CSE4::URA leu2,3-112::pGAL-3Flag-CSE4::LEU2 his3-11 trp1-1 ade2-1 can1-100 bar1-1 bud4 RAD5 htz1::HYG::pHTZ1-3HA-HTZ1::TRP cse4::KAN psh1::KAN*	*pSB1067, pSB1072, pSB1729*	
SBY12918	*MAT**a** ura3-1::pCSE4-3Flag-CSE4::URA leu2,3-112 his3-11 trp1-1 ade2-1 can1-100 bar1-1 bud4 RAD5*	*pSB1067, pSB1072*	

	htz1::HYG::pHTZ1-3HA-HTZ1::TRP cse4::KAN	
SBY12920	*MAT**a** ura3-1::pCSE4-3Flag-CSE4::URA leu2,3-112 his3-11 trp1-1 ade2-1 can1-100 bar1-1 bud4 RAD5 htz1::HYG::pHTZ1-3HA-HTZ1::TRP cse4::KAN swr1::HYG*	*pSB1067, pSB1729*
SBY12922	*MAT**a** ura3-1::pCSE4-3Flag-CSE4::URA leu2,3-112 his3-11 trp1-1 ade2-1 can1-100 bar1-1 bud4 RAD5 htz1::HYG::pHTZ1-3HA-HTZ1::TRP cse4::KAN swr1::HYG psh1::KAN*	*pSB1067, pSB1072, pSB1729*
SBY12924	*MAT**a** ura3-1::pCSE4-3Flag-CSE4::URA leu2,3-112::pGAL-3Flag-CSE4::LEU2 his3-11 trp1-1 ade2-1 can1-100 bar1-1 bud4 RAD5 htz1::HYG::pHTZ1-3HA-HTZ1::TRP cse4::KAN swr1::HYG psh1::KAN*	*pSB1067, pSB1729, pSB1072*
SBY12928	*MAT**a** ura3-1::pCSE4-3Flag-CSE4::URA leu2,3-112 his3-11 trp1-1 ade2-1 can1-100 bar1-1 bud4 RAD5 htz1::HYG::pHTZ1-3HA-HTZ1::TRP cse4::KAN nhp10::HYG psh1::KAN*	*pSB1067*
SBY12930	*MAT**a** ura3-1::pCSE4-3Flag-CSE4::URA leu2,3-112::pGAL-3Flag-CSE4::LEU2 his3-11 trp1-1 ade2-1 can1-100 bar1-1 bud4 RAD5 htz1::HYG::pHTZ1-3HA-HTZ1::TRP cse4::KAN nhp10::HYG*	*pSB1067, pSB1072, pSB1729*
SBY12956	*MAT**a** ura3-1::pCSE4-3Flag-CSE4::URA leu2,3-112::pGAL-3Flag-CSE4::LEU2 his3-11 trp1-1 ade2-1 can1-100 bar1-1 bud4 RAD5 htz1::HYG::pHTZ1-3HA-HTZ1::TRP cse4::KAN swr1::HYG*	*pSB1067, pSB1072, pSB1729*
SBY12958	*MAT**a** ura3-1::pCSE4-3Flag-CSE4::URA leu2,3-112 his3-11 trp1-1 ade2-1 can1-100 bar1-1 bud4 RAD5 htz1::HYG::pHTZ1-3HA-HTZ1::TRP cse4::KAN nhp10::HYG*	*pSB1067, pSB1072*
SBY12959	*MAT**a** ura3-1::pCSE4-3Flag-CSE4::URA leu2,3-112::pGAL-3Flag-CSE4::LEU2 his3-11 trp1-1 ade2-1 can1-100 bar1-1 bud4 RAD5 htz1::HYG::pHTZ1-3HA-HTZ1::TRP cse4::KAN nhp10::HYG psh1::KAN*	*pSB1067, pSB1072, pSB1729*
SBY13702	*MAT**a** ura3-1 leu2,3-112 his3-11 trp1-1 ade2-1 can1-100 bar1-1 bud4 rad5-535 htz1::HYG::pHTZ1-3HA-HTZ1::TRP*	*pSB1072*
SBY13998	*MAT**a** ura3-1::pCSE4-3Flag-CSE4::URA leu2,3-112 his3-11 trp1-1 ade2-1 can1-100 bar1-1 bud4 RAD5 htz1::HYG::pHTZ1-3HA-HTZ1::TRP cse4::KAN psh1::KAN*	*pSB1067, pSB1072*
SBY14482	*MAT**a** ura3-1::pCSE4-3Flag-CSE4::URA leu2,3-112::pGAL-3Flag-CSE4::LEU2 his3-11 trp1-1 ade2-1 can1-100 bar1-1 bud4 RAD5 cse4::KAN PSH1-13Myc::HIS htz1::HYG::pHTZ1-3HA-HTZ1::TRP*	*pSB1067 pSB1729*
SBY14515	*MAT**a** ura3-1 leu2,3-112::pGAL-3Flag-CSE4::LEU2 his3-11 trp1-1 ade2-1 can1-100 bar1-1 bud4 rad5-535 INO80-13Myc::HIS psh1::KAN*	*pSB1729*
SBY14526	*MAT**a** ura3-1 leu2,3-112::pGAL-3Flag-CSE4::LEU2 his3-11 trp1-1 ade2-1 can1-100 bar1-1 bud4 rad5-535 INO80-13Myc::HIS*	*pSB1729*
SBY14527	*MAT**a** ura3-1 leu2,3-112 his3-11 trp1-1 ade2-1 can1-100 bar1-1 bud4 rad5-535 INO80-13Myc::HIS*	
SBY15903	*MAT**a** ura3-1 leu2,3-112 his3-11 trp1-1 ade2-1 can1-100 bar1-1 rad5-535 2uM::pTET-CSE4::URA*	*[pSB1073]*
SBY15904	*MAT**a** ura3-1 leu2,3-112 his3-11 trp1-1 ade2-1 can1-100*	*[pSB1073]*

	bar1-1 rad5-535 2uM::pTET-CSE4::URA psh1::KAN	
SBY15906	*MAT**a** ura3-1 leu2,3-112 his3-11 trp1-1 ade2-1 can1-100 bar1-1 rad5-535 2uM::pTET-CSE4::URA psh1::KAN htz1::KAN*	*[pSB1073]*
SBY15924	*MAT**a** ura3-1 leu2,3-112 his3-11 trp1-1 ade2-1 can1-100 bar1-1 rad5-535 2uM::pTET-Empty::URA*	*[pSB416]*
SBY16018	*MAT**a** ura3-1 leu2,3-112 his3-11 trp1-1 ade2-1 can1-100 bar1-1 bud4 RAD5 psh1::KAN*	
SBY16066	*MAT**a** ura3-1 leu2,3-112::pGAL-3Flag-CSE4:LEU2 his3-11 trp1-1 ade2-1 can1-100 bar1-1 bud4 RAD5*	*pSB1729*
SBY16072	*MAT**a** ura3-1 leu2,3-112 his3-11 trp1-1 ade2-1 can1-100 bar1-1 bud4 RAD5*	
SBY16074	*MAT**a** ura3-1 leu2,3-112 his3-11 trp1-1 ade2-1 can1-100 bar1-1 bud4 RAD5 htz1::HYG*	
SBY16076	*MAT**a** ura3-1 leu2,3-112 his3-11 trp1-1::pGAL-H3::TRP1 ade2-1 can1-100 bar1-1 bud4 RAD5*	*pSB893*
SBY16080	*MAT**a** ura3-1 leu2,3-112 his3-11 trp1-1 ade2-1 can1-100 bar1-1 bud4 RAD5*	
SBY16082	*MAT**a** ura3-1 leu2,3-112 his3-11 trp1-1 ade2-1 can1-100 bar1-1 bud4 RAD5 htz1::HYG*	
SBY16084	*MAT**a** ura3-1 leu2,3-112 his3-11 trp1-1::pGAL-H3::TRP1 ade2-1 can1-100 bar1-1 bud4 RAD5*	*pSB893*
SBY16099	*MAT**a** ura3-1 leu2,3-112 his3-11 trp1-1 ade2-1 can1-100 bar1-1 bud4 RAD5 psh1::KAN*	
SBY16101	*MAT**a** ura3-1 leu2,3-112 his3-11 trp1-1 ade2-1 can1-100 bar1-1 bud4 RAD5 psh1::KAN*	
SBY16102	*MAT**a** ura3-1 leu2,3-112::pGAL-3Flag-CSE4::LEU2 his3-11 trp1-1 ade2-1 can1-100 bar1-1 bud4 RAD5*	*pSB1729*
SBY16103	*MAT**a** ura3-1 leu2,3-112::pGAL-3Flag-CSE4:LEU2 his3-11 trp1-1 ade2-1 can1-100 bar1-1 bud4 RAD5 psh1::HYG*	*pSB1729*

Supplemental Table 2.3. Plasmids used in this chapter

Plasmid Number	Description	Source
pSB1067	*pCSE4-3Flag-CSE4* + 500bp downstream, *URA3* (integrating)	(*118*)
pSB1072	*pHTZ1-3HA-HTZ1* + 250bp downstream, *TRP1* (integrating)	Biggins Lab
pSB1729	*pGAL-3Flag-CSE4* + 500bp downstream, *LEU2* (integrating)	Biggins Lab
pSB893	*pGAL-HHT1, TRP1* (integrating)	(*43*)
pSB1073	*pTET-CSE4, URA3,* 2mM	Biggins Lab
pSB416 (CM190)	*pTET-empty vector*, URA3, 2m*M*	(*188*)

Supplemental Table 2.4. Oligonucleotides used in this chapter

Oligo Number	Purpose	Sequence	Source
SB773	*CEN3* Forward	ATCAGCGCCAAACAATATGGAAAA	(*178*)
SB774	*CEN3* Reverse	GAGCAAAACTTCCACCAGTAAACG	(*178*)
SB3061	*CEN4* forward	TCACATGCTTATAATCAACTTTT	K. Krassovsky, S. Henikoff
SB3062	*CEN4* Reverse	TGTTTCGGTAATCATAAACAA	K. Krassovsky, S. Henikoff
SB3735	*SAP4* Promoter Forward	ACAGCACAACACGCTTACCA	This study
SB3736	*SAP4* Promoter Reverse	CCAGCCCTAAATCCCCTAAA	This study
SB3781	*SLP1* Promoter Forward	TCCTAGGTTATCTCATCGGTACT	This study
SB3782	*SLP1* Promoter Reverse	ACTATATCCATTGCGTCCTTTCT	This study
SB3814	*UTH1* Gene Forward	GTAACACCGCCACCTCTTGT	This study
SB3815	*UTH1* Gene Reverse	ACCATCGGAAGGTTGTTCAG	This study
SB4768 (CR2)	*RDS1* Promoter Forward	GACCCGTGCAGATCACTATTACA	(*56*)
SB4769 (CR2)	*RDS1* Promoter Reverse	GCAGTTTATCACATTTCCGTTTG	(*56*)
SB4983 (TT4412)	*rDNA (RDN25)* Forward	GCCTGTGGGAATACTGCCAG	L. Lee, T. Tsukiyama
SB4984 (TT4413)	*rDNA (RDN25)* Reverse	CCATCTTTCGGGTCCCAACAGC	L. Lee, T. Tsukiyama
SB4762	*ARE1* Gene	AAGGAATCTTTGTCCCCAGAGA	(*56*)
SB4763	*ARE1* Gene	TCTTGGGTAGTTGATCTGGTACAC	(*56*)

Supplemental Table 2.5. RNA-seq information

Sample Name	Strain number	Mapped Reads
WT t0 batch 1	SBY3939	8,052,352
psh1ΔKAN t0 batch 1	SBY16099	8,479,755
psh1ΔKAN leu2-3,112::pGAL-3Flag-CSE4:LEU2 t0 batch 1	SBY12350	7,285,227
htz1ΔHYG t0 batch 1	SBY6183	8,736,689
trp1-1::pGAL-H3:TRP1 t0 batch 1	SBY4471	8,066,430
WT t2 batch 1	SBY3939	7,748,726
psh1ΔKAN t2 batch 1	SBY16099	7,513,193
psh1ΔKAN leu2-3,112::pGAL-3Flag-CSE4:LEU2 t2 batch 1	SBY12350	7,392,085
htz1ΔHYG t2 batch 1	SBY6183	7,003,319
trp1-1::pGAL-H3:TRP1 t2 batch 1	SBY4471	7,926,433
WT t0 batch 2	SBY16072	7,652,177
psh1ΔKAN t0 batch 2	SBY16101	7,471,872
leu2-3,112::pGAL-3Flag-CSE4:LEU2 t0 batch 2	SBY16102	7,531,780
psh1ΔKAN leu2-3,112::pGAL-3Flag-CSE4:LEU2 t0 batch 2	SBY12338	6,919,807
htz1ΔHYG t0 batch 2	SBY16074	7,035,485
trp1-1::pGAL-H3:TRP1 t0 batch 2	SBY16076	6,975,987
WT t2 batch 2	SBY16072	7,227,820
psh1ΔKAN t2 batch 2	SBY16101	7,702,140
leu2-3,112::pGAL-3Flag-CSE4:LEU2 t2 batch 2	SBY16102	7,740,670
psh1ΔKAN leu2-3,112::pGAL-3Flag-CSE4:LEU2 t2 batch 2	SBY12338	6,922,124
htz1ΔHYG t2 batch 2	SBY16074	7,162,966
trp1-1::pGAL-H3:TRP1 t2 batch 2	SBY16076	7,758,302
WT t0 batch 3	SBY16080	7,239,742
psh1ΔKAN t0 batch 3	SBY16018	7,337,970
leu2-3,112::pGAL-3Flag-CSE4:LEU2 t0 batch 3	SBY16066	6,778,973
psh1ΔKAN leu2-3,112::pGAL-3Flag-CSE4:LEU2 t0 batch 3	SBY16103	7,624,807
htz1ΔHYG t0 batch 3	SBY16082	7,267,024
trp1-1::pGAL-H3:TRP1 t0 batch 3	SBY16084	7,764,848
WT t2 batch 3	SBY16080	7,854,429
psh1ΔKAN t2 batch 3	SBY16018	7,302,453
leu2-3,112::pGAL-3Flag-CSE4:LEU2 t2 batch 3	SBY16066	7,518,238
psh1ΔKAN leu2-3,112::pGAL-3Flag-CSE4:LEU2 t2 batch 3	SBY16103	7,228,229
htz1ΔHYG t2 batch 3	SBY16082	6,867,970
trp1-1::pGAL-H3:TRP1 t2 batch 3	SBY16084	7,862,726

2.9 SUPPLEMENTAL FILES

Supplemental File 2.1. RNA-seq differential gene expression data.

Supplemental File 2.2. Transcription factor enrichment analysis.

Chapter 3. HISTONE H4 FACILITATES THE PROTEOLYSIS OF THE BUDDING YEAST CENP-A^{CSE4} CENTROMERIC HISTONE VARIANT

*Modified from an article of the same title published in Genetics (*205*)

Gary M.R. Deyter[*,†,1], Erica M. Hildebrand[*,†,‡], Adrienne D. Barber[†], and Sue Biggins[†]

[*] These authors contributed equally

[†] Howard Hughes Medical Institute, Division of Basic Sciences, Fred Hutchinson Cancer Research Center, Seattle, WA 98040

[‡] Molecular and Cellular Biology Program, University of Washington, Seattle, WA 98195

[1]Department of Health Services Research, University of Texas MD Anderson Cancer Center, 1400 Pressler St., Unit 1444, Houston, TX 77030

Running title: Histone H4 regulates CENP-A proteolysis

Keywords: CENP-A^{Cse4}; H4; Psh1; proteolysis; centromere; nucleosome

Corresponding author:
Sue Biggins
1100 Fairview Ave N., A2-168
PO Box 19024
Seattle, WA 98109
206-667-1351
sbiggins@fredhutch.org

3.1 SUMMARY

The incorporation of histone variants into nucleosomes can alter chromatin-based processes. CENP-A is the histone H3 variant found exclusively at centromeres that serves as an epigenetic mark for centromere identity and is required for kinetochore assembly. CENP-A mislocalization to ectopic sites appears to contribute to genomic instability, transcriptional misregulation, and tumorigenesis, so mechanisms exist to ensure its exclusive localization to centromeres. One conserved process is proteolysis, which is mediated by the Psh1 E3 ubiquitin ligase in budding yeast. To determine whether there are features of the CENP-A nucleosome that facilitate proteolysis, we performed a genetic screen to identify histone H4 residues that regulate CENP-A^{Cse4} degradation. We found that H4-R36 is a key residue that promotes the interaction between CENP-A^{Cse4} and Psh1. Consistent with this, CENP-A^{Cse4} protein levels are stabilized in H4-R36A mutant cells and CENP-A^{Cse4} is enriched in the euchromatin. We propose that the defects in CENP-A^{Cse4} proteolysis may be related to changes in Psh1 localization, as Psh1 becomes enriched at some 3' intergenic regions in H4-R36A mutant cells. Together, these data reveal a key residue in histone H4 that is important for efficient CENP-A^{Cse4} degradation, likely by facilitating the interaction between Psh1 and CENP-A^{Cse4}.

3.2 INTRODUCTION

Chromatin structure is a barrier to many processes that must gain access to DNA to generate the biomolecules required for cellular viability (*2*). Chromatin also serves as a platform that promotes the association of supramolecular structures with DNA, such as kinetochores that form on centromeres and capping structures that assemble at telomeres (*67, 206*). The foundation of chromatin is histones, which associate with and compact DNA. Histones are therefore subject to

a variety of regulation, such as post-translational modifications and regulated incorporation or removal at various genomic regions (*26*). Chromatin is also regulated by the deposition of histone variants, which can alter chromatin structure and accessibility to regulate cellular processes (*14*). One conserved histone is the H3 variant CENP-A, which localizes to centromeres to mediate their epigenetic propagation and to serve as the foundation for kinetochore assembly (*67, 207-209*). Consistent with this, CENP-A mislocalization to euchromatin can lead to ectopic kinetochore formation, genome instability, and transcriptional misregulation (*124, 129, 131, 210*). It is therefore essential that CENP-A exclusively localizes to centromeres and does not stably incorporate into euchromatin.

One conserved mechanism that prevents ectopic CENP-A localization is ubiquitin-mediated proteolysis (*42, 111, 112, 115, 116*). The most detailed understanding of CENP-A proteolysis is in budding yeast, where the E3 ubiquitin ligase Psh1 mediates CENP-A^{Cse4} degradation to limit its incorporation into euchromatin (*43, 44*). Psh1 requires its association with the conserved FACT (Facilitates Chromatin Transcription/Transactions) complex to bind to CENP-A^{Cse4} and mediate ubiquitylation, and a loss of this interaction results in CENP-A^{Cse4} mislocalization and cell death when CENP-A^{Cse4} is overexpressed (*118*). FACT (consisting of the Spt16 and Pob3 proteins) influences many aspects of the dynamic nature of chromatin, and we previously proposed that its role in chromatin disassembly allows Psh1 to access mislocalized CENP-A^{Cse4} for ubiquitylation (*118*). Proline isomerization is also important for CENP-A^{Cse4} degradation because it is impaired in *fpr3* and *fpr4* proline isomerase mutants (*105*). CENP-A^{Cse4} has several proline residues that may require isomerization to promote an interaction with Psh1 (*105*). Although CENP-A stably associates with histone H4 in CENP-A/H4 dimers and tetramers, the

contribution of histone H4 or other features of the centromeric nucleosome to CENP-A proteolysis is unknown (*95, 211*).

Here, we report that the histone H4 residue R36 contributes to CENP-A^{Cse4} degradation. CENP-A^{Cse4} overexpression is toxic to H4-R36A mutants, and this lethality is unrelated to centromere dysfunction because kinetochore composition and chromosome segregation are normal in these cells. Instead, overexpressed CENP-A^{Cse4} is stabilized and enriched in the euchromatin in the H4-R36A mutant, indicating a role for histone H4 in preventing CENP-A^{Cse4} mislocalization. Consistent with this, the interaction between Psh1 and CENP-A^{Cse4} is decreased in the H4 mutant. In addition, Psh1 becomes enriched at 3' ends of genes, similar to the mislocalization pattern of the FACT component Spt16 in H4-R36A mutant cells (*130*). The mislocalization of Psh1 to 3' intergenic regions raises the possibility that it has reduced access to CENP-A^{Cse4} at promoters and intragenic regions, resulting in elevated CENP-A^{Cse4} levels in the euchromatin. Together, our data identify a role for histone H4 in promoting an interaction between Psh1 and CENP-A^{Cse4} to prevent the promiscuous incorporation of CENP-A^{Cse4} into euchromatin.

3.3 RESULTS

3.3.1 *H4-R36A mutant cells are sensitive to CENP-A^{Cse4} overexpression*

Because CENP-A^{Cse4} proline residues influence its degradation, we hypothesized that additional features of the CENP-A^{Cse4} nucleosome might be important for CENP-A^{Cse4} proteolysis (*105*). CENP-A^{Cse4} binds with high affinity to histone H4 before and after deposition on DNA, so we asked whether histone H4 residues are important for CENP-A^{Cse4} degradation. To do this, we took advantage of the fact that mutants defective in CENP-A^{Cse4} degradation are sensitive to

CENP-A^{Cse4} overexpression (*43, 44*). We used a previously constructed library of budding yeast histone H4 mutants where each amino acid was changed to alanine to screen for mutants that are intolerant to CENP-A^{Cse4} overexpression (*177, 212*). We transformed the H4 library with a high-copy plasmid expressing N-terminally Myc-tagged CENP-A^{Cse4} under the galactose promoter and analyzed the growth of the cells on glucose versus galactose-containing medium. After subsequent rescreening (see Materials and Methods), only one histone H4 mutant, H4-R36A, exhibited significant lethality when CENP-A^{Cse4} was overproduced (**Figure 3.1A, Supplemental Figure 3.1A**). Since arginine residues are subject to methylation in budding yeast, we created additional amino acid substitutions at H4 position 36 to test whether a post-translational modification might be involved (*26*). We replaced R36 with a similarly basic residue lysine (R36K) that would inhibit methylation by an arginine methyltransferase. H4-R36K cells grew similar to wild-type (WT) cells when CENP-A^{Cse4} was overexpressed, indicating that methylation is not involved. We also replaced H4-R36 with glutamic acid (R36E) to generate a negative charge and found it was nearly as sensitive to increased CENP-A^{Cse4} levels as H4-R36A cells (**Figure 3.1A, Supplemental Figure 3.1A**). Together, these data indicate that a basic residue at position 36 in histone H4, but not post-translational modification of the amino acid, is required to prevent sensitivity to CENP-A^{Cse4} overexpression. Also, mutation of the neighboring H4-R35 residue did not cause sensitivity to CENP-A^{Cse4} (**Figure 3.1B**, **Supplemental Figure 3.1B**), indicating a specific role for H4-R36 in protecting cells from CENP-A^{Cse4}-induced lethality. A notable feature of H4-R36 is that it is the only residue in the alpha-1 helix of H4 whose side chain interacts with nucleosomal DNA near the entry/exit site in canonical H3 nucleosomes and in octameric human CENP-A nucleosomes (**Figure 3.1C**) (*3, 213*). H4-R36 is also located in a region near to the CENP-A targeting domain (CATD) in the human CENP-A nucleosome, which is

required for Psh1 recognition of CENP-A^{Cse4} (**Figure 3.1D**) (*43, 213*). These data suggest that the interaction between H4-R36 and DNA contributes to its function in shielding cells from the potentially lethal consequences of CENP-A^{Cse4} overexpression.

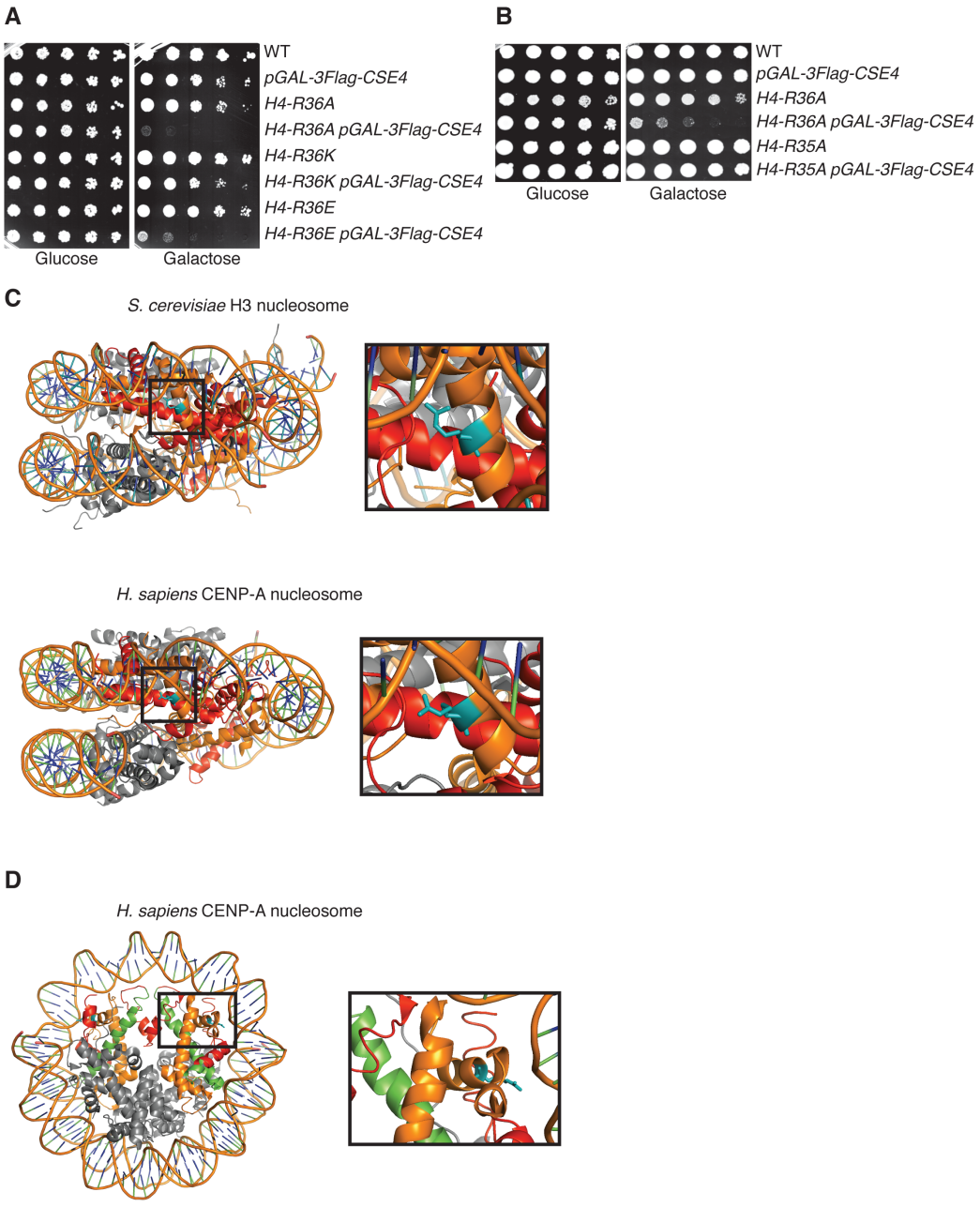

Figure 3.1. CENP-A^{Cse4} overexpression is lethal in H4-R36A cells
(A) Five-fold serial dilutions of the indicated strains (WT (SBY13389), *pGAL-3Flag-CSE4* (SBY13390), *H4-R36A* (SBY13391), *H4-R36A pGAL-3Flag-CSE4* (SBY13392), *H4-R36K* (SBY13393), *H4-R36K pGAL-3Flag-CSE4* (SBY13394), *H4-R36E* (SBY13395), *H4-R36E pGAL-3Flag-CSE4* (SBY13396)) were plated on glucose or galactose media at 23 °C. (B) Five-fold dilutions of the indicated strains (WT (SBY9401), *pGAL-3Flag-CSE4* (SBY10025), *H4-R36A* (SBY9365), *H4-R36A pGAL-3Flag-CSE4* (SBY9397), *H4-R35A* (SBY10510), *H4-R35A pGAL-3Flag-CSE4* (SBY13407)) were plated on glucose or galactose media at 23 °C. (C) Side views of crystal structures of the *S. cerevisiae* nucleosome containing histone H3 (top) and the *H. sapiens* nucleosome containing CENP-A (bottom). Histone H4 (orange) residue R36 (cyan) makes side-chain interactions with nucleosomal DNA. Red: histone H3 (left) or CENP-A (right). Larger versions of boxed regions are shown to the right of each structure. (D) Top view of the crystal structure of the *H. sapiens* nucleosome containing CENP-A as in (C), with the CATD indicated (green). Larger version of boxed region is shown to the right.

3.3.2 *Kinetochores are functional in H4-R36A cells overexpressing CENP-A^{Cse4}*

Since CENP-A^{Cse4} is essential for chromosome segregation, we asked if CENP-A^{Cse4} overexpression in H4-R36A cells altered kinetochore composition or function (*29*). There is a precedent for H4 influencing chromosome segregation, since the *hhf1-20* mutation (conferring a H4-T82I/A89V substitution) that weakens the interface between H4 and DNA causes chromosome missegregation, as do other H4 mutations that were more recently identified (*151, 177, 214*). However, H4-R36A mutants have not been identified in any of these chromosome segregation screens and H4-R36A mutant cells do not show sensitivity to mitotic spindle poisons (*212*). We confirmed that the growth of H4-R36A cells was not affected by benomyl, a microtubule-destabilizing drug that inhibits the growth of kinetochore mutants and spindle assembly checkpoint mutants such as *mad1*Δ (**Figure 3.2A**, **Supplemental Figure 3.1C**). We also tested whether CENP-A^{Cse4} still localizes to the centromere by performing chromatin immunoprecipitation (ChIP) followed by quantitative PCR (qPCR) and detected similar levels of CENP-A^{Cse4} at *CEN4* in WT and H4-R36A cells overexpressing CENP-A^{Cse4} (**Figure 3.2B**).

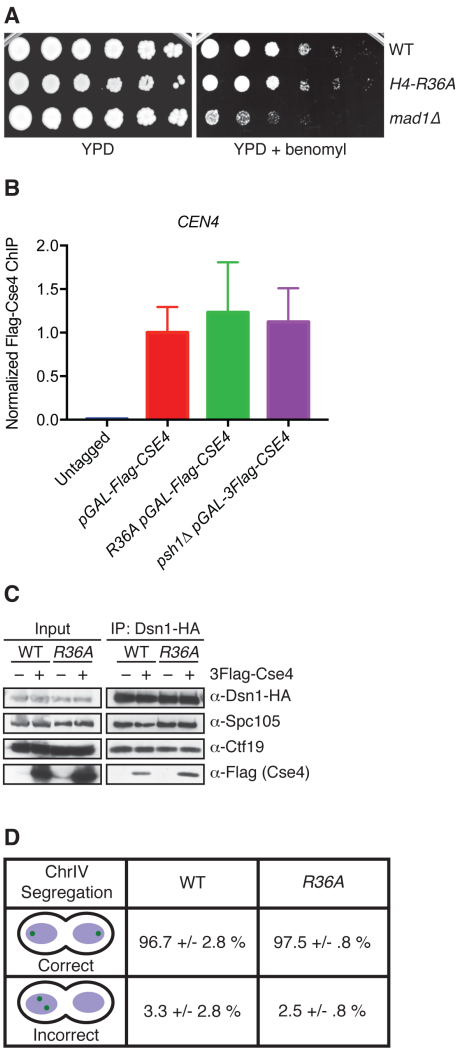

Figure 3.2. The overproduction of CENP-A^{Cse4} in the H4-R36A mutant does not perturb chromosome segregation

(A) WT (SBY9401), *H4-R36A* (SBY9979), and *mad1*Δ (SBY3256) cells were serially diluted five-fold and plated on YPD (left) or YPD + benomyl (right) medium and incubated at 23 °C. (B) 3Flag-Cse4 ChIP in WT (SBY16469) and *H4-R36A* (SBY13812) cells with *pGAL-3Flag-CSE4* overexpression. An untagged strain (SBY3) was used as a negative control. qPCR for the *CEN4* locus (using primers SB3061 + SB3062) was performed. Normalized Flag-Cse4 ChIP is the ratio of the % Input in each strain relative to the % Input in the *pGAL-3Flag-CSE4* strain. Mean Flag-Cse4 ChIP enrichment +/- 1 standard error of the mean (SEM) for three biological replicates is shown. (C) Anti-HA-conjugated beads were used to immunoprecipitate kinetochores via Dsn1-3HA from WT (SBY10450) or *H4-R36A* (SBY10453) cells containing *pGAL-3Flag-CSE4* in the presence (+) or absence (-) of galactose. The levels of Spc105 and Ctf19 were analyzed by immunoblotting with antibodies raised against the respective proteins. Immunoblotting with α-HA antibodies revealed the levels of Dsn1-3HA in the immunoprecipitates while α-Flag antibodies detected the incorporation of overexpressed 3Flag-Cse4. (D) Asynchronous cultures of WT (SBY10494) or *H4-R36A* (SBY10391) cells with *mad1*Δ and expressing *pGAL-3Flag-CSE4* were grown in galactose for 4 hours and chromosome IV segregation was monitored in anaphase cells (defined by cells with DNA masses at opposite poles). At least 100 cells were counted for each strain from two independent replicates. Percent correct or incorrect segregation +/- 1 standard deviation (SD) is shown.

We next analyzed the integrity of kinetochores by purification of the Dsn1 kinetochore protein, a method we previously developed to isolate native kinetochore particles (*107*). We immunoprecipitated Dsn1-3HA from WT and H4-R36A cells in the presence or absence of CENP-A^{Cse4} overexpression (**Figure 3.2C**). The levels of co-purifying Ctf19 and Spc105, representative components of the inner and outer kinetochore, respectively, were similar in kinetochores isolated from WT and H4-R36A cells (**Figure 3.2C**). These data suggest that the overall kinetochore composition is not affected. To assess kinetochore function, we monitored chromosome segregation in H4-R36A cells that also carried a *mad1*Δ to inactivate the spindle assembly checkpoint and ensure similar cell cycle progression for all strains (*215*). Cells containing a fluorescently marked chromosome IV were analyzed for segregation to opposite poles at anaphase (*216*). There was no significant difference in chromosome segregation between cells overexpressing CENP-A^{Cse4} in the presence or absence of the H4-R36A mutation (**Figure 3.2D**), indicating that the H4-R36 mutation does not significantly alter kinetochore composition or function.

3.3.3 *Cells with reduced H3 levels are not sensitive to CENP-A^{Cse4} overexpression*

The cellular levels of canonical H3 and CENP-A^{Cse4} are tightly regulated, and defects in H3 chromatin assembly can lead to CENP-A^{Cse4} incorporation (*42-44, 63, 117, 217-219*). Interestingly, H4-R36A is one of several histone mutants that have decreased H3 occupancy at highly transcribed genes (*220*). We therefore hypothesized that the sensitivity of H4-R36A cells to CENP-A^{Cse4} levels may be due to "gap-filling" in which defects in H3 chromatin occupancy provide nucleosome-depleted genomic regions that promote CENP-A^{Cse4} incorporation. If this were true, other histone mutants that are defective in H3 occupancy should also be sensitive to

increased CENP-A^{Cse4} levels. To test this, we analyzed the growth of three other histone mutants in this class (H3-V46A, H3-R49A, and H4-I46A) when CENP-A^{Cse4} was overexpressed (**Figure 3.3A**, **Supplemental Figure 3.2A**) (*220*). H3-V46A and H3-R49A cells exhibited a slight sensitivity to increased CENP-A^{Cse4} levels, while H4-I46A cell growth was unaffected by CENP-A^{Cse4} overproduction. Notably, the H4-I46A mutant has a reduction in H3 chromatin assembly that is comparable to R36A cells, strongly suggesting that the lethality of CENP-A^{Cse4} overexpression in H4-R36A cells is not related to gap-filling. As an additional test of this model, we directly reduced H3 levels. H3 and H4 are transcribed from two loci, *HHT1-HHF1* and *HHT2-HHF2*. The major locus is *HHT2-HHF2* and deleting this locus decreases the soluble pools of histones H3 and H4 (*221*). We therefore analyzed the growth of *hht2-hhf2*Δ cells when CENP-A^{Cse4} was overexpressed (**Figure 3.3B**, **Supplemental Figure 3.2B**) and found no growth defect, indicating that reduced H3 levels do not sensitize cells to CENP-A^{Cse4} incorporation. Additionally, H4-R36A *hht2-hhf2*Δ cells did not show a more severe phenotype with CENP-A^{Cse4} overexpression compared to H4-R36A cells. Altogether, these data suggest that altered H3 levels likely play a minimal role in the sensitivity of H4-R36A cells to increased CENP-A^{Cse4} protein.

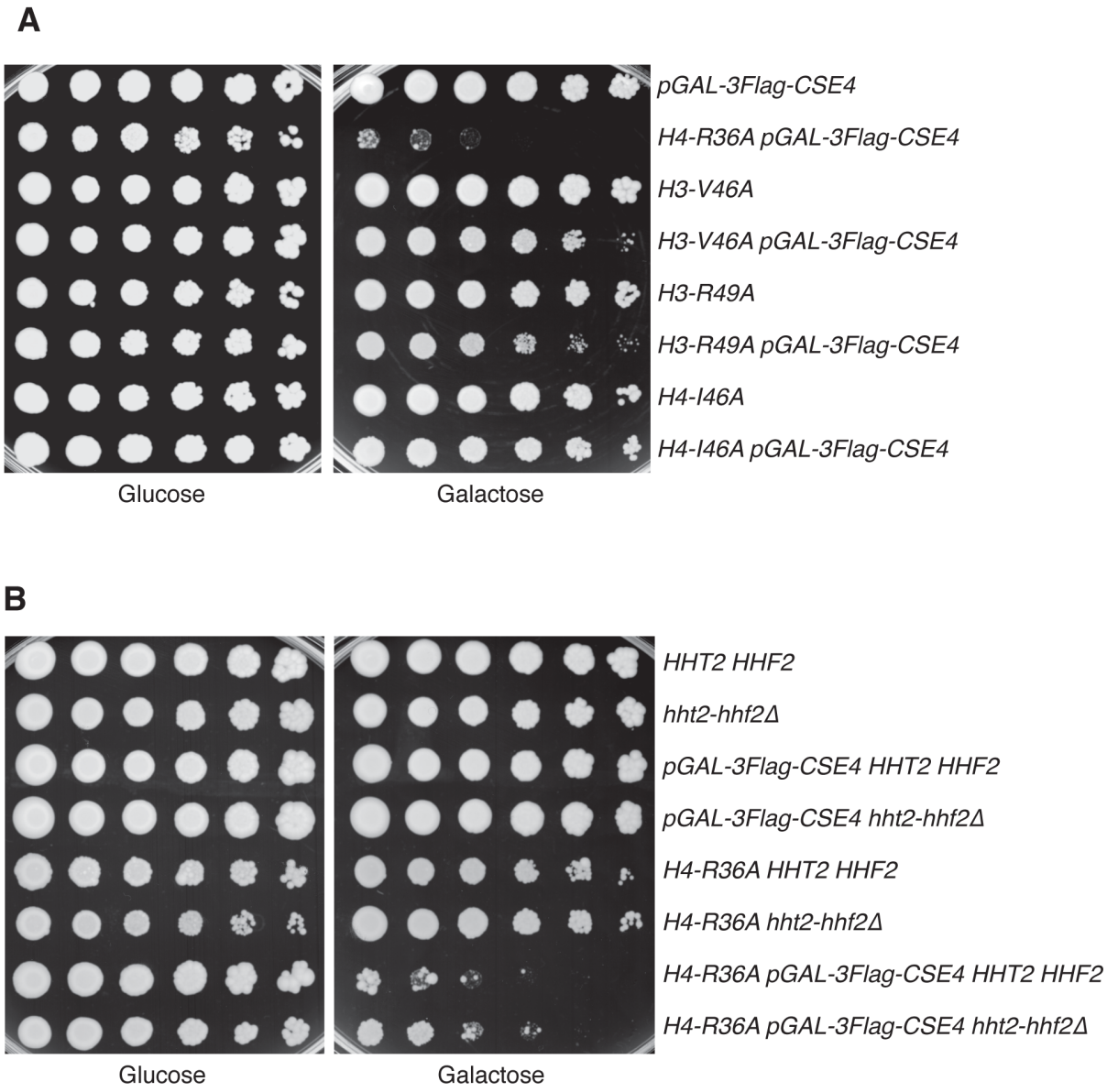

Figure 3.3. The sensitivity of H4-R36A cells to CENP-A^{Cse4} overexpression is not due to H3 depletion
(A) Five-fold serial dilutions of the indicated strains (*pGAL-3Flag-CSE4* (SBY10025), *H4-R36A pGAL-3Flag-CSE4* (SBY9397), *H3-V46A* (SBY10392), *H3-V46A pGAL-3Flag-CSE4* (SBY10511), *H3-R49A* (SBY10393), *H3-R39A pGAL-3Flag-CSE4* (SBY10512), *H4-I46A* (SBY10394), *H4-I46A pGAL-3Flag-CSE4* (SBY10513)) were plated on glucose or galactose media at 23 °C. (B) Five-fold dilutions of the indicated strains (*HHT2-HHF2* (SBY9401), *hht2-hhf2*Δ (SBY10730), *pGAL-3Flag-CSE4 HHT2-HHF2* (SBY10025), *pGAL-3Flag-CSE4 hht2-hhf2*Δ (SBY10734), *H4-R36A HHT2-HHF2* (SBY9365), *H4-R36A hht2-hhf2*Δ (SBY10778), *H4-R36A pGAL-3Flag-CSE4 HHT2-HHF2* (SBY9397), *H4-R36A pGAL-3Flag-CSE4 hht2-hhf2*Δ (SBY10782)) were plated on glucose or galactose media at 23 °C.

3.3.4 *CENP-A^{Cse4} is mislocalized in H4-R36A cells*

Because the sensitivity of cells to CENP-A^{Cse4} overexpression correlates with the level of CENP-A^{Cse4} misincorporation into euchromatin, we asked whether CENP-A^{Cse4} localizes to euchromatin in H4-R36A cells (*43, 44, 131*). To test this, we compared the levels of overexpressed CENP-A^{Cse4} in soluble and chromatin fractions from WT, H4-R36A, and *psh1*Δ cells. As we previously showed, the levels of CENP-A^{Cse4} are higher in *psh1*Δ than WT since CENP-A^{Cse4} is stabilized (*43*) (**Figure 3.4A**). Similarly, CENP-A^{Cse4} levels are also higher in H4-R36A cells compared to WT cells, and it is enriched in the chromatin fraction of H4-R36A cells, although to a lesser extent than *psh1*Δ cells (**Figure 3.4A**, **Supplemental Figure 3.3**).

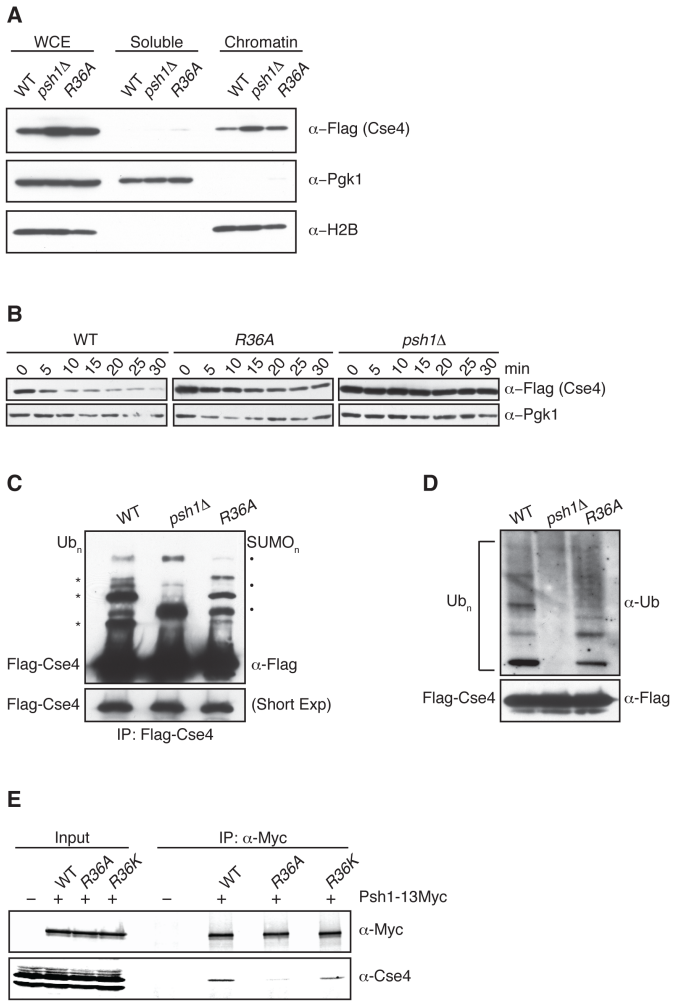

Figure 3.4. H4-R36A cells have defects in CENP-A^{Cse4} degradation
(A) Whole cell extracts (WCE) from WT (SBY10025), *psh1*Δ (SBY10590), and *H4-R36A* (SBY9397) cells expressing *pGAL-3Flag-CSE4* were fractionated into soluble and chromatin fractions. 3Flag-Cse4 levels were monitored in each fraction with α-Flag antibodies. Pgk1 and H2B are markers of the soluble and chromatin fractions, respectively. Note that a longer exposure of the blot for CENP-A^{Cse4} is included in Figure S3, which shows CENP-A^{Cse4} in the soluble fraction. (B) WT (SBY10025), *H4-R36A* (SBY9397), and *psh1*Δ (SBY10590) cells expressing *pGAL-3Flag-CSE4* were grown in galactose, protein synthesis was inhibited by cycloheximide addition at time zero, and lysates were monitored for 3Flag-Cse4 levels at the indicated time points with α-Flag antibodies. Pgk1 served as a loading control. (C) WT (SBY10025), *psh1*Δ (SBY10590), and *H4-R36A* (SBY9397) cells expressing *pGAL-3Flag-CSE4* were grown in galactose and 3Flag-Cse4 was immunoprecipitated with α-Flag antibodies. Unmodified 3Flag-Cse4 and its higher-mobility species (Ub$_n$) were detected on immunoblots by probing with α-Flag antibodies, these bands are marked on the left by asterisks. Note that SUMO conjugates appear on Cse4 in the absence of ubiquitylation (SUMO$_n$), these bands are marked on the right by black dots (*106*). The lower panel shows a shorter exposure of the immunoblot to display the levels of unmodified 3Flag-Cse4 in the immunoprecipitates and serves as a loading control. (D) An immunoblot probed with a-ubiquitin antibodies of the α-Flag immunoprecipitates isolated from the strains denoted in (C) reveals the ubiquitin conjugates of 3Flag-Cse4. The lower panel shows the levels of unmodified 3Flag-Cse4 by immunoblotting with α-Flag antibodies. (E) Psh1-13Myc was immunoprecipitated from WT (SBY15335), *H4-R36A* (SBY15624), and *H4-R36K* (SBY16468) cells, and immunoblots were probed with α-Myc and α-Cse4 antibodies. Cells expressing untagged Psh1 (SBY3) served as a control. The Cse4/Psh1 ratio +/- 1 SEM was calculated vs. WT for *H4-R36A* (0.5 +/- 0.03) and *H4-R36K* (3.0 +/- 0.6) from 3 biological replicates.

3.3.5 *The interaction between Psh1 and CENP-A^{Cse4} is altered in the H4-R36A mutant*

The increased CENP-A^{Cse4} protein levels in H4-R36A cells suggested a defect in CENP-A^{Cse4} proteolysis because there are no changes in *PSH1* or *CSE4* transcription in these cells (*222*). To determine if CENP-A^{Cse4} degradation is impaired in H4-R36A cells, we monitored CENP-A^{Cse4} protein levels after transient overexpression followed by translational repression with cycloheximide. CENP-A^{Cse4} was partially stabilized in H4-R36A cells compared to WT cells (**Figure 3.4B**). To determine whether this is a result of a reduction in ubiquitin-mediated proteolysis, we analyzed the level of CENP-A^{Cse4} ubiquitin conjugates in WT, *psh1*Δ, and H4-R36A cells. As expected, CENP-A^{Cse4} isolated from WT cells displayed several higher mobility species, most of which correspond to ubiquitin conjugates of CENP-A^{Cse4} (**Figure 3.4C**, **D**). Consistent with previous work, ubiquitin conjugates of CENP-A^{Cse4} are decreased in *psh1*Δ cells (*43, 44*). The upper CENP-A^{Cse4} forms that are present in the *psh1*Δ cells correspond to SUMO-conjugates that become detectable when ubiquitylation is reduced (*43, 106*) (**Figure 3.4C** and data not shown). CENP-A^{Cse4} isolated from H4-R36A cells showed lower levels of most ubiquitin conjugates and increased sumoylation compared to WT cells, consistent with its partial stabilization. Together, these results show that H4-R36A cells are partially defective in CENP-A^{Cse4} degradation and accumulate CENP-A^{Cse4} in euchromatin.

The increased stability of CENP-A^{Cse4} in H4-R36A cells suggested that the interaction between CENP-A^{Cse4} and Psh1 might be altered in the mutant. Indeed, the association between Psh1 and CENP-A^{Cse4} is reduced when Psh1 is immunoprecipitated from H4-R36A cells compared to WT cells (**Figure 3.4E**). The CENP-A^{Cse4}/Psh1 ratio +/- 1 standard error of the mean (SEM) vs. WT for H4-R36A cells was 0.5 +/- 0.03. Consistent with our data suggesting that residue 36 of H4 needs to be basic to protect cells from lethality when CENP-A^{Cse4} is

overproduced (**Figure 3.1**), the Psh1-CENP-A^{Cse4} interaction is retained in the H4-R36K mutant that restores the basic charge (**Figure 3.4E**). The CENP-A^{Cse4}/Psh1 ratio +/- 1 SEM vs. WT for H4-R36K cells was 3.0 +/- 0.6. Taken together, these results suggest that the defects in CENP-A^{Cse4} proteolysis are likely due to a decreased interaction between Psh1 and CENP-A^{Cse4} in H4-R36A.

3.3.6 *Psh1 is enriched at the 3' ends of genes in H4-R36A*

The altered Psh1-CENP-A^{Cse4} interaction could be due to a change in CENP-A^{Cse4} nucleosome structure that directly affects the binding of CENP-A^{Cse4} to Psh1, and/or it could be due to changes in the localization of Psh1 such that it is no longer available to bind to CENP-A^{Cse4} nucleosomes. Psh1 is present in both the soluble and chromatin fractions of cells, however its euchromatic localization pattern has not been analyzed (*43, 44*). In addition, Psh1 is known to associate with FACT (*43, 118*), although their level of co-localization throughout the genome is unknown. The FACT complex exhibits an altered localization pattern in H4-R36A mutants and becomes enriched at the 3' untranslated region (UTR) of highly transcribed genes (*130*). This phenotype is also shared with other histone mutants including H4-R31E and H3-L61W (*130, 223*). These residues map to a distinct area of the nucleosome, and it was proposed that this nucleosomal region releases FACT from the end of transcribed units, although the exact mechanism or signal for the dissociation remains unclear (*130, 223*).

Because Psh1 association with FACT is important for CENP-A^{Cse4} ubiquitylation and degradation (*118*), we analyzed Psh1 localization in WT vs. H4-R36A cells at the 5', 3' and coding regions of two highly transcribed genes, *ADH1* and *PMA1*. It was previously found that the Spt16 component of FACT is mislocalized to the 3' UTRs of these genes in H4-R36A or H3-

L61W mutant cells (*130, 223*). We confirmed the enrichment of Spt16 to the 3' UTRs of the *ADH1* and *PMA1* genes in the H4-R36A mutants in our strain background using ChIP-PCR (data not shown). Strikingly, ChIP-qPCR revealed that Psh1 also shows a strong enrichment at the 3' UTRs of these genes in H4-R36A cells compared to WT, while the levels at the promoter and gene regions were similar to WT cells (**Figure 3.5A-D**). The H4-R36K mutant, which rescues the Psh1-CENP-A^{Cse4} interaction, also restores the WT Psh1 localization pattern (**Figure 3.5C, D**). Together, these data suggest that altered Psh1 localization could contribute to the CENP-A^{Cse4} stability phenotype in H4-R36A mutant cells.

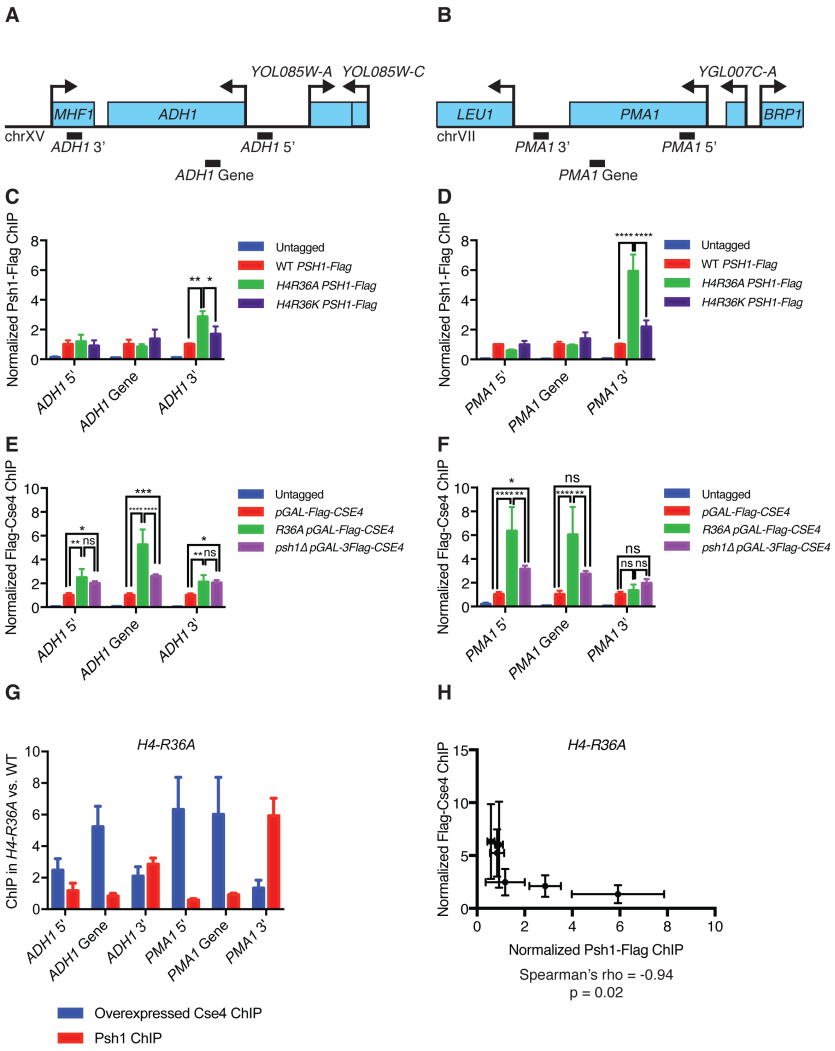

Figure 3.5. Psh1 and CENP-A^{Cse4} are mislocalized in the H4-R36A mutant cells
(A) Diagram of the *ADH1* genomic locus showing regions amplified by 5', 3', and intragenic primer sets (not to scale). (B) Diagram of the *PMA1* genomic locus showing regions amplified by the 5', 3', and intragenic primer sets (not to scale). (C) Psh1-3Flag ChIP from WT (SBY13723), *H4-R36A* (SBY13725), and *H4-R36K* (SBY16594) cells. Cells expressing untagged Psh1 (SBY3) were used as controls. qPCR was performed for the primer sets shown in (A), *ADH1* 5' (SB5059 and SB5060), *ADH1* Gene (SB4470 and SB4471), and *ADH1* 3' (SB4472 and SB4473). Normalized Psh1-Flag ChIP is the ratio of the % Input in each strain relative to the % Input in the WT *PSH1-Flag* strain. Mean Psh1-Flag ChIP enrichment +/- 1 SEM from 3 biological replicates is shown. Results from two-way ANOVA with Tukey's multiple comparisons test are shown. * $p \leq 0.05$, ** $p \leq 0.01$, *** $p \leq 0.001$, **** $p \leq 0.0001$. (D) Psh1-Flag ChIP as in (C), with PCR primers as shown in (B) for *PMA1* 5' (SB5029 and SB5030), *PMA1* Gene (SB4076 and SB4077), and *PMA1* 3' (SB5027 and SB5028). (E) ChIP of overexpressed Flag-Cse4 from WT (SBY16469), *H4-R36A* (SBY13812), and *psh1*Δ (SBY11189) strains. Cells expressing untagged CENP-A^{Cse4} were used as a control (SBY3). PCR primers at the *ADH1* locus were used as in (C). qPCR was performed, normalized Flag-Cse4 ChIP is the ratio of the % Input in each strain relative to the % Input in the *pGAL-3Flag-CSE4* strain. Mean Flag-Cse4 ChIP enrichment +/- 1 SEM from 3 biological replicates is shown. Results from two-way ANOVA with Tukey's multiple comparisons test are shown. * $p \leq 0.05$, ** $p \leq 0.01$, *** $p \leq 0.001$, **** $p \leq 0.0001$. (F) Flag-Cse4 ChIP as in (E) for *PMA1* primers as in (D). (G) Bar plot of the average CENP-A^{Cse4} (blue) or Psh1 (red) ChIP signal at each locus for the *H4-R36A* strains +/- 1 SEM from 3 biological replicates. (H) Scatter plot of Psh1 ChIP signal vs. CENP-A^{Cse4} ChIP signal at each locus as in (G) (average +/- 1 SD) in the *H4-R36A* strains. Spearman's correlation coefficient was calculated from these data (rho = -0.94, p = 0.02).

3.3.7 *CENP-A^{Cse4} mislocalization is negatively correlated with Psh1 enrichment in H4-R36A cells*

We previously discovered that overexpressed CENP-A^{Cse4} is mislocalized to nucleosomes in both tandem and divergent intergenic regions in the absence of Psh1 (*131*). To test whether this is also true in the H4-R36A mutant cells, we performed ChIP-qPCR on overexpressed CENP-A^{Cse4} from WT, H4-R36A, and *psh1*Δ cells, and analyzed CENP-A^{Cse4} enrichment at the *ADH1* and *PMA1* promoters, genes, and 3' regions compared to the WT *pGAL-3Flag-CSE4* strain. For both genes, overexpressed CENP-A^{Cse4} is enriched in the promoter and coding regions in H4-R36A cells compared to WT and *psh1*Δ mutant cells (**Figure 3.5E**, **F**). In contrast, the level of CENP-A^{Cse4} mislocalization at the 3' ends of these genes is either much lower (at the *ADH1* 3' end) or not enriched at all (at the *PMA1* 3' end). Strikingly, correlation analysis of Psh1 and CENP-A^{Cse4} localization in the H4-R36A strain reveals a significant negative correlation (Spearman's rho = -0.9429, p = 0.0167) (**Figure 3.5G**, **H**). This finding is consistent with the possibility that the local enrichment of Psh1 mediates the ubiquitylation and degradation of CENP-A^{Cse4} at specific regions.

3.4 DISCUSSION

In this study, we performed the first systematic screen to identify mutations in H4 that affect the regulation of the histone variant CENP-A^{Cse4}. The H4 mutant R36A exhibited the strongest sensitivity to CENP-A^{Cse4} overexpression of those analyzed. Our genetic and biochemical analyses support a model whereby a positive charge at this residue is required for CENP-A^{Cse4} regulation by ensuring that the Psh1 ubiquitin ligase interacts with CENP-A^{Cse4}.

The H4-R36A cells overexpressing CENP-A^{Cse4} are most likely inviable due to mislocalization of the centromeric histone variant to the euchromatin. We previously determined that CENP-A^{Cse4} overexpression is lethal in cells lacking Psh1 due to ectopic localization of the centromeric histone variant, and here we found that Psh1 exhibits reduced binding to its substrate in the H4-R36A mutant cells (*43, 118*). Consistent with this, there was an increase in CENP-A^{Cse4} stability and a reduction in its ubiquitylated forms in the H4-R36A mutant cells. Since H4-R36A cells have transcriptional defects as well as decreased nucleosome occupancy at transcribed genes, it is possible that increased transcriptional stress in the presence of mislocalized CENP-A^{Cse4} contributes to cell death (*130, 131, 212, 220, 222*). However, the lethality induced by CENP-A^{Cse4} overexpression is rescued in the H4-R36K mutant, which restores the interaction between Psh1 and CENP-A^{Cse4} but not all of the other H4-R36A phenotypes (*212*). Together, these data strongly suggest that the reduced interaction between Psh1 and CENP-A^{Cse4} is related to the cell death caused by CENP-A^{Cse4} overexpression.

The reduced Psh1-CENP-A^{Cse4} interaction in the H4-R36A mutant cells could be due to a change in the nucleosome or (CENP-A^{Cse4}-H4)$_2$ tetramer structure that directly alters the binding site of Psh1 for CENP-A^{Cse4}. The CENP-A targeting domain (CATD) of CENP-A^{Cse4} is required for Psh1 binding and H4-R36 is not predicted to directly contact the CATD in an octameric nucleosome (*43, 213*). However, H4-R36 contacts the DNA near the DNA entry/exit site on the nucleosome and this region is close to the CATD (*9, 213*). Therefore, this residue may directly contribute to Psh1 recognition of the nucleosome and help distinguish nucleosome-bound versus soluble CENP-A^{Cse4}.

The decreased binding between Psh1 and CENP-A^{Cse4} may also be due to an indirect mechanism related to altered localization of the ubiquitin ligase. We found that Psh1 becomes

enriched at 3' UTRs in H4-R36A cells at two loci. If this is a widespread phenomenon, it could explain the decreased Psh1-CENP-A^{Cse4} interaction, since Psh1 may be sequestered at 3' UTRs. Consistent with this, there appears to be a negative correlation between the enrichment of Psh1 and CENP-A^{Cse4} in H4-R36A cells at these loci, raising the possibility that there is localized degradation of CENP-A^{Cse4} at the 3' sites where Psh1 accumulates. In the future, ChIP-seq assays to determine the genome-wide mislocalization pattern of CENP-A^{Cse4} and Psh1 in H4-R36A cells may further elucidate the underlying mechanism.

It is unclear what mechanism underlies the Psh1 3' UTR enrichment. This mislocalization pattern is similar to what has been seen for the FACT complex component Spt16 in H4-R36A cells (*130*). Since Psh1 binds to Spt16 and this interaction is essential for controlling CENP-A^{Cse4} localization *in vivo*, one possibility is that the mislocalization of FACT in H4-R36A cells leads to Psh1 enrichment at 3' UTRs (*43, 118*). However, there are intragenic Spt16 suppressors that relieve its accumulation at the 3' UTR in the H4-R36A mutant cells, but only some of them suppress the lethality of CENP-A^{Cse4} overexpression (data not shown) (*130, 223*). Therefore, the underlying mechanism appears to be more complicated than just FACT mislocalization leading to the accumulation of Psh1 at 3' UTR regions. Consistent with this, while both Psh1 and Spt16 are enriched at 3' UTRs in H4-R36A cells, only Spt16 shows depletion at promoters and intragenic regions (*130*).

While the precise reason for the Psh1 mislocalization to 3' ends of genes is not clear, it is correlated with altered CENP-A^{Cse4} localization. We therefore propose that Psh1 needs to dynamically associate with chromatin to regulate CENP-A^{Cse4} (**Figure 3.6**). This is consistent with our previous conclusion that Psh1 needs to be traveling with FACT and elongating RNA polymerases to recognize CENP-A^{Cse4} that is incorporated into nucleosomes (*118*). By disrupting

chromatin, FACT would allow Psh1 to access the CATD, which is normally buried in the core of the nucleosome. The position of H4-R36 near the nucleosome entry/exit site may facilitate the ability of FACT to disrupt nucleosome structure. When this residue is disrupted, it may alter Psh1 and FACT localization in a manner that impairs CENP-A^{Cse4} proteolysis, possibly by preventing the dynamic movement of FACT and Psh1 (**Figure 3.6**).

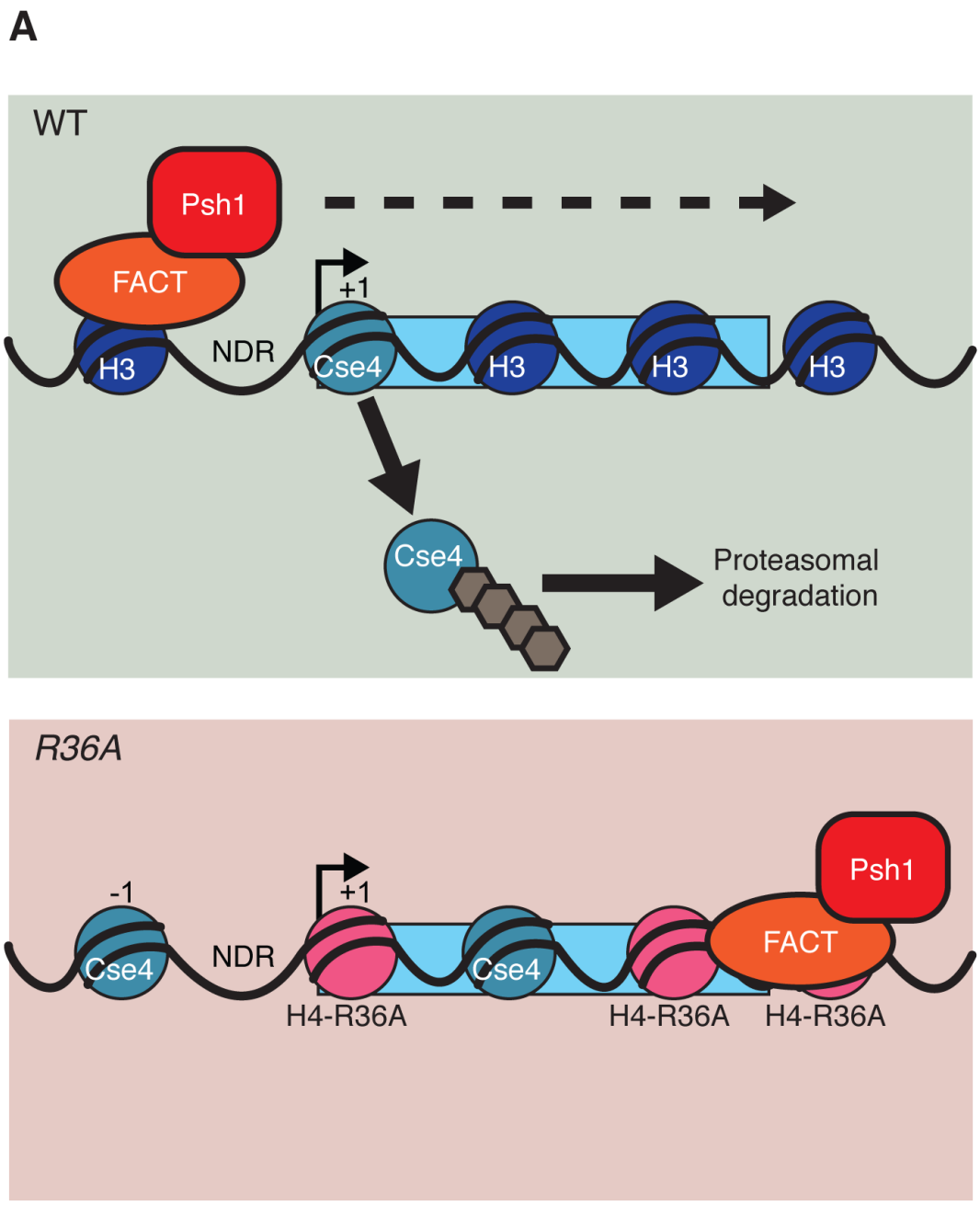

Figure 3.6. Model for control of CENP-A^{Cse4} localization via a dynamic Psh1-chromatin interaction
In WT cells containing canonical nucleosomes (dark blue), Psh1 (red) and FACT (orange) interact dynamically with genes during transcription (dynamic interaction is indicated by dashed arrow). This allows Psh1 to recognize mislocalized CENP-A^{Cse4} (teal) at 5', intragenic, and 3' regions and mediate its ubiquitylation (brown), leading to its proteasomal degradation. Psh1-mediated recognition and degradation enables the cells to control CENP-A^{Cse4} localization and to live when CENP-A^{Cse4} is overexpressed (green shaded box). When H4-R36 is mutated to alanine (pink), FACT and Psh1 lose their dynamic interaction with transcribed genes and are sequestered at 3' UTRs, compromising the Psh1/CENP-A^{Cse4} interaction. CENP-A^{Cse4} that incorporates at 5' or intragenic regions is not adequately ubiquitylated and is retained at ectopic sites, leading to cell death (red shaded box).

In sum, our work has identified another facet of the regulation of CENP-A^{Cse4} protein levels and localization. Histone H4 residue (R36) facilitates the Psh1-CENP-A^{Cse4} physical interaction, likely by allowing Psh1 and FACT to travel dynamically through genes during transcription to facilitate CENP-A^{Cse4} removal and degradation. Because it is essential to maintain the exclusive localization of the centromeric histone to prevent genomic instability and transcriptional misregulation (*43, 44, 131*), it will be important to further elucidate the precise nature of the interaction between Psh1 and the centromeric nucleosome as well as the dynamics of Psh1 localization to chromatin in the future.

3.5 MATERIALS AND METHODS

3.5.1 *Yeast strain construction and microbial techniques*

Microbial techniques and media were performed as described (*118*). For all experiments involving induction of epitope-tagged *pGAL-CSE4*, budding yeast cells of the indicated strains were grown to log phase (OD 0.55-0.8, Bio-Rad SmartSpec^{TM} 3000) in lactic acid media at 23 °C and induced for 2 hours with 2% galactose, unless otherwise indicated. Yeast strains were constructed using standard genetic techniques (*173, 174*). Epitope-tagged proteins were constructed using either a PCR integration technique or by the integration of plasmids after restriction digestion (*175*). Specific plasmids and yeast strains used in this study are described in **Supplemental Table 3.1** and **Supplemental Table 3.2**, respectively. A *pGAL-3Flag-CSE4, LEU2* 2-micron vector (pSB1730) was constructed by digesting vector YEplac181 with *Kpn*I and *Sac*I (*224*). The vector was ligated with a *pGAL-3Flag-CSE4* fragment that was isolated by digesting pSB839 (*43*) with the same enzymes to create a 2-micron, *LEU2* plasmid with *pGAL-3Flag-CSE4* (pSB1730).

3.5.2 *Genetic screen of histone mutant library*

A previously constructed budding yeast histone H4 library was used to screen for mutants that are sensitive to CENP-A^{Cse4} overexpression (*177, 212*). Each H4 amino acid was singly changed to alanine by integrating plasmids from a Histone Mutant Library version 2.1 (HMLv2.1) that had been digested with *Bci*VI to target the *HHT2-HHF2* locus in a *hht1-hhf1*Δ background (*177, 212*). For convenience in the initial screen, we used a previously constructed library in our lab that also contained an Ipl1-degron protein (*177*). However, the strains were grown under conditions that did not promote Ipl1 degradation. First, the H4 library was transformed in 96 well plate format with a high-copy plasmid expressing Myc-tagged CENP-A^{Cse4} under the galactose promoter (pSB830, (*42*)) and subsequently plated on selective medium containing glucose in 100 x 15 mm plates. After 5 days of growth at 23 °C, transformants were patched onto selective medium containing glucose and incubated at 23 °C. Replica plating was performed to analyze the growth of the transformed library on glucose versus galactose-containing medium. Hits were selected as strains that grew at 23 °C on glucose but exhibited defective growth on galactose-containing medium. To eliminate histone mutants that are defective in galactose metabolism, positive hits were rescreened to compare their growth on galactose with a control vector (YEplac181, (*224*)) with that of the *pGAL-Myc-CSE4* plasmid (pSB830, (*42*)). Hits were also streaked onto selective medium containing glucose or galactose to confirm the replica plating results. This initial round of screening identified six histone H4 mutants that appeared to have defective growth when CENP-A^{Cse4} was overexpressed: H4-I34A, H4-R36A, H4-K44A, H4-Y51A, H4-T80A, and H4-D85A. Second, the six H4 mutants were obtained from the same initial H4 mutant library and were retransformed with YEplac181 (vector control), pSB830 (*Myc-CSE4* plasmid), and pSB1730 (*pGAL-3Flag-CSE4,* which expresses CENP-A^{Cse4} at higher levels

compared to the *pGAL-Myc-CSE4* plasmid) to reanalyze their growth on galactose-containing medium. This approach eliminated three of the mutants, leaving H4-R36A, H4-K44A, and H4-Y51A for further testing. These three H4 mutants were then regenerated in an otherwise wildtype background, where both histone loci were replaced with the mutants in contrast to the parent strains that had a single *HHF1-HHT1* locus replaced in the presence of an *HHF2-HHT2* deletion. These strains were made for each histone mutant of interest by integrating plasmids from a Histone Mutant Library version 3.0 (HMLv3.0) (a kind gift from Junbiao Dai, Tsinghua University) that were digested with *Bci*VI to target the *HHT1-HHF1* locus. The plasmids that were used to make the histone mutants were sequenced to confirm the presence of the desired mutation. They were subsequently crossed to strains with the histone mutant of interest at the *HHT2-HHF2* locus to obtain strains with replacements at both histone loci. Plate spot assays (with yeast transformed with YEplac181 or pSB1730) were used to analyze the growth of the mutants on glucose and galactose medium for the final three candidates. The plasmids used to make these strains are listed in **Supplemental Table 3.1**.

3.5.3 *PyMOL structures*

Preparation of structural figures of the human CENP-A (PDBID 3AN2, (*213*) and yeast H3 (PDBID 1ID3, (*9*) nucleosomes were performed using the PyMOL Molecular Graphics System (Schrodinger, LLC).

3.5.4 *Protein and immunoprecipitation techniques*

Protein extracts to analyze total CENP-A^{Cse4} levels were prepared as described (*131, 176*). Immunoblots using chemiluminescence were performed as previously described (*131, 176*). For

all immunoblots, the antibody dilutions were as follows: mouse α-Pgk1 monoclonal antibodies (Invitrogen Catalog # 459250) at a 1:10,000 dilution were used as a loading control. Mouse α-Flag M2 monoclonal antibodies (Sigma-Aldrich Catalog # F3165) were used at a 1:3000 dilution, mouse α-HA 12CA5 monoclonal antibodies (Roche Catalog # 1-583-816) were used at a 1:10,000 dilution, rabbit α-H2B polyclonal antibodies (Active Motif Catalog # 39237) were used at a 1:3,000 dilution, and mouse α-Myc 9E10 monoclonal antibodies were used at a 1:10,000 dilution (Covance Catalog # MMS-150R). Rabbit α-Spc105 antibodies were used at a 1:1,000 dilution (*107*). Rabbit α-Ctf19 antibodies (generous gift from Arshad Desai) were used at a 1:15,000 dilution. Quantitative immunoblots were carried out according to (*177*) with the modification of using 4% non-fat milk in PBS as the blocking agent for the α-Cse4 immunoblot. Briefly, IRDye anti-mouse and anti-rabbit secondary antibodies from LI-COR were used at a 1:5,000 dilution. The immunoblots were imaged on a LI-COR imaging system, and the protein levels were quantified using Image Studio Lite.

Kinetochore purifications were performed from 50 ml cultures as previously described (*107*). For experiments analyzing ubiquitin conjugates of Cse4, NEM (N-ethylmaleimide) was added to the lysis and wash buffers to a final concentration of 5 mM (*118*). Immunoprecipitates were separated by SDS-PAGE and analyzed by immunoblotting. Co-immunoprecipitation experiments were performed as previously described for Psh1-Myc and Spt16-Flag strains using Protein G Dynabeads conjugated with α-Myc (A-14, SC-789) and separated on an SDS-PAGE gel (*118.*).

3.5.5 *Chromatin fractionation*

Chromatin fractionation assays were performed as described, followed by analysis on immunoblots (*118*). α-PGK1 was used as a marker and loading control for the soluble fraction, and α-H2B was used as a marker and loading control for the chromatin fraction (*118*).

3.5.6 *CENP-A^{Cse4} stability assays*

CENP-A^{Cse4} stability assays were performed as in (*118*). Briefly, cells were grown in YEP + lactic acid until mid-log phase, followed by a 2 hour 3Flag-Cse4 induction with 2% galactose. Glucose was added to a final concentration of 2% to further inhibit 3Flag-Cse4 transcription, and cycloheximide was added to a final concentration of 50 μg/mL. Time point 0 was taken immediately, followed by sample collection at the indicated time points. Extracts were prepared and analyzed as described (*176*).

3.5.7 *Chromosome segregation assay*

Analysis of GFP-LacI was performed as described (*216, 225*). The lacO array was integrated at the *TRP1* locus, ~12.5 Kb from *CEN4*.

3.5.8 *Chromatin immunoprecipitation (ChIP)*

ChIP was performed from 50 ml asynchronous yeast cultures with 1% formaldehyde to mediate crosslinking followed by sonication to fragment DNA, as previously described (*71*). α-Flag M2 antibodies conjugated to protein G dynabeads were used for both Flag-Cse4 and Psh1-Flag ChIPs. Quantitative polymerase chain reaction (qPCR) was performed as previously described (*131*), on an AppliedBiosystems™ QuantStudio 5 qPCR machine. Oligonucleotide sequences are

available in **Supplemental Table 3.3**. Graphpad Prism 7 was used for two-way ANOVA with Tukey's multiple comparison tests to analyze Psh1 or CENP-A^{Cse4} enrichment, and to calculate Spearman's correlation coefficient for the Psh1 vs. CENP-A^{Cse4} data in the H4-R36A strain. Normalized ChIP signal for Psh1-Flag and Flag-Cse4 ChIPs was calculated as the mean of the ratio of the % Input for each strain relative to % Input for the WT *PSH1-Flag* or *pGAL-Flag-CSE4* strain, respectively, for 3 biological replicates.

3.5.9 *PSH1 and CSE4 gene expression analysis*

Gene expression of *PSH1* and *CSE4* in H4-R36A compared to WT cells was determined using published microarray data (*222*). The microarray data was accessed using the NCBI GEO accession viewer (GSE29059). A .txt file containing the log2 ratio of each gene in each histone mutant compared to WT was downloaded from this record (GSE29059_log2_mut_wt_ratio.txt.gz). This was imported into Microsoft Excel, and the log2 ratio for the H4-R36A mutant compared to the WT cells was looked up using the Microsoft Excel search function for *CSE4* (YKL049C, log2 H4-R36A vs. WT = 0.94562094), and *PSH1* (YOLO54W, log2 H4-R36A vs. WT = 0.15504214). The paper that published the microarray data used a cutoff of > 1.5 fold up or down-regulation to determine which genes were differentially regulated, and both *CSE4* and *PSH1* have less than 1.5 fold change compared to WT (*222*).

3.5.10 *Reagent and data availability*

All strains and plasmids are available upon request. **Supplemental Table 3.1** describes the plasmids used to construct yeast strains, **Supplemental Table 3.2** lists the genotypes of all yeast strains, and **Supplemental Table 3.3** reports all oligonucleotide sequences used in this study.

3.6 ACKNOWLEDGEMENTS

We thank Junbiao Dai for providing the plasmids required to generate the histone mutant strains, and Arshad Desai for sharing α-Ctf19 antibodies. We thank members of the Tsukiyama and Biggins laboratories for helpful discussions and advice and T. Tsukiyama and M. Basrai for critical reading of the manuscript. Research was funded by a National Institutes of Health grant Regulation of Centromeric Chromatin (R01 GM078069) to SB, an American Cancer Society fellowship to G.M.R.D., a National Institutes of Health Chromosome Metabolism and Cancer Training Grant (T32CA009657) and the National Science Foundation Graduate Research Fellowship Program to EH. SB is an Investigator of the Howard Hughes Medical Institute.

3.7 AUTHOR CONTRIBUTIONS

EH, GD, and SB designed the experiments. EH, GD, and SB interpreted data and prepared the manuscript. GD, EH, and AB performed the experiments.

3.8 SUPPLEMENTAL FIGURES

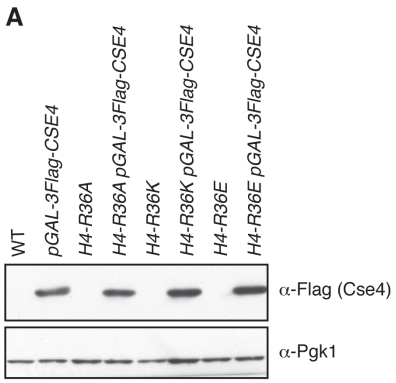

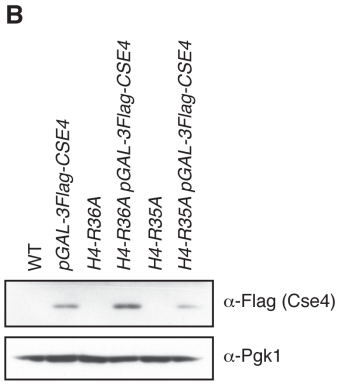

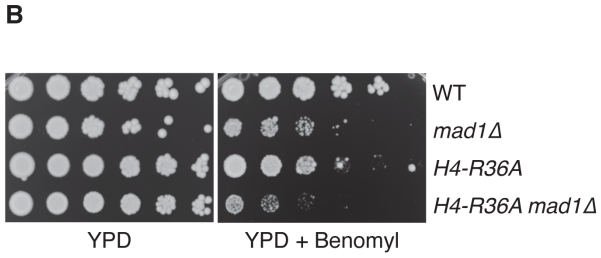

Supplemental Figure 3.1. CENP-A^{Cse4} overexpression analysis for Figure 3.1
(A) Immunoblots of overexpressed 3Flag-Cse4 in the following strains (WT (SBY13389), *pGAL-3Flag-CSE4* (SBY13390), *H4-R36A* (SBY13391), *H4-R36A pGAL-3Flag-CSE4* (SBY13392), *H4-R36K* (SBY13393), *H4-R36K pGAL-3Flag-CSE4* (SBY13394), *H4-R36E* (SBY13395), *H4-R36E pGAL-3Flag-CSE4* (SBY13396)), corresponding to the serial dilution assay in **Figure 3.1A**. Pgk1 serves as a loading control. (B) Immunoblots of overexpressed 3Flag-Cse4 in the following strains (WT (SBY9401), *pGAL-3Flag-CSE4* (SBY10025), *H4-R36A* (SBY9365), *H4-R36A pGAL-3Flag-CSE4* (SBY9397), *H4-R35A* (SBY10510), *H4-R35A pGAL-3Flag-CSE4* (SBY13407)), corresponding to the serial dilution assay in **Figure 3.1B**. Pgk1 serves as a loading control. (C) Serial dilution assay on YPD or YPD + 10% benomyl for WT (SBY13729), *mad1*Δ (SBY10494), *H4-R36A* (SBY9566), and *mad1*Δ *H4-R36A* (SBY10391). Note that while all strains also contain *pGAL-Flag-CSE4*, they were grown on glucose containing media to repress expression from the *pGAL* promoter.

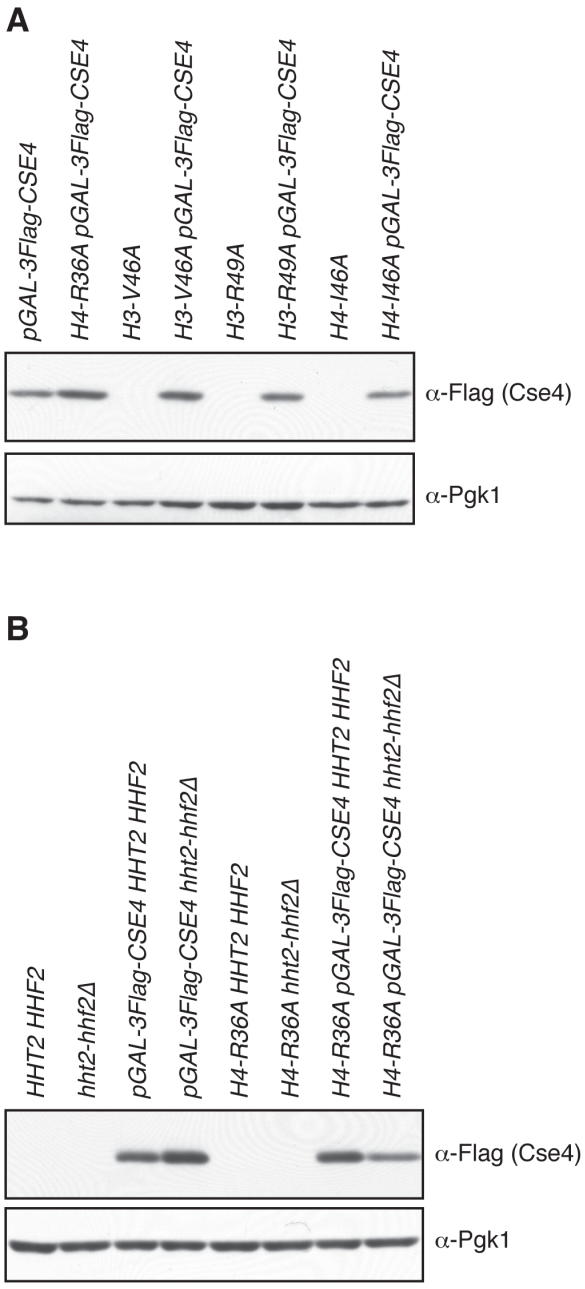

Supplemental Figure 3.2. CENP-A^{Cse4} overexpression analysis for Figure 3.3
(A) Immunoblots of overexpressed 3Flag-Cse4 in the following strains (*pGAL-3Flag-CSE4* (SBY10025), *H4-R36A pGAL-3Flag-CSE4* (SBY9397), *H3-V46A* (SBY10392), *H3-V46A pGAL-3Flag-CSE4* (SBY10511), *H3-R49A* (SBY10393), *H3-R49A pGAL-3Flag-CSE4* (SBY10512), *H4-I46A* (SBY10394), *H4-I46A pGAL-3Flag-CSE4* (SBY10513)), corresponding to the serial dilution assay in **Figure 3.3A**. Pgk1 serves as a loading control. (B) Immunoblots of overexpressed 3Flag-Cse4 in the following strains (*HHT2-HHF2* (SBY9401), *hht2-hhf2*Δ (SBY10730), *pGAL-3Flag-CSE4 HHT2-HHF2* (SBY10025), *pGAL-3Flag-CSE4 hht2-hhf2*Δ (SBY10734), *H4-R36A HHT2-HHF2* (SBY9365), *H4-R36A hht2-hhf2*Δ (SBY10778), *H4-R36A pGAL-3Flag-CSE4 HHT2-HHF2* (SBY9397), *H4-R36A pGAL-3Flag-CSE4 hht2-hhf2*Δ (SBY10782)), corresponding to the serial dilution assay in **Figure 3.3B**. Pgk1 serves as a loading control.

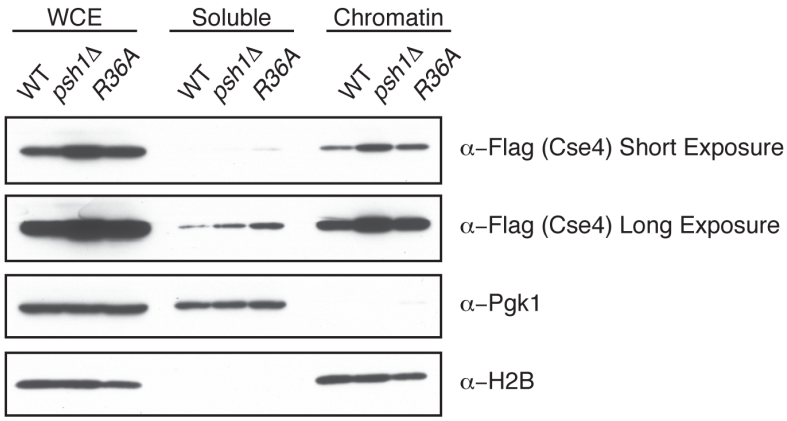

Supplemental Figure 3.3. Chromatin fractionation in H4-R36A
Chromatin fractionation from **Figure 3.4A** with a long exposure of the Flag-Cse4 blot to detect CENP-A^{Cse4} in the soluble fraction. Whole cell extracts (WCE) from WT (SBY10025), *psh1*Δ (SBY10590), and *H4-R36A* (SBY9397) cells expressing *pGAL-3Flag-CSE4* were fractionated into soluble and chromatin fractions. 3Flag-Cse4 levels were monitored in each fraction with α-Flag antibodies. Pgk1 and H2B are markers of the soluble and chromatin fractions, respectively.

3.9 SUPPLEMENTAL TABLES

Supplemental Table 3.1. Plasmids used in this chapter

Plasmid Number	Description	Source
pAFS52	*LacO(256), TRP1* (integrating)	(*216*)
pSB116	*pHIS3-pCUP1-GFP12-LacI12, HIS3* (integrating)	(*225*)
pSB1665	*pGAL-3Flag-CSE4, URA3 (*integrating*)*	(*43*)
pSB1673	*H4 synthetic WT HYG (HHT1-HHF1* integrating*), chloramphenicol* [1]	Gift from J. Dai
pSB1729	*pGAL-3Flag-CSE4*, *LEU2* (integrating)	(*131*)
pSB1730	*2 micron, LEU2, pGAL-3Flag-CSE4*	This study
pSB1749	*H4-R36A (HHT1-HHF1* integrating*), HYG, chloramphenicol* [1]	Gift from J. Dai
pSB2576	H3-R49A (*HHT1-HHF1* integrating), HYG, chloramphenicol [1]	Gift from J. Dai
pSB2577	*H3-V46A (HHT1-HHF1* integrating*), HYG, chloramphenicol* [1]	Gift from J. Dai
pSB2578	*H3-R49A (HHT2-HHF2* integrating*), URA, amp*[2]	(*212*)
pSB2579	*H3-V46A (HHT2-HHF2* integrating*), URA, amp* [2]	(*212*)
pSB2580	*H4-R36K (HHT1-HHF1* integrating*), HYG, chloramphenicol* [1]	Gift from J. Dai
pSB2581	*H4-R36E (HHT1-HHF1* integrating*), HYG, chloramphenicol* [1]	Gift from J. Dai
pSB2582	*H4-R36K* (*HHT2-HHF2* integrating), URA, amp [2]	(*212*)
pSB2583	*H4-R36E (HHT2-HHF2* integrating*), URA, amp* [2]	(*212*)
pSB2584	*H4 synthetic WT (HHT2-HHF2* integrating*) URA amp* [2]	(*212*)
pSB2585	*H4-R36A (HHT2-HHF2* integrating*), URA, amp* [2]	(*212*)
pSB2586	*H4-I46A (HHT1-HHF1* integrating*), HYG, chloramphenicol* [1]	Gift from J. Dai
pSB2587	*H4-R35A (HHT1-HHF1* integrating*), HYG, chloramphenicol* [1]	Gift from J. Dai
pSB2588	*H4-I46A (HHT2-HHF2* integrating*), URA, amp* [2]	(*212*)
pSB2589	*H4-R35A (HHT2-HHF2* integrating*), URA, amp* [2]	(*212*)
pSB830	*2 micron, LEU2, pGAL-Myc-CSE4*	(*42*)
YEplac181	*2 micron, LEU2*	(*224*)

[1] From Histone Mutant Library version 3.0 (HMLv3.0). Kind gift from Junbiao Dai, Tsinghua University

[2] From Histone Mutant Library version 2.1 (HMLv2.1). 212. J. Dai *et al.*, Probing nucleosome function: a highly versatile library of synthetic histone H3 and H4 mutants. *Cell.* **134**, 1066-1078 (2008).

Supplemental Table 3.2. Yeast strains used in this chapter

All strains are isogenic to W303

Strain	Genotype	Integrated and [replicating] plasmids
SBY3	*MATa ura3-1 leu2,3-112 his3-11 trp1-1 ade2-1 can1-100 bar1-1 rad5-535*	
SBY3256	*MATa ura3-1 leu2,3-112 his3-11 trp1-1 ade2-1 can1-100 bar1-1 rad5-535 mad1::HIS3*	
SBY9365	*MATα ura3-1 leu2,3-112 his3-11 trp1-1 ade2-1 can1-100 bar1-1 rad5-535 hht1-hhf1::HHT1-synthetic-hhf1-R36A:HYG hht2-hhf2::HHT2-synthetic-hhf2-R36A:URA3*	pSB1749, pSB2585
SBY9397	*MATα ura3-1::pGAL-3Flag-CSE4:URA3 leu2,3-112 his3-11 trp1-1 ade2-1 can1-100 bar1-1 rad5-535 hht1-hhf1::HHT1-synthetic-hhf1-R36A:HYG hht2-hhf2::HHT2-synthetic-hhf2-R36A:URA3*	pSB1665, pSB1749, pSB2585
SBY9401	*MATa ura3-1 leu2,3-112 his3-11 trp1-1 ade2-1 can1-100 bar1-1 rad5-535 hht1-hhf1::HHT1-synthetic-HHF1-synthetic:HYG hht2-hhf2::HHT2-synthetic-HHF2-synthetic:URA3*	pSB1673, pSB2584
SBY9566	*MATα ura3-1::pGAL-3Flag-CSE4:URA3 leu2,3-112 his3-11::pCUP1-GFP12-LacI12:HIS3 trp1-1::LacO(256 repeats):TRP1 ade2-1 can1-100 bar1-1 hht1-hhf1::HHT1-synthetic-hhf1-R36A:HYG hht2-hhf2::HHT2-synthetic-hhf2-R36A:URA3 mad1::HIS3*	pSB1665, pAFS52, pSB116, pSB1749, pSB2585
SBY9979	*MATa ura3-1 leu2,3-112 his3-11 trp1-1 ade2-1 can1-100 bar1-1 rad5-535 hht1-hhf1::HHT1-synthetic-hhf1-R36A:HYG hht2-hhf2::HHT2-synthetic-hhf2-R36A:URA3*	pSB1749, pSB2585
SBY10025	*MATα ura3-1::pGAL-3Flag-CSE4:URA3 leu2,3-112 his3-11 trp1-1 ade2-1 can1-100 bar1-1 rad5-535 hht1-hhf1::HHT1-synthetic-HHF1-synthetic:HYG hht2-hhf2::HHT2-synthetic-HHF2-synthetic:URA3*	pSB1665 pSB1673, pSB2584
SBY10391	*MATα ura3-1::pGAL-3Flag-CSE4:URA3 leu2,3-112 his3-11::pCUP1-GFP12-LacI12:HIS3 trp1-1::LacO(256 repeats):TRP1 ade2-1 can1-100 bar1-1 hht1-hhf1::HHT1-synthetic-hhf1-R36A:HYG hht2-hhf2::HHT2-synthetic-hhf2-R36A:URA3 mad1::HIS3*	pSB1665, pAFS52, pSB116, pSB1749, pSB2585
SBY10392	*MATα ura3-1 leu2,3-112 his3-11 trp1-1 ade2-1 can1-100 bar1-1 rad5-535 hht1-hhf1::hht1-V46A-HHF1-synthetic:HYG hht2-hhf2::hht2-V46A-HHF2-synthetic:URA3*	pSB2577, pSB2579
SBY10393	*MATα ura3-1 leu2,3-112 his3-11 trp1-1 ade2-1 can1-100 bar1-1 rad5-535 hht1-hhf1::hht1-R49A-HHF1-synthetic:HYG hht2-hhf2::hht2-R49A-HHF2-synthetic:URA3*	pSB2576, pSB2578
SBY10394	*MATα ura3-1 leu2,3-112 his3-11 trp1-1 ade2-1 can1-100 bar1-1 rad5-535 hht1-hhf1::HHT1-synthetic-hhf1-I46A:HYG hht2-hhf2::HHT2-synthetic-hhf2-I46A:URA*	pSB2586, pSB2588
SBY10450	*MATα ura3-1::pGAL-3Flag-CSE4:URA3 leu2,3-112 his3-11 trp1-1 ade2-1 can1-100 bar1-1 rad5-535 hht1-hhf1::HHT1-synthetic-HHF1-synthetic:HYG hht2-hhf2::HHT2-synthetic-HHF2-synthetic:URA3 DSN1-3HA:HIS3 MTW1-13Myc:KanMX*	pSB1665, pSB1673, pSB2584
SBY10453	*MATα ura3-1::pGAL-3Flag-CSE4:URA3 leu2,3-112 his3-11 trp1-1 ade2-1 can1-100 bar1-1 rad5-535 hht1-hhf1::HHT1-synthetic-hhf1-R36A:HYG hht2-hhf2::HHT2-synthetic-hhf2-R36A:UR3A DSN1-3HA:HIS3 MTW1-13Myc:KanMX*	pSB1665, pSB1749, pSB2585
SBY10494	*MATα ura3-1::pGAL-3Flag-CSE4:URA3 leu2,3-112 his3-11::pCUP1-GFP12-LacI12:HIS3 trp1-1::LacO(256 repeats):TRP1 ade2-1 can1-*	pSB1665, pAFS52,

	100 bar1-1 hht1-hhf1::HHT1-synthetic-HHF1-synthetic:HYG hht2-hhf2::HHT2-synthetic-HHF2-synthetic:URA3 mad1::HIS3	pSB116, pSB1673, pSB2584
SBY10510	*MATα ura3-1 leu2,3-112 his3-11 trp1-1 ade2-1 can1-100 bar1-1 -535 hht1-hhf1::HHT1-synthetic-hhf1-R35A:HYG hht2-hhf2::HHT2-synthetic-hhf2-R35A:URA3*	pSB2587, pSB2589
SBY10511	*MATα ura3-1::pGAL-3Flag-CSE4:URA3 leu2,3-112 his3-11 trp1-1 ade2-1 can1-100 bar1-1-535 hht1-hhf1::hht1-V46A-HHF1-synthetic:HYG hht2-hhf2::hht2-V46A-HHF2-synthetic:URA3*	pSB1665, pSB2577, pSB2579
SBY10512	*MATα ura3-1::pGAL-3Flag-CSE4:URA3 leu2,3-112 his3-11 trp1-1 ade2-1 can1-100 bar1-1 rad5-535 hht1-hhf1::hht1-R49A-HHF1-synthetic:HYG hht2-hhf2::hht2-R49A-HHF2-synthetic:URA3*	pSB1665, pSB2576, pSB2578
SBY10513	*MATα ura3-1::pGAL-3Flag-CSE4:URA3 leu2,3-112 his3-11 trp1-1 ade2-1 can1-100 bar1-1 rad5-535 hht1-hhf1::HHT1-synthetic-hhf1-I46A:HYG hht2-hhf2::HHT2-synthetic-hhf2-I46A:URA3*	pSB1665, pSB2586, pSB2588
SBY10590	*MATα ura3-1::pGAL-3Flag-CSE4:URA3 leu2,3-112 his3-11 trp1-1 ade2-1 can1-100 bar1-1 rad5-535 hht1-hhf1::HHT1-synthetic-HHF1-synthetic:HYG hht2-hhf2::HHT2-synthetic-HHF2-synthetic:URA3 psh1::KanMX*	pSB1665, pSB1673, pSB2584
SBY10730	*MATα ura3-1 leu2,3-112 his3-11 trp1-1 ade2-1 can1-100 bar1-1 rad5-535 hht1-hhf1::HHT1-synthetic-HHF1-synthetic:HYG hht2-hhf2::NAT*	pSB1673
SBY10734	*MATα ura3-1::pGAL-3Flag-CSE4:URA3 leu2,3-112 his3-11 trp1-1 ade2-1 can1-100 bar1-1 rad5-535 hht1-hhf1::HHT1-synthetic-HHF1-synthetic:HYG hht2-hhf2::NAT*	pSB1665, pSB1673
SBY10778	*MATα ura3-1 leu2,3-112 his3-11 trp1-1 ade2-1 can1-100 bar1-1 rad5-535 hht1-hhf1::HHT1-synthetic-hhf1-R36A:HYG hht2-hhf2::NAT*	pSB1749
SBY10782	*MATα ura3-1::pGAL-3Flag-CSE4:URA3 leu2,3-112 his3-11 trp1-1 ade2-1 can1-100 bar1-1 rad5-535 hht1-hhf1::HHT1-synthetic-hhf1-R36A:HYG hht2-hhf2::NAT*	pSB1665, pSB1749
SBY11189	*MATa ura3-1 leu2,3-112::pGAL-3Flag-CSE4:LEU2 his3-11 trp1-1 ade2-1 can1-100 bar1-1 rad5-535 psh1::KanMX*	pSB1729
SBY13213	*MATα ura3-1::pGAL-3Flag-CSE4:URA3 leu2,3-112 his3-11 trp1-1 ade2-1 can1-100 bar1-1 rad5-535 hht1-hhf1::HHT1-synthetic-HHF1-synthetic:HYG hht2-hhf2::HHT2-synthetic-HHF2-synthetic:URA3 Psh1-13Myc::HIS3*	pSB1665, pSB1673, pSB2584
SBY13215	*MATα ura3-1::pGAL-3Flag-CSE4:URA3 leu2,3-112 his3-11 trp1-1 ade2-1 can1-100 bar1-1 rad5-535 hht1-hhf1::HHT1-synthetic-hhf1-R36A:HYG hht2-hhf2::HHT2-synthetic-hhf2-R36A:URA3 Psh1-13Myc::HIS3*	pSB1665, pSB1749, pSB2585
SBY13389	*MATa ura3-1 leu2,3-112 his3-11 trp1-1 ade2-1 can1-100 bar1-1 rad5-535 hht1-hhf1::HHT1-synthetic-HHF1 synthetic:HYG hht2-hhf2::HHT2-synthetic-HHF2 synthetic:URA3 [2 micron, LEU2]*	[pSB291], pSB1673, pSB2584
SBY13390	*MATa ura3-1 leu2,3-112 his3-11 trp1-1 ade2-1 can1-100 bar1-1 rad5-535 hht1-hhf1::HHT1-synthetic-HHF1 synthetic:HYG hht2-hhf2::HHT2-synthetic-HHF2 synthetic:URA3 [2 micron, LEU2, pGAL-3Flag-CSE4]*	[pSB1730], pSB1673, pSB2584
SBY13391	*MATα ura3-1 leu2,3-112 his3-11 trp1-1 ade2-1 can1-100 bar1-1 rad5-535 hht1-hhf1::HHT1-synthetic-hhf1-R36A:HYG hht2-hhf2::HHT2-synthetic-hhf2-R36A:URA3 [2 micron, LEU2]*	[pSB291], pSB1749, pSB2585
SBY13392	*MATα ura3-1 leu2,3-112 his3-11 trp1-1 ade2-1 can1-100 bar1-1 rad5-535 hht1-hhf1::HHT1-synthetic-hhf1-R36A:HYG hht2-hhf2::HHT2-synthetic-hhf2-R36A:URA3 [2 micron, LEU2, pGAL-3Flag-CSE4]*	[pSB1730], pSB1749, pSB2585
SBY13393	*MATa ura3-1 leu2,3-112 his3-11 trp1-1 ade2-1 can1-100 bar1-1 rad5-535 hht1-hhf1::HHT1-synthetic-hhf1-R36K:HYG hht2-hhf2::HHT2-synthetic-hhf2-R36K:URA3 [2 micron, LEU2]*	[pSB291], pSB2580, pSB2582

SBY13394	*MATa ura3-1 leu2,3-112 his3-11 trp1-1 ade2-1 can1-100 bar1-1 rad5-535 hht1-hhf1::HHT1-synthetic-hhf1-R36K:HYG hht2-hhf2::HHT2-synthetic-hhf2-R36K:URA3 [2 micron, LEU2, pGAL-3Flag-CSE4]*	[pSB1730], pSB2580, pSB2582
SBY13395	*MATα ura3-1 leu2,3-112 his3-11 trp1-1 ade2-1 can1-100 bar1-1 rad5-535 hht1-hhf1::HHT1-synthetic-hhf1-R36E:HYG hht2-hhf2::HHT2-synthetic-hhf2-R36E:URA3 [2 micron, LEU2]*	[pSB291], pSB2581, pSB2583
SBY13396	*MATα ura3-1 leu2,3-112 his3-11 trp1-1 ade2-1 can1-100 bar1-1 rad5-535 hht1-hhf1::HHT1-synthetic-hhf1-R36E:HYG hht2-hhf2::HHT2-synthetic-hhf2-R36E:URA3 [2 micron, LEU2, pGAL-3Flag-CSE4]*	[pSB1730], pSB2581, pSB2583
SBY13407	*MATα ura3-1::pGAL-3Flag-CSE4:URA3 leu2,3-112 his3-11 trp1-1 ade2-1 can1-100 bar1-1 rad5-535 hht1-hhf1::HHT1-synthetic-hhf1-R36K:HYG hht2-hhf2::HHT2-synthetic-hhf2-R36K:URA3*	pSB1665, pSB2580, pSB2582
SBY13723	*MATa ura3-1 leu2,3-112 his3-11 trp1-1 ade2-1 can1-100 bar1-1 rad5-535 hht1-hhf1::HHT1-synthetic-HHF1-synthetic:HYG hht2-hhf2::HHT2-synthetic-HHF2-synthetic:URA3 PSH1-3Flag:TRP1*	pSB1673, pSB2584
SBY13725	*MATa ura3-1 leu2,3-112 his3-11 trp1-1 ade2-1 can1-100 bar1-1 rad5-535 hht1-hhf1::HHT1-synthetic-hhf1-R36A:HYG hht2-hhf2::HHT2-synthetic-hhf2-R36A:URA3 PSH1-3Flag:TRP1*	pSB1749, pSB2585
SBY13729	*MATα ura3-1::pGAL-3Flag-CSE4:URA3 leu2,3-112 his3-11::pCUP1-GFP12-LacI12:HIS3 trp1-1::LacO(256 repeats):TRP1 ade2-1 can1-100 bar1-1 hht1-hhf1::HHT1-synthetic-HHF1-synthetic:HYG hht2-hhf2::HHT2-synthetic-HHF2-synthetic:URA3*	pSB1665, pAFS52, pSB116, pSB1673, pSB2584
SBY13812	*MATa ura3-1 leu2,3-112::pGAL-3Flag-CSE4:LEU2 his3-11 trp1-1 ade2-1 can1-100 bar1-1 rad5-535 hht1-hhf1::HHT1-synthetic-hhf1-R36A:HYG hht2-hhf2::HHT2-synthetic-hhf2-R36A:URA3*	pSB1729, pSB1749, pSB2585
SBY15335	*MATa ura3-1 leu2,3-112 his3-11 trp1-1 ade2-1 can1-100 bar1-1 rad5-535 hht1-hhf1::HHT1-synthetic-HHF1-synthetic:HYG hht2-hhf2::HHT2-synthetic-HHF2-synthetic:URA3 PSH1-13Myc:HIS3 SPT16-3Flag:KanMX*	pSB1673, pSB2584
SBY15624	*MATa ura3-1 leu2,3-112 his3-11 trp1-1 ade2-1 can1-100 bar1-1 rad5-535 hht1-hhf1::HHT1-synthetic-hhf1-R36A:HYG hht2-hhf2::HHT2-synthetic-hhf2-R36A:URA3 PSH1-13Myc:HIS3 SPT16-3Flag:KanMX*	pSB1749, pSB2585
SBY16468	*MATa ura3-1 leu2,3-112 his3-11 trp1-1 ade2-1 can1-100 bar1-1 rad5-535 hht1-hhf1::HHT1-synthetic-hhf1-R36K:HYG hht2-hhf2::HHT2-synthetic-hhf2-R36K:URA3 PSH1-13Myc:HIS3 SPT16-3Flag:KanMX*	pSB2580, pSB2582
SBY16469	*MATα ura3-1 leu2,3-112::pGAL-3Flag-CSE4:LEU2 his3-11 trp1-1 ade2-1 can1-100 bar1-1 rad5-535 hht1-hhf1::HHT1-synthetic-HHF1-synthetic:HYG hht2-hhf2::HHT2-synthetic-HHF2-synthetic:URA3*	pSB1729, pSB1673, pSB2584
SBY16594	*MATa ura3-1 leu2,3-112 his3-11 trp1-1 ade2-1 can1-100 bar1-1 rad5-535 hht1-hhf1::HHT1-synthetic-hhf1-R36K:HYG hht2-hhf2::HHT2-synthetic-hhf2-R36K:URA3 PSH1-3Flag:TRP1*	pSB2580, pSB2582

Supplemental Table 3.3. Oligonucleotides used in this chapter

Oligo Number	Purpose	Sequence (5' to 3')	Source
FO1798 (SB4470)	*ADH1* gene Forward	ACGCTTGGCACGGTGACTG	(*223*)
FO1800 (SB4471)	*ADH1* gene Reverse	ACCGTCGTGGGTGTAACCAGA	(*223*)
FO1803 (SB4472)	*ADH1* 3' Forward	CCCAACTGAAGGCTAGGCTGTGG	(*223*)
FO1804 (SB4473)	*ADH1* 3' Reverse	ACCGGCATGCCGAGCAAATGCCTG	(*223*)
FO1814 (SB4076)	*PMA1* gene Forward	CTATTATTGATGCTTTGAAGACCTCC AG	(*223*)
FO1815 (SB4077)	*PMA1* gene Reverse	TGCCCAAAATAATAGACATACCCCA TAA	(*223*)
OAD383 (SB5027)	*PMA1* 3' Forward	CGTAAGCGAGACTTCCAAATGG	(*226*)
OAD384 (SB5028)	*PMA1* 3' Reverse	TCCTGCCCAGCTCTTCTATAATACTT	(*226*)
OAD394 (SB5029)	*PMA1* 5' Forward	AGTTGCCGCCGGTGAA	(*226*)
OAD395 (SB5030)	*PMA1* 5' Reverse	CCGTAAGATGGGTCAGTTTGTAAAT	(*226*)
SB773	*CEN3* Forward	ATCAGCGCCAAACAATATGGAAAA	(*178*)
SB774	*CEN3* Reverse	GAGCAAAACTTCCACCAGTAAACG	(*178*)
SB5059	*ADH1* 5' Forward	CGACAAAGACAGCACCAACA	This study
SB5060	*ADH1* 5' Reverse	TGTGCGTGAATGAAGGAAGG	This study

Chapter 4. CONCLUSIONS AND PERSPECTIVE

In this dissertation I have presented a detailed analysis of the pattern and consequences of CENP-A^{Cse4} mislocalization in the absence of proteolysis. In addition, I have investigated other chromatin-based mechanisms that contribute to CENP-A^{Cse4} regulation in budding yeast. Below, I highlight the important findings, discuss how my findings relate to other published studies, and comment on future directions for this field.

4.1 CONSERVATION OF CENP-A MISLOCALIZATION PATTERNS AND MECHANISMS

In Chapter 2, my ChIP-seq experiment showed that overexpression of CENP-A^{Cse4}, both in *psh1*Δ and in WT cells, leads to mislocalization to promoter nucleosomes in budding yeast. The absolute level of mislocalization is much higher in the *psh1*Δ background, and this is the only condition where significant misregulation of transcription is also observed. Meta-analysis of CENP-A^{Cse4} mislocalization at 5' and 3' ends of genes showed that both divergent and tandem intergenic regions were susceptible to CENP-A^{Cse4} mislocalization. Interestingly, the mislocalization pattern was different in the H4-R36A mutant, as I present in Chapter 3. In H4-R36A, ChIP-PCR at two representative loci show that CENP-A^{Cse4} is mislocalized to divergent promoters upon overexpression, but at tandem promoters the H4-R36A mutant has no increase in CENP-A^{Cse4} ChIP signal compared to overexpression alone. I propose that this difference in mislocalization pattern may be related to the FACT and Psh1 mislocalization to 3' ends of genes in the H4-R36A mutant, which could be allowing Psh1 to clear CENP-A^{Cse4} at intergenic regions that contain 3' ends of genes, including tandem intergenic regions, while CENP-A^{Cse4} at divergent intergenic regions builds up due to the loss of Psh1 and FACT dynamics.

Table 4.1. Observed CENP-A mislocalization patterns by organism

Organism	Mislocalization pattern	Mutant/condition	Proposed Mechanism	Reference
***Saccharomyces cerevisiae* (Budding Yeast)**	Promoter nucleosomes	*psh1*Δ with highly overexpressed CENP-A^{Cse4}	INO80-C dependent, H2A.Z^{Htz1} containing nucleosomes enriched, high turnover might be involved	Chapter 2, (*131*)
	Promoter nucleosomes	Slightly overexpressed CENP-A^{Cse4}	High H3 turnover	(*88*)
	Promoter nucleosomes	*cac1*Δ *hir1*Δ	Turnover is decreased at promoters in this mutant, may be related to mislocalization pattern	(*63*)
	Highly transcribed genes	C-terminal tagged CENP-A^{Cse4}, sonication ChIP-seq	Could be due to high chromatin accessibility at these regions	(*122, 123*)
	CLRs (AT rich, intergenic, near ARS and tRNA sites)	C-terminal tagged Cse4, sonication ChIP-seq	Could be due to high chromatin accessibility at these regions	(*121, 123*)
	Intergenic regions without 3' ends of genes	H4-R36A	Psh1 is mislocalized with FACT to 3' ends of genes in this condition.	Chapter 3
	Increased CENP-A^{Cse4} enrichment at rDNA and telomeres, slightly decreased at centromeres.	*ubp8*Δ	Removal of a short ubiquitin chain by Ubp8 might be important for Psh1 to further ubiquitylate and degrade ectopic CENP-A^{Cse4}. Also, Ubp8 may protect CENP-A^{Cse4} at centromeres.	(*108*)
	CENP-A^{Cse4} is stabilized in the euchromatin, but specific regions were not identified.	*slx5*Δ	Slx5 ubiquitylates CENP-A^{Cse4} after SUMOylation, potentially in a parallel pathway to Psh1	(*106*)
	CENP-A^{Cse4} is enriched at high turnover nucleosomes in euchromatin	*snf2*Δ	Mislocalization may be nucleosome turnover dependent	(*119*)
	Intergenic and intragenic regions	Overexpressed CENP-A^{Cse4}-K16R. H3 overexpression rescues localization and phenotype	Altered dosage and mislocalization of H3 and CENP-A^{Cse4} lead to chromosome loss/problems	(*227*)

	CENP-A^{Cse4} is enriched at repetitive regions such as Ty elements, telomeres, and rDNA.	C-terminally tagged CENP-A^{Cse4}-myc, with and without overexpression	Could be a hypomorphic allele due to C-terminal tag, or could be overexpressed compared to untagged CENP-A^{Cse4}	(*154*)
	CENP-A^{Cse4} is stabilized in the euchromatin, but specific regions were not identified.	*spt4-138*	Spt4 is important for preventing CENP-A^{Cse4} mislocalization, mechanism seems to be related to heterochromatin formation and gene silencing	(*228*)
	CENP-A^{Cse4} is enriched at the rDNA and at promoter nucleosomes	*cka2*Δ	Deletion of Cka2 (which phosphorylates and activates Psh1) leads to increased incorporation of CENP-A^{Cse4} due to decreased Psh1 activity	(*102*)
***Schizosaccharomyces pombe* (Fission Yeast)**	Increased centromeric CENP-A^{Cnp1}, also some promoter mislocalization	*top3-105*, other topoisomerases may also have an effect	Regulation of DNA topology is important for controlling CENP-A^{Cnp1} localization	(*229*)
	CENP-A^{Cnp1} is enriched at pericentric and chromosome arm regions	*spt16-18* with overexpressed CENP-A^{Cnp1}	Spt16 is important for maintaining H3 chromatin integrity, loss of this integrity may lead to increased CENP-A^{Cnp1} mislocalization	(*99*)
	CENP-A^{Cnp1} is enriched at pericentric and subtelomeric regions	*pst2*Δ mutant	Clr6-complex II is required to maintain H3 chromatin integrity, this loss of integrity may leads to increased CENP-A^{Cnp1} mislocalization	(*99*)
	CENP-A^{Cnp1} is mislocalized near heterochromatin boundaries in both mitotic and meiotic cells, as well as near telomeres. Ectopic kinetochores form, and mislocalization persists for multiple generations. Mislocalization is	Overexpression of CENP-A^{Cnp1}	Kinetochore mislocalization, has to do with heterochromatin boundaries and is usually controlled by ubiquitin-mediated proteolysis.	(*143*)

	CATD dependent. The N-terminus of CENP-A^{Cnp1} is important for preventing mislocalization, and mediates ubiquitin-mediated degradation.			
	Ectopic centromeres form in regions with low H2A.Z, such as subtelomeric regions and rDNA repeats. and rDNA repeats.	Deletion of the endogenous centromere.	Scm3 efficiently maintains CENP-A^{Cnp1} at regions with low H2A.Z	(*127*)
	CENP-A^{Cnp1} is mislocalized to subtelomeric and pericentromeric regions	Overexpression of CENP-A^{Cnp1}	CENP-A^{Cnp1} seems to be attracted to heterochromatin when mislocalized, but heterochromatin is not strictly required	(*126*)
Drosophila melanogaster **(Fruit flies)**	CENP-A^{CID} localization to sites of DNA damage. Ectopic kinetochore formation and genetic instability.	CHRAC14 mutant. Has problems with DNA damage repair and CENP-A^{CID} mislocalization. Ectopic kinetochore formation and genetic instability	CHRAC14 interacts with CENP-A^{CID}, normally prevents its association with DNA break sites	(*230*)
	CENP-A^{CID} becomes mislocalized to pericentric heterochromatin and telomeres (heterochromatin boundaries) when pulse overexpressed. Generally goes to transcriptionally silent, intergenic domains.	Pulse overexpression of CENP-A^{CID}	Low nucleosome turnover, transcriptionally inactive regions are permissive for CENP-A^{CID} mislocalization. Possible evolutionary link between telomeres and centromeres	(*125*)
Homo sapiens **(Human cells)**	CENP-A is overexpressed in human lung adenocarcinoma cells, this is correlated with decreased survival,	Overexpression of CENP-A in cancer cells	Overexpression may cause problems with kinetochore function	(*231*)

CENP-A shows general nuclear staining by immunohistochemistry			
CENP-A is mislocalized to DNAse I hypersensitive sites which are transcription factor hotspots at promoters of oncogenes and tumor suppressors in human colorectal cancer cells. Also to regions of high nucleosome turnover and subtelomeric and pericentric sites, which are regions with high levels of translocations. CENP-A Associates with H3, ATRX and DAXX.	Overexpression of CENP-A in cancer cells	Ectopic CENP-A nucleosomes form octamers, mislocalization may leads to chromosome instability. ATRX/DAXX, not HJURP, found at ectopic sites.	(*145*)
Intergenic CENP-A mislocalization, to CTCF peaks, enhancers, and active promoters. Correlated with H3.3 and H2A.Z nucleosomes, which have higher turnover.	Overexpression of CENP-A either from cancer cell lines or by an inducible promoter	DAXX dependent mislocalization, likely due to high turnover, near CTCF and H2A.Z peaks. CENP-A forms heterotypic nucleosomes with H3.3.	(*120*)
CENP-A is mislocalized in primary colorectal cancer cells	Overexpression of CENP-A in cancer cells	Overexpression is related to mistargeting of CENP-A	(*129*)

The different mislocalization patterns observed in these two conditions was intriguing, and I was curious how these are similar to or different from the CENP-A mislocalization patterns in both other mutants in budding yeast and in other organisms. I therefore surveyed the literature for CENP-A mislocalization patterns in budding yeast, fission yeast, fruit flies, and humans, as

these are the most well studied species in this field. The results of this analysis are summarized in **Table 4.1**. One key finding from this comparison is that there are two main types of mislocalization patterns for CENP-A, which can be divided based on organism. Human cells and budding yeast both show a predominant mislocalization pattern of CENP-A incorporation at promoter nucleosomes, and this seems to be related to both histone variant composition and high histone turnover at these regions. In addition, mislocalization of CENP-A in these species seems to be independent of the normal CENP-A chaperone (Scm3 or HJURP). Instead, complexes such as DAXX/ATRX in humans and INO80 in budding yeast seem to be required for incorporation of CENP-A to chromosome arms (*44, 120, 131, 145*).

In contrast, fission yeast and fruit flies show a different pattern of mislocalization. Instead of being incorporated at promoters, CENP-A in these species tends to become mislocalized to borders between euchromatin and heterochromatin, both at pericentromeres and at sub-telomeric regions (*99, 124-126*). In fission yeast, the centromeric CENP-A chaperone (Scm3) is also required for incorporation of CENP-A at non-centromeric sites (*127*). I think it is possible that differences in ectopic CENP-A chaperone use may determine which of the two types of mislocalization patterns are observed, and I am interested to know which type of chaperone fruit flies use for mislocalized CENP-A^{CID} incorporation.

The consequence of CENP-A mislocalization in different species and mutants is another interesting area of study. The two types of mislocalization discussed above are also correlated with the ability of CENP-A to nucleate ectopic kinetochores. It is simple to picture cell death due to ectopic kinetochore formation, which would lead to DNA breaks during mitosis due to dicentric chromosomes. However, while ectopic kinetochores can form in both fruit flies and fission yeast with CENP-A overexpression, they have not been convincingly observed with only

overexpression of CENP-A in budding yeast or human cells (*124, 125, 143*). Instead, mislocalization of CENP-A^{Cse4} to promoters in budding yeast seems to be correlated to changes in transcription, which could be causing cell death indirectly by affecting other cellular processes (*131*). In human cells, promoter mislocalization of CENP-A due to overexpression is correlated with only small transcriptional changes, but if a ubiquitin ligase is identified that controls CENP-A levels in humans, it is possible that the combination of a mutant in that ligase with overexpression of the centromeric histone variant would have more drastic transcriptional effects (*120*). Some human cancer cells have been identified that overexpress CENP-A, and it is currently unknown how this might be affecting cell growth (*120, 129, 145, 231*). Interestingly, one study found CENP-A mislocalization to occur at promoters of oncogenes and tumor suppressors, so it is possible that CENP-A mislocalization is affecting oncogene or tumor suppressor expression, and that this could be a mechanism by which CENP-A misregulation contributes to oncogenesis (*145*).

4.2 ORGANIZATION OF THE CENP-A^{CSE4} LOCALIZATION REGULATION NETWORK IN BUDDING YEAST

Following the discovery of Psh1, multiple other CENP-A^{Cse4} degradation pathways have also been identified in budding yeast (**Figure 4.1**). Two other ubiquitin ligases, Rcy1, which is an F-box protein that interacts with the SCF complex, and Slx5, a SUMO-targeted ubiquitin ligase, have been shown to mediate CENP-A^{Cse4} proteolysis (*104, 106*). In addition, regulatory aspects are also starting to be understood. The peptidyl-prolyl *cis-trans* isomerase Fpr3 is required to change CENP-A^{Cse4} proline conformation to allow Psh1 to interact with CENP-A^{Cse4}, while Doa1, a binding partner of Cdc48, is required for CENP-A^{Cse4} N-terminal ubiquitylation in an

unknown mechanism that may involve control of cellular ubiquitin pools (*103, 105*). Slx5 mediated CENP-A^{Cse4} ubiquitylation requires CENP-A^{Cse4} to first be SUMOylated by the Siz1/Siz2 SUMO-ligases, providing an extra layer of regulation (*106*). Recent work from the Biggins' lab identified the FACT complex as an essential component of the Psh1 regulatory pathway, which is required for Psh1 to ubiquitylate CENP-A^{Cse4} when it is incorporated into chromatin (*118*). This appears to be related to the study described in Chapter 3 of this dissertation, as the H4-R36A mutant perturbs FACT and Psh1 localization, and decreases the ability of Psh1 to bind to and ubiquitylate CENP-A^{Cse4}.

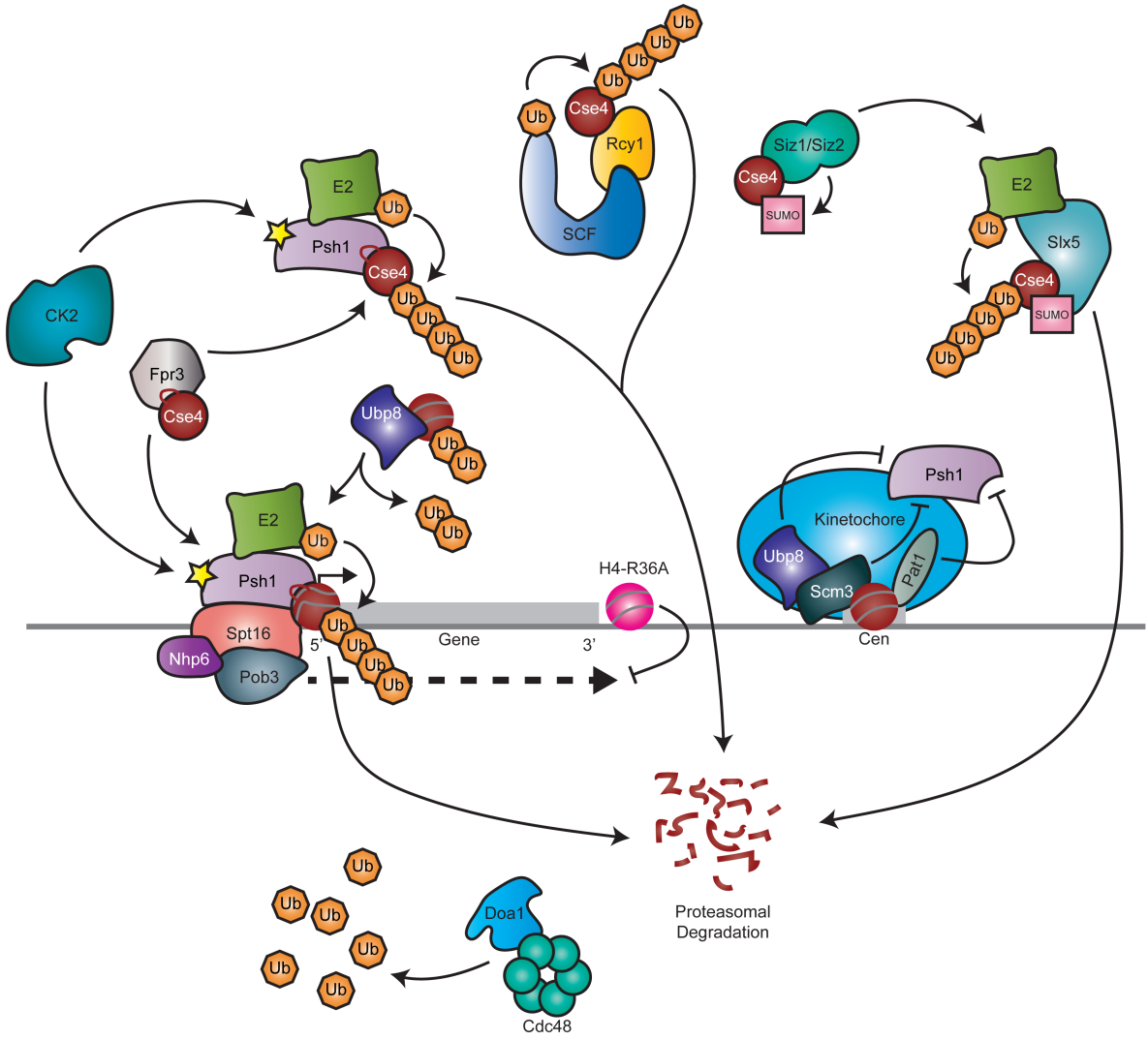

Figure 4.1. Model synthesizing the multiple degradation pathways identified for CENP-A^{Cse4} in budding yeast
CENP-A^{Cse4} ubiquitylation is mediated by the E3 ubiquitin ligases Psh1, Rcy1, and Slx5. Psh1 is activated by CK2 phosphorylation, and requires Fpr3 mediated CENP-A^{Cse4} proline isomerization to bind to CENP-A^{Cse4}. Psh1 also requires FACT (Spt16, Pob3, Nhp6) to mediate ubiquitylation of CENP-A^{Cse4} in a chromatin bound state. The H4 mutant R36A perturbs FACT and Psh1 localization and increases CENP-A^{Cse4} mislocalization. Slx5 is a SUMO-targeted ubiquitin ligase and requires CENP-A^{Cse4} SUMOylation by Siz1/Siz2 before it can mediate CENP-A^{Cse4} ubiquitylation. Rcy1 is an F-box ubiquitin ligase, and interacts with the SCF complex. Doa1, which binds to Cdc48, is required for CENP-A^{Cse4} N-terminal ubiquitylation, and also is important for maintaining cellular ubiquitin pools. At the kinetochore, Pat1 and Scm3 block Psh1 from accessing CENP-A^{Cse4} and the deubiquitinase Ubp8 opposes Psh1 mediated degradation. Ubp8 also has a role outside of the kinetochore, where it is required for efficient Psh1-mediated degradation of CENP-A^{Cse4}.

As centromeric CENP-A^{Cse4} is highly stable, and Psh1 binds to the centromere by ChIP and is purified with kinetochore components, mechanisms that protect CENP-A^{Cse4} at the kinetochore have also been an active area of research (*42, 44, 107*). The kinetochore protein Pat1 and the CENP-A^{Cse4} chaperone Scm3 both block Psh1 activity at the centromere, likely due to physically impeding Psh1 access to centromere bound CENP-A^{Cse4} (*44, 109*). Psh1 is activated by Casein Kinase 2 (CK2) phosphorylation. While the details of where in the cell CK2 is active towards Psh1 are not yet known, it is possible that kinetochore bound Psh1 is in the inactive, unphosphorylated form, and therefore is not active towards the centromeric pool of CENP-A^{Cse4} (*102*). Finally, the deubiquitinase Ubp8 has been identified to oppose Psh1 mediated ubiquitylation, and seems to protect CENP-A^{Cse4} from degradation at the centromere. Ubp8 also appears to be required for Psh1 to mediate polyubiquitylation and degradation of ectopically bound CENP-A^{Cse4}, perhaps by removing a short ubiquitin chain from CENP-A^{Cse4} to relieve a block on Psh1 activity (*108*).

How this regulatory network fits together to control CENP-A^{Cse4} localization is still an open question in the field. My work characterizing the mislocalization pattern of CENP-A^{Cse4} in the *psh1*Δ mutant opens up a new way of thinking about the different pathways, as they may affect separate pools of CENP-A^{Cse4}. In the *psh1*Δ mutant, CENP-A^{Cse4} became mislocalized mainly to promoters, so it seems like either there is still an intact mechanism preventing localization to intragenic regions in this strain or promoter regions are more permissive for CENP-A^{Cse4} mislocalization than intragenic chromatin. An interesting future direction would be to compare CENP-A^{Cse4} mislocalization patterns genome-wide in mutants of each branch of the regulatory network to determine which are responsible for control of promoter localization, intragenic localization, soluble CENP-A^{Cse4}, nucleosomal CENP-A^{Cse4}, etc. There may also be a layer of

cell cycle control of these different degradation pathways, which would be important to understand in the future. Finally, while no human homolog of Psh1 has yet been identified, the discovery of other ubiquitin ligases besides Psh1 that act on CENP-A^{Cse4} suggests the possibility of finding their homologs in the human genome, which would allow future studies on the importance of ubiquitin-mediated proteolysis on human centromeric histone variant localization.

APPENDIX A: CENP-A^{CSE4} IS SYNTHETIC DOSAGE LETHAL WITH *RTS1*Δ

Introduction:

An epistatic miniarray profile (E-MAP) was previously used to identify genes that showed strong negative interactions with Psh1, in collaboration with Nevan Krogan (UCSF) (*232*). One gene that had a strong negative interaction with Psh1 was *RTS1*, which encodes for a B' (B56) regulatory subunit of the PP2A phosphatase (*233*). Rts1 is one of two B type PP2A subunits in budding yeast, and it has broad specificity (*233*). One role of PP2A-Rts1 is at the pericentromere, where it is required for biorientation of the kinetochore and for tension sensing (*234-237*). For the tension sensing role, lack of tension brings Sgo1 to the centromere via Bub1 phosphorylation of H2A-S121. Sgo1 then recruits PP2A-Rts1 and other pericentric factors required for kinetochore biorientation. PP2A-Rts1 phosphatase activity is important for releasing Sgo1 when proper kinetochore-microtubule attachments are made.

Results:

The E-MAP result of a negative genetic interaction with *psh1*Δ was supported in the W303 strain background (**Figure A.1A**). In addition, overexpression of CENP-A^{Cse4} is lethal with *rts1*Δ, to a similar extent as with *psh1*Δ (**Figure A.1B**). Deletion of the other B type PP2A subunit, Cdc55, is only slightly sensitive to CENP-A^{Cse4} overexpression (**Figure A.1C**). *rts1*Δ is not sensitive to canonical histone H3 overexpression, so this is specific for the centromeric histone variant (**Figure A.1D**).

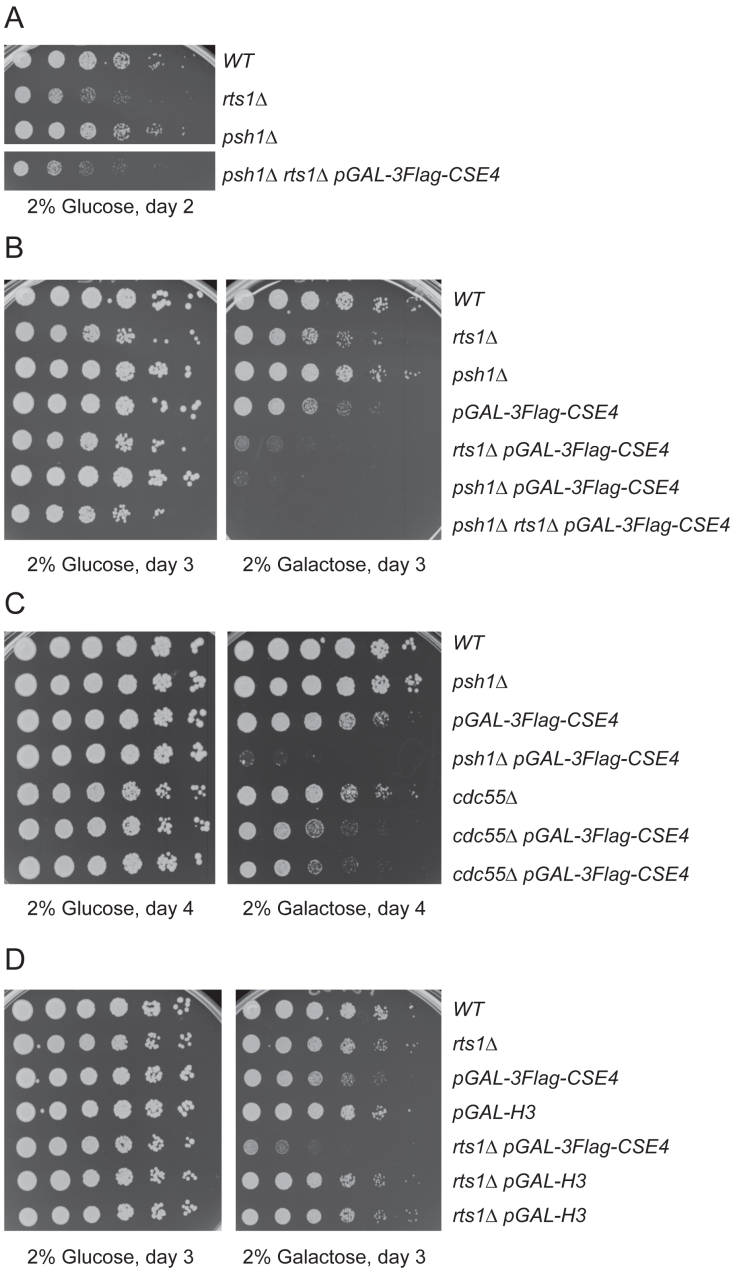

Figure A.1. *rts1*Δ dies with overexpression of CENP-A^{Cse4}

(A) Serial dilution growth assay of WT (SBY3), *rts1*Δ (SBY8182), *psh1*Δ (SBY8336), and *psh1*Δ *rts1*Δ *pGAL-3Flag-CSE4* (SBY13402) plated on 2% glucose, so Cse4 is not overexpressed. (B) Serial dilution growth assay of WT (SBY3), *rts1*Δ (SBY8182), *psh1*Δ (SBY8336), *pGAL-3Flag-CSE4* (SBY9540), *rts1*Δ *pGAL-3Flag-CSE4* (SBY13131), *psh1*Δ *pGAL-3Flag-CSE4* (SBY11189), and *psh1*Δ *rts1*Δ *pGAL-3Flag-CSE4* (SBY13042) plated on 2% glucose (no Cse4 overexpression) or 2% galactose (Cse4 overexpression). (C) Serial dilution growth assay of WT (SBY3), *psh1*Δ (SBY8336), *pGAL-3Flag-CSE4* (SBY9540), *psh1*Δ *pGAL-3Flag-CSE4* (SBY11189), *cdc55*Δ (SBY8181), *cdc55*Δ *pGAL-3Flag-CSE4* isolate 1 (SBY13949), *cdc55*Δ *pGAL-3Flag-CSE4* isolate 2 (SBY13950) plated on 2% glucose (no Cse4 overexpression) or 2% galactose (Cse4 overexpression). (D) Serial dilution growth assay of WT (SBY2), *rts1*Δ (SBY8182), *pGAL-3Flag-CSE4* (SBY9540), *pGAL-H3* (SBY4471), *rts1*Δ *pGAL-3Flag-CSE4* (SBY13131), *rts1*Δ *pGAL-H3* (SBY13452) and *rts1*Δ *pGAL-H3* (duplicate) (SBY13442) plated on 2% glucose (no Cse4 overexpression) or 2% galactose (Cse4 overexpression).

CENP-A^{Cse4} is destabilized in *rts1*Δ (**Figure A.2A**), and *psh1*Δ *rts1*Δ CENP-A^{Cse4} stability seems to be the same as *psh1*Δ alone (**Figure A.2B**). However, levels of endogenous CENP-A^{Cse4} are not decreased at the centromere, pericentromere, or *SAP4* promoter in *rts1*Δ by ChIP-PCR (**Figure A.2C**).

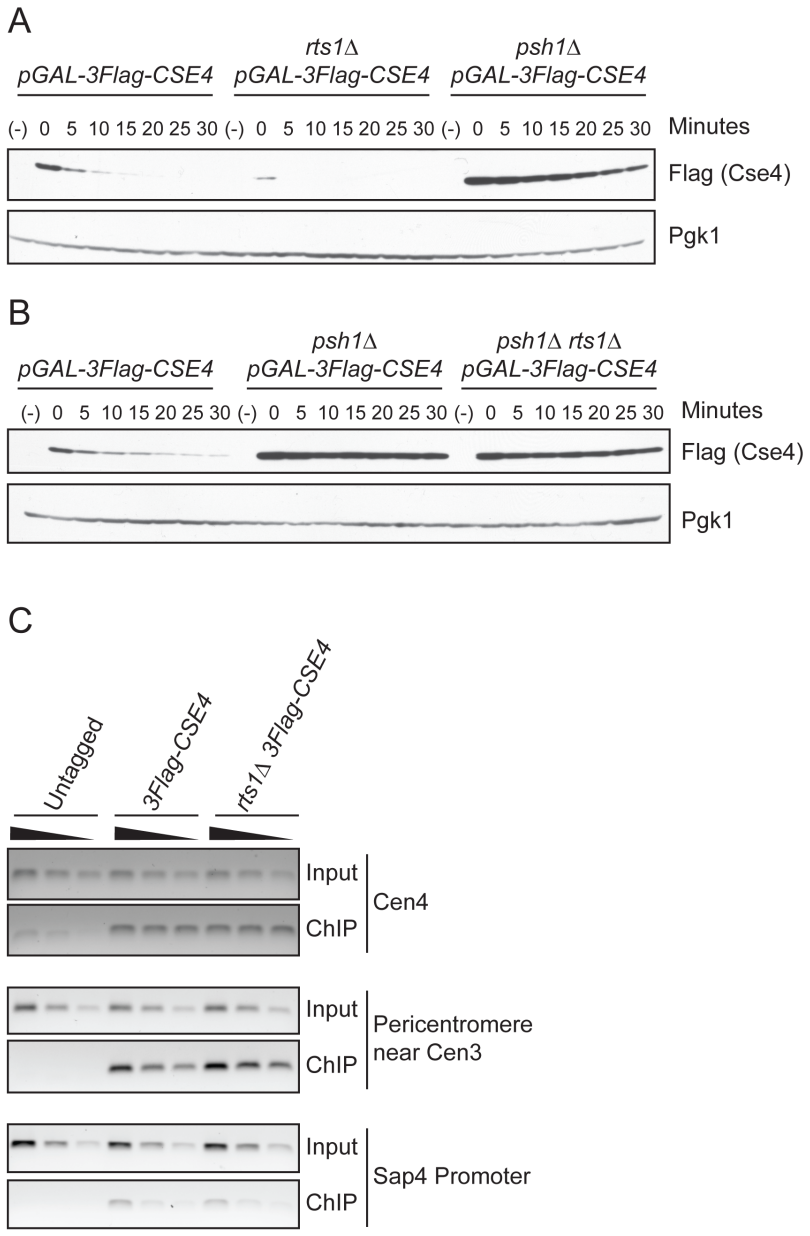

Figure A.2. CENP-A^{Cse4} is destabilized in *rts1*Δ
(A) Western blot showing CENP-A^{Cse4} stability after 2 hours of overexpression with 2% galactose followed by addition of 2% glucose and cyclohexamide to stop transcription and translation of CENP-A^{Cse4}, samples taken for protein lysates at the timepoints shown. anti-Flag shows CENP-A^{Cse4} and anti-Pgk1 is the loading control. Strains are *pGAL-3Flag-CSE4* (SBY9540), *rts1*Δ *pGAL-3Flag-CSE4* (SBY13131), and *psh1*Δ *pGAL-3Flag-CSE4* (SBY11189). (B) CENP-A^{Cse4} stability assay as in A with the following strains: *pGAL-3Flag-CSE4* (SBY9540), *psh1*Δ *pGAL-3Flag-CSE4* (SBY11189), *rts1*Δ *psh1*Δ *pGAL-3Flag-CSE4* (SBY13402). (C) Flag-Cse4 ChIP at Cen4, the pericentromere near Cen3, and the *SAP4* promoter in an untagged control (SBY3), *3Flag-CSE4* (SBY10419), and *rts1*Δ *3Flag-CSE4* (SBY13465). 3 fold dilutions of Input (1:100, 1:300, 1:900) and ChIP (1:3, 1:9, 1:27) were used for PCR analysis.

One possible model to explain these results is that the *rts1*Δ with overexpressed CENP-A^{Cse4} synthetic dosage lethality phenotype may be mediated through Sgo1 activity, since *rts1*Δ cells have increased Sgo1 at the centromere, and both *rts1*Δ and *sgo1-3A* cells are defective in the tension checkpoint and have biorientation defects (*234-237*). It is possible that overexpressed CENP-A^{Cse4} is interfering with biorientation, and that this is causing a problem in *rts1*Δ because there is extra Sgo1 at the centromere. I tested the *sgo1-3A* mutant, which disrupts the PP2A-Sgo1 interaction, and found that it is sick with CENP-A^{Cse4} overexpression (**Figure A.3A**). This suggests there may be a biorientation defect. In support of this hypothesis, Pds1 is stabilized in *rts1*Δ when CENP-A^{Cse4} is overexpressed (Figure A.3B), and this is partially rescued in a spindle checkpoint mutant (**Figure A.3C**). *mad3*Δ does not rescue growth of *rts1*Δ with overexpressed CENP-A^{Cse4} (**Figure A.3D**) so it is likely due to a chromosome segregation and/or biorientation defect, rather than over-activation of the spindle checkpoint. In the future, this hypothesis can be tested by sister spot assays to monitor chromosome segregation defects in *rts1*Δ *mad3*Δ +/- overexpressed CENP-A^{Cse4}.

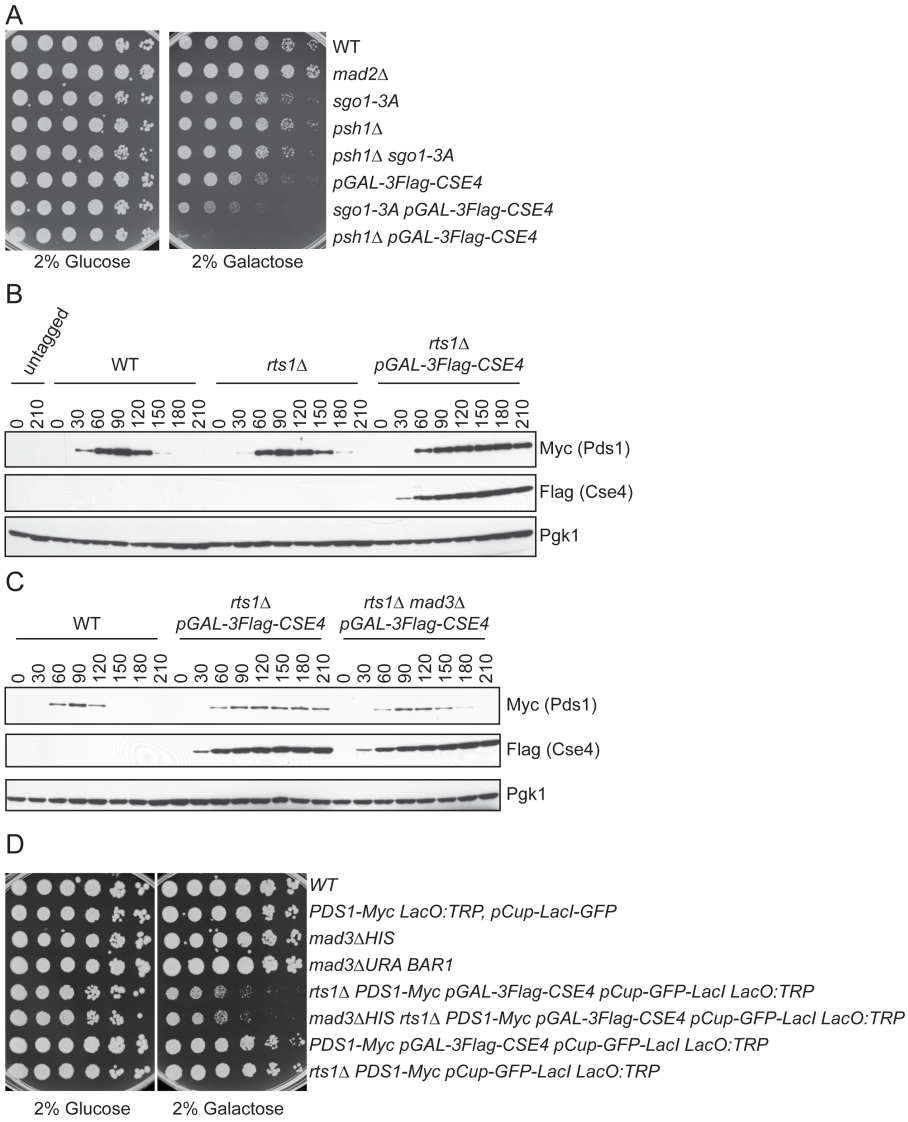

Figure A.3. Overexpression of CENP-A^{Cse4} in *rts1*Δ may cause a biorientation defect
(A) *sgo1-3A* is sensitive to CENP-A^{Cse4} overexpression. Serial dilution growth assay of WT (SBY3), *mad2*Δ (SBY292), *sgo1-3A* (SBY13415), *psh1*Δ (SBY8336), *psh1*Δ *sgo1-3A* (SBY13519), *pGAL-3Flag-CSE4* (SBY9540), *sgo1-3A pGAL-3Flag-CSE4* (SBY13520), and *psh1*Δ *pGAL-3Flag-CSE4* (SBY11189) plated on 2% glucose (no Cse4 overexpression) and 2% galactose (Cse4 overexpression). (B) Pds1-Myc timecourse with alpha factor arrest and release into YEP + lactic acid media + 2% galactose to induce CENP-A^{Cse4} overexpression. Alpha factor was re-added at t=60 to prevent cells from continuing into next cell cycle. Western blot analysis was performed for Myc-Pds1 (Securin), Flag-Cse4, and Pgk1 (loading control). Strains: untagged (SBY3), WT *PDS1-Myc* (SBY818), *rts1*Δ *PDS1-Myc* (SBY14509), *rts1*Δ *PDS1-Myc pGAL-3Flag-CSE4* (SBY14736). (C) Pds1-Myc timecourse as in B with the following strains: WT *PDS1-Myc* (SBY818), *rts1*Δ *pGAL-3Flag-CSE4 PDS1-Myc* (SBY14736), *rts1*Δ *mad3*Δ *pGAL-3Flag-CSE4 PDS1-Myc* (SBY15371). D. Serial dilution growth assay of WT (SBY3), *PDS1-Myc LacO:TRP pCup-LacI-GFP* (SBY818), *mad3*Δ*HIS* (SBY11071), *mad3*Δ*URA BAR1* (SBY293), *rts1*Δ *PDS1-Myc pGAL-3Flag-CSE4 pCup-GFP-LacI LacO:TRP* (SBY14736), *mad3*Δ*HIS rts1*Δ *PDS1-Myc pGAL-3Flag-CSE4 pCup-GFP-LacI LacO:TRP* (SBY15371), *PDS1-Myc pGAL-3Flag-CSE4 pCup-GFP-LacI LacO:TRP* (SBY15347), *rts1*Δ *PDS1-Myc pCup-GFP-LacI LacO:TRP* (SBY14509), plated on 2% glucose (no Cse4 overexpression) and 2% galactose (Cse4 overexpression).

APPENDIX B: THE EFFECT OF *PSH1*Δ ON KINETOCHORE COMPOSITION

Results:

Based on the observation of Psh1 at centromeric DNA by ChIP-chip, combined with the presence of Psh1 in purified yeast kinetochores by mass spectrometry, I was interested in the role of Psh1 at the kinetochore in budding yeast (*44, 107*). To investigate the kinetochore composition in a *psh1*Δ strain, I purified kinetochores from WT vs. *psh1*Δ strains using either Flag-tagged Dsn1 or a mini-chromosome based kinetochore purification, as previously described (*107, 238*). For the Dsn1-Flag purification, both a 2L blender protocol and a 200ml bead-beat protocol were used. The silver stained kinetochores from the 2L blender lysis kinetochore purification look similar for the two strains, although mass spectrometry has not been performed to quantitatively compare kinetochore composition (**Figure B.1A**). Western blot analysis of inner and outer kinetochore components from the 2L blender kinetochore purification show a difference only for CENP-A^{Cse4}, which is decreased in the kinetochore purified from *psh1*Δ cells compared to WT kinetochores (**Figure B.1B**). This result was consistent with the result from 200ml bead-beat kinetochore purification, which also showed decreased CENP-A^{Cse4} purified with *psh1*Δ kinetochores compared to WT (**Figure B.1C**). In contrast, no difference in CENP-A^{Cse4} protein levels was seen on kinetochores purified by the minichromosome method, when normalized to LacI-Flag levels in the IPs (**Figure B.1D**). Overall, the difference in CENP-A^{Cse4} levels at *psh1*Δ kinetochores is intriguing, but should be repeated using the freezer mill lysis method and using quantitative mass spectrometry to determine if there are any compositional differences for both the Dsn1-Flag and mini-chromosome purification methods in the future.

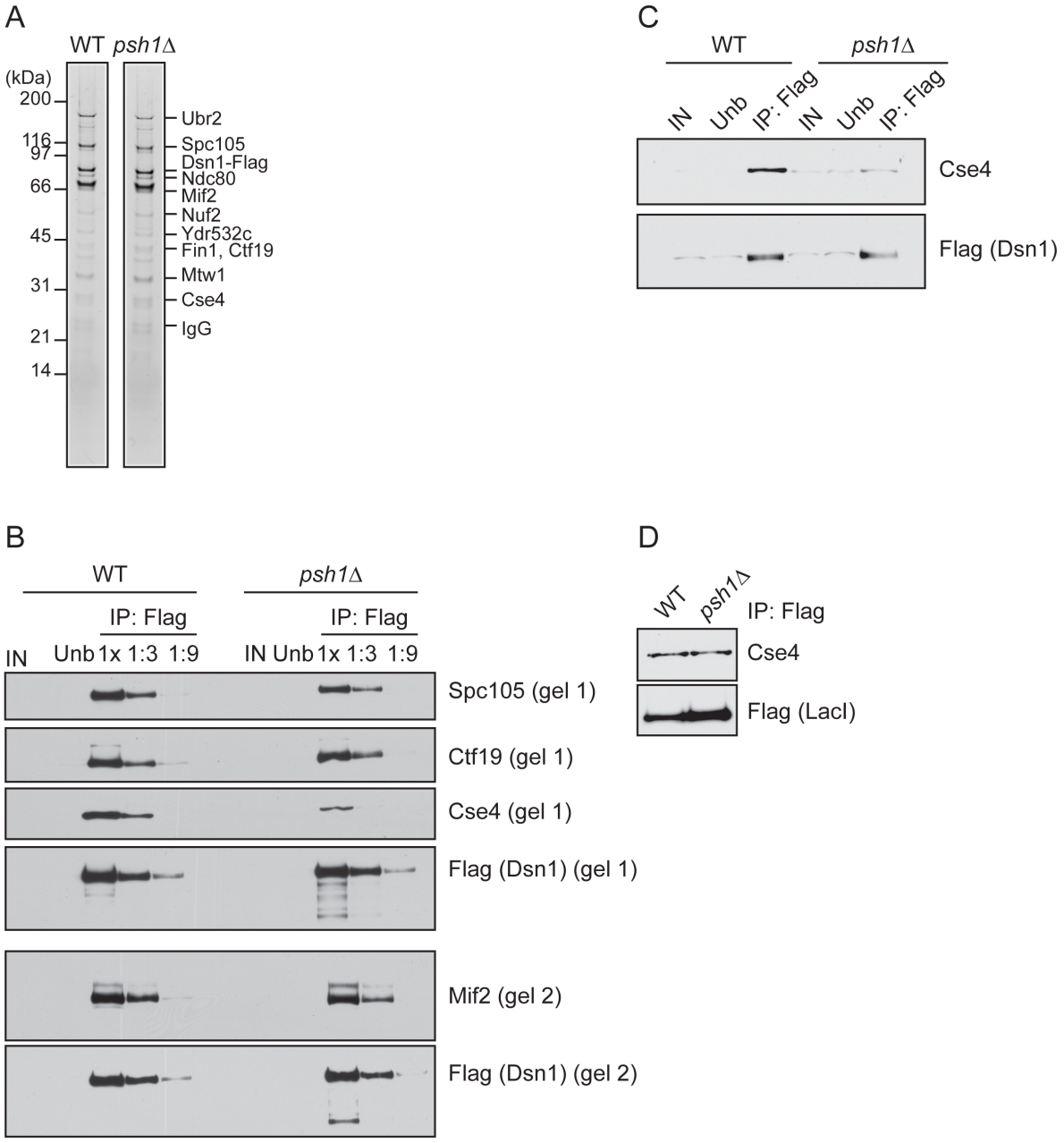

Figure B.1. Kinetochore composition in *psh1*Δ
(A) Silver stained 2L blender kinetochore purifications from WT *DSN1-HIS-Flag* (SBY8253) and *psh1*Δ *DSN1-HIS-Flag* (SBY9363). (B) Western blot kinetochore proteins from a 2L blender kinetochore purification from strains as in (A), two gels were run with the same samples, as indicated by the "gel 1" and "gel 2" labels. (C) Western blot of Dsn1-HIS-Flag and CENP-A^{Cse4} from a 200ml bead-beat kinetochore purifications from strains as in (A). (D) Western blot of LacI-Flag and CENP-A^{Cse4} from a mini-chromosome purification from WT mini-chromosome (SBY5203) and *psh1*Δ mini-chromosome (SBY9369) strains.

References

1. R. D. Kornberg, Chromatin structure: a repeating unit of histones and DNA. *Science.* **184**, 868-871 (1974).
2. S. Venkatesh, J. L. Workman, Histone exchange, chromatin structure and the regulation of transcription. *Nat Rev Mol Cell Biol.* **16**, 178-189 (2015).
3. K. Luger, A. W. Mader, R. K. Richmond, D. F. Sargent, T. J. Richmond, Crystal structure of the nucleosome core particle at 2.8 A resolution. *Nature.* **389**, 251-260 (1997).
4. C. L. Woodcock, R. P. Ghosh, Chromatin Higher-order Structure and Dynamics. *Cold Spring Harbor Perspectives in Biology.* **2**, a000596-a000596 (2010).
5. T. H. Hsieh *et al.*, Mapping Nucleosome Resolution Chromosome Folding in Yeast by Micro-C. *Cell.* **162**, 108-119 (2015).
6. J. M. Belton, J. Dekker, Measuring Chromatin Structure in Budding Yeast. *Cold Spring Harb Protoc.* **2015**, 614-618 (2015).
7. J. H. Gibcus, J. Dekker, The hierarchy of the 3D genome. *Mol Cell.* **49**, 773-782 (2013).
8. E. Lieberman-Aiden *et al.*, Comprehensive mapping of long-range interactions reveals folding principles of the human genome. *Science.* **326**, 289-293 (2009).
9. C. L. White, R. K. Suto, K. Luger, Structure of the yeast nucleosome core particle reveals fundamental changes in internucleosome interactions. *Embo J.* **20**, 5207-5218 (2001).
10. C. R. Clapier, B. R. Cairns, The biology of chromatin remodeling complexes. *Annu Rev Biochem.* **78**, 273-304 (2009).
11. K. Bloom, A. Joglekar, Towards building a chromosome segregation machine. *Nature.* **463**, 446-456 (2010).

12. O. K. Smith, M. I. Aladjem, Chromatin structure and replication origins: determinants of chromosome replication and nuclear organization. *J Mol Biol.* **426**, 3330-3341 (2014).

13. K. Struhl, E. Segal, Determinants of nucleosome positioning. *Nat Struct Mol Biol.* **20**, 267-273 (2013).

14. M. Li, Y. Fang, Histone variants: the artists of eukaryotic chromatin. *Sci China Life Sci.* **58**, 232-239 (2015).

15. O. J. Rando, Combinatorial complexity in chromatin structure and function: revisiting the histone code. *Curr Opin Genet Dev.* **22**, 148-155 (2012).

16. B. Bartholomew, Regulating the chromatin landscape: structural and mechanistic perspectives. *Annu Rev Biochem.* **83**, 671-696 (2014).

17. G. E. Blake, E. D. Watson, Unravelling the complex mechanisms of transgenerational epigenetic inheritance. *Curr Opin Chem Biol.* **33**, 101-107 (2016).

18. R. Bar-Ziv, Y. Voichek, N. Barkai, Chromatin dynamics during DNA replication. *Genome Res.* (2016).

19. R. T. Kamakaka, S. Biggins, Histone variants: deviants? *Genes Dev.* **19**, 295-310 (2005).

20. B. Biterge, R. Schneider, Histone variants: key players of chromatin. *Cell Tissue Res.* **356**, 457-466 (2014).

21. I. Albert *et al.*, Translational and rotational settings of H2A.Z nucleosomes across the *Saccharomyces cerevisiae* genome. *Nature.* **446**, 572-576 (2007).

22. E. Luk *et al.*, Stepwise histone replacement by SWR1 requires dual activation with histone H2A.Z and canonical nucleosome. *Cell.* **143**, 725-736 (2010).

23. R. M. Raisner *et al.*, Histone variant H2A.Z marks the 5' ends of both active and inactive genes in euchromatin. *Cell.* **123**, 233-248 (2005).

24. V. Subramanian, P. A. Fields, L. A. Boyer, H2A.Z: a molecular rheostat for transcriptional control. *F1000Prime Rep.* **7**, 01 (2015).

25. J. Zlatanova, A. Thakar, H2A.Z: view from the top. *Structure.* **16**, 166-179 (2008).

26. O. J. Rando, F. Winston, Chromatin and transcription in yeast. *Genetics.* **190**, 351-387 (2012).

27. C. M. Weber, S. Ramachandran, S. Henikoff, Nucleosomes are context-specific, H2A.Z-modulated barriers to RNA polymerase. *Mol Cell.* **53**, 819-830 (2014).

28. M. F. Dion *et al.*, Dynamics of Replication-Independent Histone Turnover in Budding Yeast. *Science.* **315**, 1405-1408 (2007).

29. S. Stoler, K. C. Keith, K. E. Curnick, M. Fitzgerald-Hayes, A mutation in *CSE4*, an essential gene encoding a novel chromatin-associated protein in yeast, causes chromosome nondisjunction and cell cycle arrest at mitosis. *Genes Dev.* **9**, 573-586 (1995).

30. P. B. Meluh, P. Yang, L. Glowczewski, D. Koshland, M. M. Smith, Cse4p is a component of the core centromere of *Saccharomyces cerevisiae*. *Cell.* **94**, 607-613 (1998).

31. W. C. Earnshaw, N. Rothfield, Identification of a family of human centromere proteins using autoimmune sera from patients with scleroderma. *Chromosoma.* **91**, 313-321 (1985).

32. D. K. Palmer, K. O'Day, M. H. Wener, B. S. Andrews, R. L. Margolis, A 17-kD centromere protein (CENP-A) copurifies with nucleosome core particles and with histones. *J Cell Biol.* **104**, 805-815 (1987).

33. G. Wieland, S. Orthaus, S. Ohndorf, S. Diekmann, P. Hemmerich, Functional Complementation of Human Centromere Protein A (CENP-A) by Cse4p from *Saccharomyces cerevisiae*. *Mol Cell Biol.* **24**, 6620-6630 (2004).

34. I. M. Cheeseman, The kinetochore. *Cold Spring Harb Perspect Biol.* **6**, a015826 (2014).

35. C. C. Chen, B. G. Mellone, Chromatin assembly: Journey to the CENter of the chromosome. *J Cell Biol.* **214**, 13-24 (2016).

36. D. du Sart *et al.*, A functional neo-centromere formed through activation of a latent human centromere and consisting of non-alpha-satellite DNA. *Nat Genet.* **16**, 144-153 (1997).

37. S. Furuyama, S. Biggins, Centromere identity is specified by a single centromeric nucleosome in budding yeast. *Proc Natl Acad Sci U S A.* **104**, 14706-14711 (2007).

38. G. Mizuguchi, H. Xiao, J. Wisniewski, M. M. Smith, C. Wu, Nonhistone Scm3 and histones CenH3-H4 assemble the core of centromere-specific nucleosomes. *Cell.* **129**, 1153-1164 (2007).

39. S. Stoler *et al.*, Scm3, an essential *Saccharomyces cerevisiae* centromere protein required for G2/M progression and Cse4 localization. *Proc Natl Acad Sci U S A.* **104**, 10571-10576 (2007).

40. R. Camahort *et al.*, Scm3 is Essential to Recruit the Histone H3 Variant Cse4 to Centromeres and to Maintain a Functional Kinetochore. *Mol Cell.* **26**, 853-865 (2007).

41. E. M. Dunleavy *et al.*, HJURP is a cell-cycle-dependent maintenance and deposition factor of CENP-A at centromeres. *Cell.* **137**, 485-497 (2009).

42. K. A. Collins, S. Furuyama, S. Biggins, Proteolysis contributes to the exclusive centromere localization of the yeast Cse4/CENP-A histone H3 variant. *Curr Biol.* **14**, 1968-1972 (2004).

43. P. Ranjitkar *et al.*, An E3 ubiquitin ligase prevents ectopic localization of the centromeric histone H3 variant via the centromere targeting domain. *Mol Cell.* **40**, 455-464 (2010).

44. G. Hewawasam *et al.*, Psh1 is an E3 ubiquitin ligase that targets the centromeric histone variant Cse4. *Mol Cell.* **40**, 444-454 (2010).

45. C. L. Liu *et al.*, Single-Nucleosome Mapping of Histone Modifications in *S. cerevisiae*. *PLoS Biol.* **3**, e328 (2005).

46. Z. A. Gurard-Levin, J. P. Quivy, G. Almouzni, Histone chaperones: assisting histone traffic and nucleosome dynamics. *Annu Rev Biochem.* **83**, 487-517 (2014).

47. C. Raynaud *et al.*, Chromatin meets the cell cycle. *J Exp Bot.* **65**, 2677-2689 (2014).

48. Q. Li, R. Burgess, Z. Zhang, All roads lead to chromatin: Multiple pathways for histone deposition. *BBA - Gene Regulatory Mechanisms.* **1819**, 238-246 (2012).

49. D. Doenecke, Chromatin dynamics from S-phase to mitosis: contributions of histone modifications. *Cell Tissue Res.* **356**, 467-475 (2014).

50. I. Whitehouse, O. J. Rando, J. Delrow, T. Tsukiyama, Chromatin remodelling at promoters suppresses antisense transcription. *Nature.* **450**, 1031-1035 (2007).

51. M. N. Prioleau, D. M. MacAlpine, DNA replication origins-where do we begin? *Genes Dev.* **30**, 1683-1697 (2016).

52. H. A. Cole, V. Nagarajavel, D. J. Clark, Perfect and imperfect nucleosome positioning in yeast. *BBA - Gene Regulatory Mechanisms.* (2012).

53. M. L. Eaton, K. Galani, S. Kang, S. P. Bell, D. M. MacAlpine, Conserved nucleosome positioning defines replication origins. *Genes Dev.* **24**, 748-753 (2010).

54. N. J. Krogan *et al.*, A Snf2 family ATPase complex required for recruitment of the histone H2A variant Htz1. *Mol Cell.* **12**, 1565-1576 (2003).

55. M. S. Kobor *et al.*, A protein complex containing the conserved Swi2/Snf2-related ATPase Swr1p deposits histone variant H2A.Z into euchromatin. *PLoS Biol.* **2**, E131 (2004).

56. G. Mizuguchi *et al.*, ATP-driven exchange of histone H2AZ variant catalyzed by SWR1 chromatin remodeling complex. *Science.* **303**, 343-348 (2004).

57. E. Luk *et al.*, Chz1, a nuclear chaperone for histone H2AZ. *Mol Cell.* **25**, 357-368 (2007).

58. A. Ranjan *et al.*, Nucleosome-free region dominates histone acetylation in targeting SWR1 to promoters for H2A.Z replacement. *Cell.* **154**, 1232-1245 (2013).

59. M. Papamichos-Chronakis, S. Watanabe, O. J. Rando, C. L. Peterson, Global regulation of H2A.Z localization by the INO80 chromatin-remodeling enzyme is essential for genome integrity. *Cell.* **144**, 200-213 (2011).

60. K. Yen, V. Vinayachandran, B. F. Pugh, SWR-C and INO80 chromatin remodelers recognize nucleosome-free regions near +1 nucleosomes. *Cell.* **154**, 1246-1256 (2013).

61. F. Wang, A. Ranjan, D. Wei, C. Wu, Comment on "A histone acetylation switch regulates H2A.Z deposition by the SWR-C remodeling enzyme". *Science.* **353**, 358 (2016).

62. M. Udugama, A. Sabri, B. Bartholomew, The INO80 ATP-dependent chromatin remodeling complex is a nucleosome spacing factor. *Mol Cell Biol.* **31**, 662-673 (2011).

63. J. L. da Rosa, J. Holik, E. M. Green, O. J. Rando, P. D. Kaufman, Overlapping regulation of CenH3 localization and histone H3 turnover by CAF-1 and HIR proteins in *Saccharomyces cerevisiae*. *Genetics.* **187**, 9-19 (2011).

64. C. Jin, G. Felsenfeld, Nucleosome stability mediated by histone variants H3.3 and H2A.Z. *Genes Dev.* **21**, 1519-1529 (2007).

65. F. Malvezzi, S. Westermann, "Uno, nessuno e centomila": the different faces of the budding yeast kinetochore. *Chromosoma.* **123**, 447-457 (2014).

66. L. Clarke, J. Carbon, Isolation of a yeast centromere and construction of functional small circular chromosomes. *Nature.* **287**, 504-509 (1980).

67. J. S. Verdaasdonk, K. Bloom, Centromeres: unique chromatin structures that drive chromosome segregation. *Nature Publishing Group.* **12**, 320-332 (2011).

68. T. Fukagawa, W. C. Earnshaw, The centromere: chromatin foundation for the kinetochore machinery. *Developmental Cell.* **30**, 496-508 (2014).

69. M. Fitzgerald-Hayes, L. Clarke, J. Carbon, Nucleotide sequence comparisons and functional analysis of yeast centromere DNAs. *Cell.* **29**, 235-244 (1982).

70. J. Lechner, J. Ortiz, The *Saccharomyces cerevisiae* kinetochore. *FEBS Lett.* **389**, 70-74 (1996).

71. T. M. Ng, W. G. Waples, B. D. Lavoie, S. Biggins, Pericentromeric sister chromatid cohesion promotes kinetochore biorientation. *Mol Biol Cell.* **20**, 3818-3827 (2009).

72. A. L. Marston, Chromosome segregation in budding yeast: sister chromatid cohesion and related mechanisms. *Genetics.* **196**, 31-63 (2014).

73. A. Belmont, Mitotic chromosome structure and condensation. *Current Opinion in Cell Biology.* **18**, 632-638 (2006).

74. E. Duro, A. L. Marston, From equator to pole: splitting chromosomes in mitosis and meiosis. *Genes Dev.* **29**, 109-122 (2015).

75. J. S. Choy, R. Acuna, W. C. Au, M. A. Basrai, A role for histone H4K16 hypoacetylation in *Saccharomyces cerevisiae* kinetochore function. *Genetics.* **189**, 11-21 (2011).

76. J. S. Choy, P. K. Mishra, W. C. Au, M. A. Basrai, Insights into assembly and regulation of centromeric chromatin in *Saccharomyces cerevisiae*. *BBA - Gene Regulatory Mechanisms.* **1819**, 776-783 (2012).

77. K. L. McKinley, I. M. Cheeseman, The molecular basis for centromere identity and function. *Nat Rev Mol Cell Biol.* **17**, 16-29 (2016).

78. S. Biggins, The composition, functions, and regulation of the budding yeast kinetochore. *Genetics.* **194**, 817-846 (2013).

79. J. Lechner, J. Carbon, A 240 kd multisubunit protein complex, CBF3, is a major component of the budding yeast centromere. *Cell.* **64**, 717-725 (1991).

80. P. Y. Goh, J. V. Kilmartin, *NDC10*: a gene involved in chromosome segregation in *Saccharomyces cerevisiae*. *J. Cell Biol.* **121**, 503-512 (1993).

81. C. Connelly, P. Hieter, Budding yeast *SKP1* encodes a evolutionarily conserved kinetochore protein required for cell cycle progression. *Cell.* **86**, 275-285 (1996).

82. O. Stemmann, J. Lechner, The *Saccharomyces cerevisiae* kinetochore contains a cyclin-CDK complexing homologue, as identified by *in vitro* reconstitution. *Embo J.* **15**, 3611-3620 (1996).

83. U.-S. Cho, S. C. Harrison, Ndc10 is a platform for inner kinetochore assembly in budding yeast. *Nature Structural & Molecular Biology.* **19**, 48-55 (2011).

84. U.-S. Cho, S. C. Harrison, Recognition of the centromere-specific histone Cse4 by the chaperone Scm3. *Proceedings of the National Academy of Sciences.* (2011).

85. Z. Zhou *et al.*, Structural basis for recognition of centromere histone variant CenH3 by the chaperone Scm3. *Nature.* **472**, 234-237 (2011).

86. H. Xiao *et al.*, Nonhistone Scm3 binds to AT-rich DNA to organize atypical centromeric nucleosome of budding yeast. *Mol Cell.* **43**, 369-380 (2011).

87. S. Henikoff, T. Furuyama, The unconventional structure of centromeric nucleosomes. *Chromosoma.* **121**, 341-352 (2012).

88. K. Krassovsky, J. G. Henikoff, S. Henikoff, Tripartite organization of centromeric chromatin in budding yeast. *Proceedings of the National Academy of Sciences.* **109**, 243-248 (2012).

89. T. Furuyama, S. Henikoff, Centromeric nucleosomes induce positive DNA supercoils. *Cell.* **138**, 104-113 (2009).

90. S. Henikoff *et al.*, The budding yeast Centromere DNA Element II wraps a stable Cse4 hemisome in either orientation in vivo. *Elife.* **3**, e01861 (2014).

91. T. Furuyama, C. A. Codomo, S. Henikoff, Reconstitution of hemisomes on budding yeast centromeric DNA. *Nucleic Acids Res.* (2013).

92. J. Wisniewski *et al.*, Imaging the fate of histone Cse4 reveals *de novo* replacement in S phase and subsequent stable residence at centromeres. *Elife.* **3**, e02203 (2014).

93. S. Henikoff, J. G. Henikoff, "Point" centromeres of Saccharomyces harbor single centromere-specific nucleosomes. *Genetics.* **190**, 1575-1577 (2012).

94. I. J. Kingston, J. S. Y. Yung, M. R. Singleton, Biophysical characterization of the centromere-specific nucleosome from budding yeast. *Journal of Biological Chemistry.* **286**, 4021-4026 (2011).

95. N. Sekulic, E. A. Bassett, D. J. Rogers, B. E. Black, The structure of (CENP-A-H4)2 reveals physical features that mark centromeres. *Nature.* **467**, 347-351 (2010).

96. M. Durand-Dubief *et al.*, SWI/SNF-Like Chromatin Remodeling Factor Fun30 Supports Point Centromere Function in *S. cerevisiae*. *PLoS Genet.* **8**, e1002974 (2012).

97. A. L. Chambers *et al.*, The INO80 chromatin remodeling complex prevents polyploidy and maintains normal chromatin structure at centromeres. *Genes Dev.* **26**, 2590-2603 (2012).

98. J. m. Hsu, J. Huang, P. B. Meluh, B. C. Laurent, The yeast RSC chromatin-remodeling complex is required for kinetochore function in chromosome segregation. *Mol Cell Biol.* **23**, 3202-3215 (2003).

99. E. S. Choi *et al.*, Factors that promote H3 chromatin integrity during transcription prevent promiscuous deposition of CENP-A(Cnp1) in fission yeast. *PLoS Genet.* **8**, e1002985 (2012).

100. E. Lejeune *et al.*, The chromatin-remodeling factor FACT contributes to centromeric heterochromatin independently of RNAi. *Curr Biol.* **17**, 1219-1224 (2007).

101. D. Finley, H. D. Ulrich, T. Sommer, P. Kaiser, The ubiquitin-proteasome system of *Saccharomyces cerevisiae*. *Genetics.* **192**, 319-360 (2012).

102. G. S. Hewawasam *et al.*, Phosphorylation by casein kinase 2 facilitates Psh1 protein-assisted degradation of Cse4 protein. *J Biol Chem.* **289**, 29297-29309 (2014).

103. W.-C. Au *et al.*, A novel role of the N terminus of budding yeast histone H3 variant Cse4 in ubiquitin-mediated proteolysis. *Genetics.* **194**, 513-518 (2013).

104. H. Cheng, X. Bao, H. Rao, The F-box protein Rcy1 is involved in the degradation of histone H3 variant Cse4 and genome maintenance. *J Biol Chem.* **291**, 10372-10377 (2016).

105. K. Ohkuni, R. Abdulle, K. Kitagawa, Degradation of centromeric histone H3 variant Cse4 requires the Fpr3 peptidyl-prolyl c*is-trans* isomerase. *Genetics.* **196**, 1041-1045 (2014).

106. K. Ohkuni *et al.*, SUMO-Targeted Ubiquitin Ligase (STUbL) Slx5 regulates proteolysis of centromeric histone H3 variant Cse4 and prevents its mislocalization to euchromatin. *Mol Biol Cell.* (2016).

107. B. Akiyoshi *et al.*, Tension directly stabilizes reconstituted kinetochore-microtubule attachments. *Nature.* **468**, 576-579 (2010).

108. C. Canzonetta *et al.*, SAGA DUB-Ubp8 Deubiquitylates Centromeric Histone Variant Cse4. *G3.* **6**, 287-298 (2016).

109. P. K. Mishra *et al.*, Pat1 protects centromere-specific histone H3 variant Cse4 from Psh1-mediated ubiquitination. *Mol Biol Cell.* **26**, 2067-2079 (2015).

110. E. Herrero, P. H. Thorpe, Synergistic control of kinetochore protein levels by Psh1 and Ubr2. *PLoS Genet.* **12**, e1005855 (2016).

111. O. Moreno-Moreno, S. Medina-Giró, M. Torras-Llort, F. Azorín, The F box protein partner of paired regulates stability of *Drosophila* centromeric histone H3, CenH3^{CID}. *Current Biology.* 1-6 (2011).

112. O. Moreno-Moreno, M. Torras-Llort, F. Azorin, Proteolysis restricts localization of CID, the centromere-specific histone H3 variant of *Drosophila*, to centromeres. *Nucleic Acids Res.* **34**, 6247-6255 (2006).

113. D. Bade, A.-L. Pauleau, A. Wendler, S. Erhardt, The E3 ligase CUL3/RDX controls centromere maintenance by ubiquitylating and stabilizing CENP-A in a CAL1-dependent manner. *Developmental Cell.* **28**, 508-519 (2014).

114. K. Maehara, K. Takahashi, S. Saitoh, CENP-A reduction induces a p53-dependent cellular senescence response to protect cells from executing defective mitoses. *Mol Cell Biol.* **30**, 2090-2104 (2010).

115. S. Gross, F. Catez, H. Masumoto, P. Lomonte, Centromere architecture breakdown induced by the viral E3 ubiquitin ligase ICP0 protein of herpes simplex virus type 1. *PloS one.* **7**, e44227 (2012).

116. P. Lomonte, K. F. Sullivan, R. D. Everett, Degradation of nucleosome-associated centromeric histone H3-like protein CENP-A induced by herpes simplex virus type 1 protein ICP0. *J Biol Chem.* **276**, 5829-5835 (2001).

117. J. A. Sharp, A. A. Franco, M. A. Osley, P. D. Kaufman, Chromatin assembly factor I and Hir proteins contribute to building functional kinetochores in *S. cerevisiae*. *Genes Dev.* **16**, 85-100 (2002).

118. G. M. R. Deyter, S. Biggins, The FACT complex interacts with the E3 ubiquitin ligase Psh1 to prevent ectopic localization of CENP-A. *Genes Dev.* **28**, 1815-1826 (2014).

119. T. Gkikopoulos *et al.*, The SWI/SNF complex acts to constrain distribution of the centromeric histone variant Cse4. *Embo J.* (2011).

120. N. Lacoste *et al.*, Mislocalization of the centromeric histone variant CenH3/CENP-A in human cells depends on the chaperone DAXX. *Mol Cell.* **53**, 631-644 (2014).

121. P. Lefrançois, R. K. Auerbach, C. M. Yellman, G. S. Roeder, M. Snyder, Centromere-like regions in the budding yeast genome. *PLoS Genet.* **9**, e1003209 (2013).

122. P. Lefrancois *et al.*, Efficient yeast ChIP-Seq using multiplex short-read DNA sequencing. *BMC Genomics.* **10**, 1-18 (2009).

123. L. Teytelman, D. M. Thurtle, J. Rine, A. van Oudenaarden, Highly expressed loci are vulnerable to misleading ChIP localization of multiple unrelated proteins. *Proceedings of the National Academy of Sciences.* 1-6 (2013).

124. P. Heun *et al.*, Mislocalization of the *Drosophila* centromere-specific histone CID promotes formation of functional ectopic kinetochores. *Dev Cell.* **10**, 303-315 (2006).

125. A. M. Olszak *et al.*, Heterochromatin boundaries are hotspots for *de novo* kinetochore formation. *Nature Cell Biology.* **13**, 1-11 (2011).

126. A. G. Castillo *et al.*, Telomeric Repeats Facilitate CENP-ACnp1 Incorporation via Telomere Binding Proteins. *PloS one.* **8**, e69673 (2013).

127. Y. Ogiyama, Y. Ohno, Y. Kubota, K. Ishii, Epigenetically induced paucity of histone H2A.Z stabilizes fission-yeast ectopic centromeres. *Nat Struct Mol Biol.* 1-12 (2013).

128. S. G. Zeitlin *et al.*, Double-strand DNA breaks recruit the centromeric histone CENP-A. *Proc Natl Acad Sci U S A.* **106**, 15762-15767 (2009).

129. T. Tomonaga *et al.*, Overexpression and mistargeting of centromere protein-A in human primary colorectal cancer. *Cancer Res.* **63**, 3511-3516 (2003).

130. H. T. Nguyen, W. Wharton, 2nd, J. A. Harper, J. R. Dornhoffer, A. A. Duina, A nucleosomal region important for ensuring proper interactions between the transcription

elongation factor Spt16 and transcribed genes in *Saccharomyces cerevisiae*. *G3.* **3**, 929-940 (2013).

131. E. M. Hildebrand, S. Biggins, Regulation of budding yeast CENP-A levels prevents misincorporation at promoter nucleosomes and transcriptional defects. *PLoS Genet.* **12**, e1005930 (2016).

132. K. Sarma, D. Reinberg, Histone variants meet their match. *Nature Reviews Molecular Cell Biology.* **6**, 139-149 (2005).

133. Y. Yamagishi, T. Sakuno, Y. Goto, Y. Watanabe, Kinetochore composition and its function: lessons from yeasts. *FEMS microbiology reviews.* **38**, 185-200 (2014).

134. C. B. Gerhold, S. M. Gasser, INO80 and SWR complexes: relating structure to function in chromatin remodeling. *Trends in Cell Biology.* **24**, 619-631 (2014).

135. B. Li *et al.*, Preferential occupancy of histone variant H2AZ at inactive promoters influences local histone modifications and chromatin remodeling. *Proc Natl Acad Sci U S A.* **102**, 18385-18390 (2005).

136. S. Henikoff, in *Epigenomics,* A. C. Ferguson-Smith, Greally, John., Martienssen, Rob A., Ed. (Springer, Netherlands, 2009), pp. 101-118.

137. A. Y. Wang, M. J. Aristizabal, C. Ryan, N. J. Krogan, M. S. Kobor, Key functional regions in the histone variant H2A.Z C-terminal docking domain. *Mol Cell Biol.* **31**, 3871-3884 (2011).

138. T. J. Wood, A. Thistlethwaite, M. R. Harris, S. C. Lovell, C. B. Millar, Mutations in non-acid patch residues disrupt H2A.Z's association with chromatin through multiple mechanisms. *PloS one.* **8**, e76394 (2013).

139. S. Watanabe, M. Radman-Livaja, O. J. Rando, C. L. Peterson, A histone acetylation switch regulates H2A.Z deposition by the SWR-C remodeling enzyme. *Science.* **340**, 195-199 (2013).

140. D. R. Foltz *et al.*, Centromere-specific assembly of CENP-A nucleosomes is mediated by HJURP. *Cell.* **137**, 472-484 (2009).

141. S. Muller, G. Almouzni, A network of players in H3 histone variant deposition and maintenance at centromeres. *Biochim Biophys Acta.* **1839**, 241-250 (2014).

142. W. C. Earnshaw, B. R. Migeon, Three related centromere proteins are absent from the inactive centromere of a stable isodicentric chromosome. *Chromosoma.* **92**, 290-296 (1985).

143. M. Gonzalez, H. He, Q. Dong, S. Sun, F. Li, Ectopic centromere nucleation by CENP-A in fission yeast. *Genetics.* **198**, 1433-1446 (2014).

144. K. E. Gascoigne *et al.*, Induced ectopic kinetochore assembly bypasses the requirement for CENP-A nucleosomes. *Cell.* **145**, 410-422 (2011).

145. R. K. Athwal *et al.*, CENP-A nucleosomes localize to transcription factor hotspots and subtelomeric sites in human cancer cells. *Epigenetics & chromatin.* **8**, 2 (2015).

146. A. Strålfors, J. Walfridsson, H. Bhuiyan, K. Ekwall, The FUN30 chromatin remodeler, Fft3, protects centromeric and subtelomeric domains from euchromatin formation. *PLoS Genet.* **7**, e1001334 (2011).

147. K. A. Collins, R. Camahort, C. Seidel, J. L. Gerton, S. Biggins, The overexpression of a *Saccharomyces cerevisiae* centromeric histone H3 variant mutant protein leads to a defect in kinetochore biorientation. *Genetics.* **175**, 513-525 (2007).

148. D. Rangasamy, I. Greaves, D. J. Tremethick, RNA interference demonstrates a novel role for H2A.Z in chromosome segregation. *Nat Struct Mol Biol.* **11**, 650-655 (2004).

149. I. K. Greaves, D. Rangasamy, P. Ridgway, D. J. Tremethick, H2A.Z contributes to the unique 3D structure of the centromere. *Proc Natl Acad Sci U S A.* **104**, 525-530 (2007).

150. N. J. Krogan *et al.*, Regulation of chromosome stability by the histone H2A variant Htz1, the Swr1 chromatin remodeling complex, and the histone acetyltransferase Nua4. *Proc Natl Acad Sci U S A.* **101**, 13513-13518 (2004).

151. S. Kawashima *et al.*, Global analysis of core histones reveals nucleosomal surfaces required for chromosome bi-orientation. *Embo J.* 1-15 (2011).

152. J. G. Henikoff, J. A. Belsky, K. Krassovsky, D. M. MacAlpine, S. Henikoff, Epigenome characterization at single base-pair resolution. *Proceedings of the National Academy of Sciences.* **108**, 18318-18323 (2011).

153. T. B. D. Team, BSgenome.Scerevisiae.UCSC.sacCer3: *Saccharomyces cerevisiae* (Yeast) full genome (UCSC version sacCer3). *R package* **version 1.3.1000**.

154. R. Camahort *et al.*, Cse4 is part of an octameric nucleosome in budding yeast. *Mol Cell.* **35**, 794-805 (2009).

155. E. F. Glynn *et al.*, Genome-wide mapping of the cohesin complex in the yeast *Saccharomyces cerevisiae*. *PLoS Biol.* **2**, E259 (2004).

156. S. A. Weber *et al.*, The kinetochore is an enhancer of pericentric cohesin binding. *PLoS Biol.* **2**, E260 (2004).

157. U. Nagalakshmi *et al.*, The transcriptional landscape of the yeast genome defined by RNA sequencing. *Science.* **320**, 1344-1349 (2008).

158. F. P. Roth, J. D. Hughes, P. W. Estep, G. M. Church, Finding DNA regulatory motifs within unaligned noncoding sequences clustered by whole-genome mRNA quantitation. *Nat Biotechnol.* **16**, 939-945 (1998).

159. A. Lengronne *et al.*, Cohesin relocation from sites of chromosomal loading to places of convergent transcription. *Nature.* **430**, 573-578 (2004).

160. A. N. Yadon *et al.*, Chromatin remodeling around nucleosome-free regions leads to repression of noncoding RNA transcription. *Mol Cell Biol.* **30**, 5110-5122 (2010).

161. M. Adam, F. Robert, M. Larochelle, L. Gaudreau, H2A.Z is required for global chromatin integrity and for recruitment of RNA polymerase II under specific conditions. *Mol Cell Biol.* **21**, 6270-6279 (2001).

162. C. Jeronimo, S. Watanabe, C. D. Kaplan, C. L. Peterson, F. Robert, The histone chaperones FACT and Spt6 restrict H2A.Z from intragenic locations. *Mol Cell.* (2015).

163. X. Shen, G. Mizuguchi, A. Hamiche, C. Wu, A chromatin remodelling complex involved in transcription and DNA processing. *Nature.* **406**, 541-544 (2000).

164. A. Tosi *et al.*, Structure and subunit topology of the INO80 chromatin remodeler and its nucleosome complex. *Cell.* **154**, 1207-1219 (2013).

165. X. Shen, R. Ranallo, E. Choi, C. Wu, Involvement of actin-related proteins in ATP-dependent chromatin remodeling. *Mol Cell.* **12**, 147-155 (2003).

166. A. J. Morrison *et al.*, Mec1/Tel1 phosphorylation of the INO80 chromatin remodeling complex influences DNA damage checkpoint responses. *Cell.* **130**, 499-511 (2007).

167. M. Morillo-Huesca, M. Clemente-Ruiz, E. Andújar, F. Prado, The SWR1 histone replacement complex causes genetic instability and genome-wide transcription misregulation in the absence of H2A.Z. *PloS one.* **5**, e12143 (2010).

168. M. D. Meneghini, M. Wu, H. D. Madhani, Conserved histone variant H2A.Z protects euchromatin from the ectopic spread of silent heterochromatin. *Cell.* **112**, 725-736 (2003).

169. M. V. Granovskaia *et al.*, High-resolution transcription atlas of the mitotic cell cycle in budding yeast. *Genome Biol.* **11**, R24 (2010).

170. M. D. Robinson, D. J. McCarthy, G. K. Smyth, edgeR: a Bioconductor package for differential expression analysis of digital gene expression data. *Bioinformatics.* **26**, 139-140 (2010).

171. Z. Xiao, J. T. McGrew, A. J. Schroeder, M. Fitzgerald-Hayes, *CSE1* and *CSE2,* two new genes required for accurate mitotic chromosome segregation in *Saccharomyces cerevisiae. Mol Cell Biol.* **13**, 4691-4702 (1993).

172. C. M. Gustafsson *et al.*, Identification of new mediator subunits in the RNA polymerase II holoenzyme from *Saccharomyces cerevisiae*. *J Biol Chem.* **273**, 30851-30854 (1998).

173. F. Sherman, G. Fink, C. Lawrence, *Methods in Yeast Genetics*. (Cold Spring Harbor Laboratory Press, Cold Spring Harbor, New York, 1974).

174. M. D. Rose, F. Winston, P. Heiter, *Methods in Yeast Genetics*. (Cold Spring Harbor Laboratory Press, Cold Spring Harbor, N. Y., 1990), pp. p. 198.

175. M. S. Longtine *et al.*, Additional modules for versatile and economical PCR-based gene deletion and modification in *Saccharomyces cerevisiae*. *Yeast.* **14**, 953-961 (1998).

176. J. Minshull *et al.*, Protein phosphatase 2A regulates MPF activity and sister chromatid cohesion in budding yeast. *Curr. Biol.* **6**, 1609-1620 (1996).

177. T. M. Ng *et al.*, Kinetochore function and chromosome segregation rely on critical residues in histones H3 and H4 in budding yeast. *Genetics.* **195**, 795-807 (2013).

178. K. A. Collins, A. R. Castillo, S. Y. Tatsutani, S. Biggins, *De novo* kinetochore assembly requires the centromeric histone H3 variant. *Mol Biol Cell.* **16**, 5649-5660 (2005).

179. H. Li, R. Durbin, Fast and accurate short read alignment with Burrows-Wheeler transform. *Bioinformatics.* **25**, 1754-1760 (2009).

180. H. Li *et al.*, The Sequence Alignment/Map format and SAMtools. *Bioinformatics.* **25**, 2078-2079 (2009).

181. R. C. Gentleman *et al.*, Bioconductor: open software development for computational biology and bioinformatics. *Genome Biol.* **5**, R80 (2004).

182. M. Lawrence, R. Gentleman, V. Carey, rtracklayer: an R package for interfacing with genome browsers. *Bioinformatics.* **25**, 1841-1842 (2009).

183. M. Lawrence *et al.*, Software for computing and annotating genomic ranges. *PLoS Comput Biol.* **9**, e1003118 (2013).

184. K. Chen *et al.*, DANPOS: Dynamic analysis of nucleosome position and occupancy by sequencing. *Genome Research.* **23**, 341-351 (2013).

185. J. T. Robinson *et al.*, Integrative genomics viewer. *Nat Biotechnol.* **29**, 24-26 (2011).

186. H. Thorvaldsdottir, J. T. Robinson, J. P. Mesirov, Integrative Genomics Viewer (IGV): high-performance genomics data visualization and exploration. *Brief Bioinform.* **14**, 178-192 (2013).

187. C. G. Pearson *et al.*, Stable kinetochore-microtubule attachment constrains centromere positioning in metaphase. *Curr Biol.* **14**, 1962-1967 (2004).

188. E. Gari, L. Piedrafita, M. Aldea, E. Herrero, A set of vectors with a tetracycline-regulatable promoter system for modulated gene expression in *Saccharomyces cerevisiae*. *Yeast.* **13**, 837-848 (1997).

189. M. A. Collart, S. Oliviero, Preparation of yeast RNA. *Current protocols in molecular biology / edited by Frederick M. Ausubel ... [et al.]*. **Chapter 13**, Unit13 12 (2001).

190. C. Trapnell, L. Pachter, S. L. Salzberg, TopHat: discovering splice junctions with RNA-Seq. *Bioinformatics.* **25**, 1105-1111 (2009).

191. S. Anders, P. T. Pyl, W. Huber, HTSeq--a Python framework to work with high-throughput sequencing data. *Bioinformatics.* **31**, 166-169 (2015).

192. A. Reiner, D. Yekutieli, Y. Benjamini, Identifying differentially expressed genes using false discovery rate controlling procedures. *Bioinformatics.* **19**, 368-375 (2003).

193. F. Halbritter, H. J. Vaidya, S. R. Tomlinson, GeneProf: analysis of high-throughput sequencing experiments. *Nat Methods.* **9**, 7-8 (2012).

194. M. W. Pfaffl, A new mathematical model for relative quantification in real-time RT-PCR. *Nucleic Acids Res.* **29**, e45 (2001).

195. P. H. Morgan M, Obenchain V, Hayden N. . (Bioconductor).

196. T. Hulsen, J. de Vlieg, W. Alkema, BioVenn - a web application for the comparison and visualization of biological lists using area-proportional Venn diagrams. *BMC Genomics.* **9**, 488 (2008).

197. M. C. Teixeira *et al.*, The YEASTRACT database: a tool for the analysis of transcription regulatory associations in *Saccharomyces cerevisiae*. *Nucleic Acids Res.* **34**, D446-451 (2006).

198. P. T. Monteiro *et al.*, YEASTRACT-DISCOVERER: new tools to improve the analysis of transcriptional regulatory associations in *Saccharomyces cerevisiae*. *Nucleic Acids Res.* **36**, D132-136 (2008).

199. D. Abdulrehman *et al.*, YEASTRACT: providing a programmatic access to curated transcriptional regulatory associations in *Saccharomyces cerevisiae* through a web services interface. *Nucleic Acids Res.* **39**, D136-140 (2011).

200. M. C. Teixeira *et al.*, The YEASTRACT database: an upgraded information system for the analysis of gene and genomic transcription regulation in *Saccharomyces cerevisiae*. *Nucleic Acids Res.* **42**, D161-166 (2014).

201. M. C. Teixeira, P. T. Monteiro, I. Sa-Correia, Predicting gene and genomic regulation in *Saccharomyces cerevisiae*, using the YEASTRACT database: a step-by-step guided analysis. *Methods Mol Biol.* **1361**, 391-404 (2016).

202. K. C. Lindstrom, J. C. Vary, Jr., M. R. Parthun, J. Delrow, T. Tsukiyama, Isw1 functions in parallel with the NuA4 and Swr1 complexes in stress-induced gene repression. *Mol Cell Biol.* **26**, 6117-6129 (2006).

203. J. A. Vincent, T. J. Kwong, T. Tsukiyama, ATP-dependent chromatin remodeling shapes the DNA replication landscape. *Nat Struct Mol Biol.* **15**, 477-484 (2008).

204. E. A. Alcid, T. Tsukiyama, ATP-dependent chromatin remodeling shapes the long noncoding RNA landscape. *Genes Dev.* **28**, 2348-2360 (2014).

205. G. M. Deyter, E. M. Hildebrand, A. D. Barber, S. Biggins, Histone H4 Facilitates the Proteolysis of the Budding Yeast CENP-A^{Cse4} Centromeric Histone Variant. *Genetics.* Early online October 28 (2016).

206. M. Kupiec, Biology of telomeres: lessons from budding yeast. *FEMS microbiology reviews.* **38**, 144-171 (2014).

207. D. K. Palmer, K. O'Day, M. H. Wener, B. S. Andrews, R. L. Margolis, A 17-kD centromere protein (CENP-A) copurifies with nucleosome core particles and with histones. *J Cell Biol.* **104**, 805-815 (1987).

208. A. A. Van Hooser *et al.*, Specification of kinetochore-forming chromatin by the histone H3 variant CENP-A. *Journal of Cell Science.* **114**, 3529-3542 (2001).

209. B. E. Black, D. W. Cleveland, Epigenetic centromere propagation and the nature of CENP-A nucleosomes. *Cell.* **144**, 471-479 (2011).

210. A. Amato, T. Schillaci, L. Lentini, A. Di Leonardo, CENPA overexpression promotes genome instability in pRb-depleted human cells. *Mol Cancer.* **8**, 119 (2009).

211. M. L. Dechassa, K. Wyns, K. Luger, Scm3 deposits a (Cse4-H4)2 tetramer onto DNA through a Cse4-H4 dimer intermediate. *Nucleic Acids Res.* **42**, 5532-5542 (2014).

212. J. Dai *et al.*, Probing nucleosome function: a highly versatile library of synthetic histone H3 and H4 mutants. *Cell.* **134**, 1066-1078 (2008).

213. H. Tachiwana *et al.*, Crystal structure of the human centromeric nucleosome containing CENP-A. *Nature.* **476**, 232-235 (2011).

214. M. M. Smith *et al.*, A novel histone H4 mutant defective in nuclear division and mitotic chromosome transmission. *Mol Cell Biol.* **16**, 1017-1026 (1996).

215. K. Hardwick, A. W. Murray, Mad1p, a phosphoprotein component of the spindle assembly checkpoint in budding yeast. *J. Cell Biol.* **131**, 709-720 (1995).

216. A. F. Straight, A. S. Belmont, C. C. Robinett, A. W. Murray, GFP tagging of budding yeast chromosomes reveals that protein-protein interactions can mediate sister chromatid cohesion. *Curr. Biol.* **6**, 1599-1608 (1996).

217. P. R. Eriksson, D. Ganguli, V. Nagarajavel, D. J. Clark, Regulation of histone gene expression in budding yeast. *Genetics.* **191**, 7-20 (2012).

218. C. F. Kurat *et al.*, Regulation of histone gene transcription in yeast. *Cell Mol Life Sci.* **71**, 599-613 (2014).

219. R. K. Singh, M.-H. M. Kabbaj, J. Paik, A. Gunjan, Histone levels are regulated by phosphorylation and ubiquitylation-dependent proteolysis. *Nature Cell Biology.* **11**, 925-933 (2009).

220. S. J. Hainer, J. A. Martens, Identification of histone mutants that are defective for transcription-coupled nucleosome occupancy. *Mol Cell Biol.* **31**, 3557-3568 (2011).

221. D. Liang, S. L. Burkhart, R. K. Singh, M. H. Kabbaj, A. Gunjan, Histone dosage regulates DNA damage sensitivity in a checkpoint-independent manner by the homologous recombination pathway. *Nucleic Acids Res.* **40**, 9604-9620 (2012).

222. I. Jung *et al.*, Global mapping of the regulatory interactions of histone residues. *FEBS Lett.* **589**, 4061-4070 (2015).

223. A. A. Duina *et al.*, Evidence that the localization of the elongation factor Spt16 across transcribed genes is dependent upon histone H3 integrity in *Saccharomyces cerevisiae*. *Genetics.* **177**, 101-112 (2007).

224. R. D. Gietz, A. Sugino, New yeast-*Escherichia coli* shuttle vectors constructed with *in vitro* mutagenized yeast genes lacking six-base pair restriction sites. *Gene.* **74**, 527-534 (1988).

225. S. Biggins *et al.*, The conserved protein kinase Ipl1 regulates microtubule binding to kinetochores in budding yeast. *Genes Dev.* **13**, 532-544 (1999).

226. C. N. Myers *et al.*, Mutant versions of the *S. cerevisiae* transcription elongation factor Spt16 define regions of Spt16 that functionally interact with histone H3. *PloS one.* **6**, e20847 (2011).

227. W. C. Au, M. J. Crisp, S. Z. DeLuca, O. J. Rando, M. A. Basrai, Altered dosage and mislocalization of histone H3 and Cse4p lead to chromosome loss in *Saccharomyces cerevisiae*. *Genetics.* **179**, 263-275 (2008).

228. L. B. Crotti, M. A. Basrai, Functional roles for evolutionarily conserved Spt4p at centromeres and heterochromatin in *Saccharomyces cerevisiae*. *Embo J.* **23**, 1804-1814 (2004).

229. U. Norman-Axelsson, M. Durand-Dubief, P. Prasad, K. Ekwall, DNA topoisomerase III localizes to centromeres and affects centromeric CENP-A levels in fission yeast. *PLoS Genet.* **9**, e1003371 (2013).

230. V. Mathew *et al.*, The histone-fold protein CHRAC14 influences chromatin composition in response to DNA damage. *CellReports.* **7**, 321-330 (2014).

231. Q. Wu *et al.*, Expression and prognostic significance of centromere protein A in human lung adenocarcinoma. *Lung Cancer.* **77**, 407-414 (2012).

232. P. Ranjitkar, Regulation of the centromeric histone H3 variant Cse4 by the E3 ubiquitin ligase, Psh1. *PhD Thesis.* 1-110 (2011).

233. U. S. Cho, W. Xu, Crystal structure of a protein phosphatase 2A heterotrimeric holoenzyme. *Nature.* **445**, 53-57 (2007).

234. O. O. Nerusheva, S. Galander, J. Fernius, D. Kelly, A. L. Marston, Tension-dependent removal of pericentromeric shugoshin is an indicator of sister chromosome biorientation. *Genes Dev.* **28**, 1291-1309 (2014).

235. K. Peplowska, A. U. Wallek, Z. Storchová, Sgo1 regulates both condensin and Ipl1/Aurora B to promote chromosome biorientation. *PLoS Genet.* **10**, e1004411 (2014).

236. K. F. Verzijlbergen *et al.*, Shugoshin biases chromosomes for biorientation through condensin recruitment to the pericentromere. *eLife.* **3**, e01374-e01374 (2014).

237. H. D. Eshleman, D. O. Morgan, Sgo1 recruits PP2A to chromosomes to ensure sister chromatid bi-orientation during mitosis. *J Cell Sci.* **127**, 4974-4983 (2014).

238. B. Akiyoshi, C. R. Nelson, J. A. Ranish, S. Biggins, Quantitative proteomic analysis of purified yeast kinetochores identifies a PP1 regulatory subunit. *Genes Dev.* **23**, 2887-2899 (2009).

CURRICULUM VITAE

ERICA M HILDEBRAND

Fred Hutchinson Cancer Research Center
Basic Sciences Division
1100 Fairview Ave N.
MS A2-168
Seattle, WA 98109
Work: (206) 667-5766

CURRENT POSITION

University of Washington/Fred Hutchinson Cancer Research Center Seattle, WA
Graduate Student 2010-Fall 2016

EDUCATION

University of Washington Seattle, WA
PhD, Molecular and Cellular Biology Graduate Program 2016
Dissertation: Regulation of centromeric nucleosome localization in budding yeast

Connecticut College New London, CT
BA, *summa cum laude* with Honors and Distinction, Biological Sciences. 2010
Certificate in Conservation Biology and Environmental Studies. Phi Beta Kappa

RESEARCH EXPERIENCE

University of Washington/Fred Hutchinson Cancer Research Center Seattle, WA
Graduate Student; Advisor: Dr. Sue Biggins 2011-Present
Regulation of CENP-A^{Cse4} localization by the E3 ubiquitin ligase Psh1 in budding yeast

- Performed and analyzed CENP-A^{Cse4} ChIP-seq to determine mislocalization pattern of CENP-A^{Cse4} when overexpressed in the *psh1*Δ background
- Determined genomic features that are permissive for CENP-A^{Cse4} mislocalization
- Identified the chromatin remodeling complex Ino80 as a putative CENP-A^{Cse4} chaperone at chromosome arms
- Measured changes in transcription by RNA-seq
- Purified kinetochores from WT vs. *psh1*Δ strains

University of Washington Seattle, WA
Graduate Rotation Student; Advisor: Dr. Bonita Brewer Winter 2011
Genetic screen for DNA replication initiation factors in budding yeast

- Conducted genetic screen in the *cdc7*Δ *mcm5-bob1* strain to identify interacting genes involved in DNA replication initiation
- Performed experimental evolution experiment to identify suppressors of the mini-chromosome maintenance defect in the *mcm5-bob1* strain

University of Washington Seattle, WA
Graduate Rotation Student: Advisor: Dr. Amy Weinmann Fall 2010
T-bet defines the Th1 cell lineage through both positive and negative gene regulation

- Studied how the transcription factor T-bet is involved in both positive and negative regulation of target genes, and how this is involved in defining Th1 cell lineage
- Mutated conserved regions of the Jumonji d3 protein to determine if the demethylase and remodeling activities localize to the same region.
- Performed endogenous Co-IPs on EL4 cells to test for the presence of BAF/BRG complex members with Jumonji d3 in different cell stimulation conditions.

Connecticut College New London, CT
Undergraduate Honors Thesis; Advisor: Dr. Deborah Eastman Fall 2009-Spring 2010
The effects of Tramtrack69 on *HLHmgamma* gene expression in *D. melanogaster*

- Transfected Drosophila S2 cell cultures with plasmid expression vectors to study the effects of TTK69 on *mgamma* gene expression and interactions with the Notch signaling pathway in *D. melanogaster*
- Measured transcriptional activation using a dual luciferase assay read by a Veritas luminometer.

Connecticut College New London, CT
Undergraduate Research Assistant; Advisor: Dr. Anne Bernhard Fall 2009
Characterization of ammonia oxidizing archaea populations in a New England salt marsh from different long term nitrogen fertilizer treatments

- Extracted DNA from sediment samples using MoBio PowerSoil DNA extraction kit.
- Amplified the archaeal ammonia oxidizing gene from environmental DNA samples using PCR.
- Constructed clone libraries of the archaeal ammonia oxidizing gene from each nitrogen treatment and analyzed using ClustalW.

Woods Hole Oceanographic Institution Woods Hole, MA
Summer Student Fellow; Advisor: Dr. Stefan Sievert Summer 2009
Microbial communities of deep-sea hydrothermal vents

- Extracted DNA from microbial population samples from deep-sea hydrothermal vents.
- Optimized PCR conditions using barcoded 454 pyrosequencing primers to metabolism related genes and rDNA.

Connecticut College New London, CT
Undergraduate Research Assistant; Advisor: Dr. Deborah Eastman Spring 2009
The effects of Tramtrack69 on *HLHmgamma* gene expression in *D. melanogaster* Summer 2008

- Studied the effects on *HLHmgamma* gene expression in *D. melanogaster*

S2 cells with addition of the putative transcriptional repressor Tramtrack69.
- Learned and used molecular biology techniques such as transfections, transformations, *D. melanogaster* S2 cell culture, qPCR, and plasmid preps.
- Optimized electroporation conditions for *D. melanogaster* S2 cells to transfect CuSO4 induced expression vectors with luciferase reporter activity.

SIT World Learning Australia: Natural and Cultural Ecology Magnetic Island, Qld, AU
Undergraduate Independent Study; Advisor: Dr. Daniella Cercarelli Fall 2008
Interspecific feeding interactions of two goatfish species, *Parupeneus inducus* and *Parupeneus ciliates* on a fringing coral reef

- Studied the interspecific feeding interactions of two goatfish species, *Parupeneus indicus* and *Parupeneus ciliates* on a fringing coral reef.
- Designed project based on previous research in the area
- Collected data on the feeding interactions of the fish species, compiled and analyzed data.

PUBLICATIONS

Deyter, G.M.*, **Hildebrand, E.M.***, Barber, A.D., Biggins, S. (2016) Histone H4 facilitates the proteolysis of the budding yeast CENP-A^{Cse4} centromeric histone variant. *Genetics*. Early online October 28. DOI: 10.1534/genetics.116.19407 (*These authors contributed equally)

Hildebrand, E.M., Biggins, S. (2016) Regulation of Budding Yeast CENP-A levels prevents misincorporation at promoter nucleosomes and transcriptional defects. *PLOS Genetics* 12(3):e1005930

Peng, X., Yando, E., **Hildebrand, E.**, Dwyer, C., Kearney, A., Waciega, A., Valiela, I., Bernhard, A.E. (2013) Differential responses of ammonia-oxidizing archaea and bacteria to long-term fertilization in a New England salt marsh. *Frontiers in Microbiology*. Jan 22;3:445.

CONFERENCE PRESENTATIONS

Hildebrand, E.M. and Biggins, S. Regulation of budding yeast CENP-A levels prevents misincorporation and promoter nucleosomes and defects in transcription. Oral presentation delivered at the CSHL Cell Biology of Yeasts Meeting, Cold Spring Harbor, NY. November 3-7, 2015.

Hildebrand, E.M. and Biggins, S. Psh1 prevents CENP-A(Cse4) mislocalization to promoter nucleosomes. Poster presentation delivered at the Seattle Genetic Instability and Cancer Symposium, Seattle, WA. June 15, 2015.

Hildebrand, E.M. and Biggins, S. Regulation of centromeric nucleosome localization by the E3 ubiquitin ligase, Psh1. Poster presentation delivered at the Yeast Genetics Meeting, Seattle, WA. July 29-August 3, 2014.

Hildebrand, E.M. and Biggins, S. Regulation of centromeric nucleosome localization in budding yeast. Poster presentation delivered at the Chromatin Structure and Function Gordon Conference, Waltham, MA. June 8-13, 2014.

Hildebrand, E, Megley, C, Eastman, D. Tramtrack69 regulates the Enhancer of split *HLHmgamma* gene in *Drosophila melanogaster*. Poster presentation delivered at the American Society for Cell Biology Meeting, San Diego, CA. December 5-9, 2009.

GRANTS AND AWARDS

Poster Contest Award 2nd Place 2015
Seattle Genetic Instability and Cancer Symposium

Genetics Society of America Poster Award 2014
Yeast Genetics Meeting

Graduate Research Fellowship Program 2012-2015
National Science Foundation

Chromosome Metabolism and Cancer Training Grant 2011-2012
Fred Hutchinson Cancer Research Center/National Institute of Health

Paul Fell Biological Research Award 2010
Connecticut College

Dorothy Richardson Prize for Sophomores in Biology 2008
Connecticut College

Keck Undergraduate Research Fellowship 2008
Connecticut College

LEADERSHIP EXPERIENCE

University of Washington/Fred Hutchinson Cancer Research Center Seattle, WA
Molecular and Cellular Biology Symposium Spring 2014
Chromatin: Navigating the Genomic Landscape
Organizing Committee Member

- Selected invited speakers
- Organized and planned event

Fred Hutchinson Cancer Research Center Seattle, WA
Graduate Student Meeting Organizer Fall 2012-Spring 2014

- Planned yearly schedule of meetings
- Recruited graduate student speakers

Fred Hutchinson Cancer Research Center Seattle, WA
Mentor, Summer Undergraduate Research Program Summer 2013

University of Washington Seattle, WA
Teaching Assistant, BIOC 442 Biochemistry Spring 2012
Teaching Assistant, BIOC 440, Biochemistry

SCIENTIFIC OUTREACH ACTIVITIES

Fred Hutchinson Cancer Research Center Seattle, WA
40th Anniversary Block Party September 15, 2015
Table Presenter

- Organized table to explain how yeast genetics is related to cancer research to the public
- Demonstrated laboratory techniques and discussed research with the public and members of the Fred Hutchinson Cancer Research Center community

Seattle Expanding Your Horizons Seattle, WA
Hands-on conference that encourages students in 6th-8th grades to explore math and science related occupations March 14, 2015
March 15, 2014
Presenter March 16, 2013

- Prepared and facilitated a workshop for middle school students to test the efficacy of household antibacterial agents March 10, 2012
- Presented information and answered questions about my career path and goals

Volunteer March 12, 2011

- Supervised and assisted participants between workshops

Fred Hutchinson Cancer Research Center Seattle, WA
Genetics Approaches and Analysis Research class from June 18, 2015
Pacific Lutheran University July 17, 2014
Lab Tour Host

- Arranged and led hands-on activity about protein purifications in the Biggins lab
- Answered questions from undergraduates about research and what it is like to be a graduate student

Northwest Association of Biological Research Seattle, WA
Student BioExpo
Judge Spring 2013

- Read, watched, and evaluated scientific research projects in the Dance/Drama section of the BioExpo
- Met with high school student participants during the BioExpo and asked questions about their projects to gauge their understanding of the topics

Mentor Fall 2011-Spring 2012

- Helped 1-2 high school students each year to plan and implement their projects for the BioExpo Fall 2012-Spring 2013

- Met with students in person once to discuss their projects and kept in touch throughout the school year via email